Parkinson's disease risk gene, *CD38*, as it relates to glial function: dysregulation of astrocyte genes and bioenergetics as a result of CD38 deficiency

Raymundo D Hernandez

Dissertation submitted to the faculty of the Virginia Polytechnic Institute and State University in partial fulfillment of the requirements for the degree of

Doctor in Philosophy
In
Translational Biology, Medicine, and Health

Michelle L. Olsen
Michael A. Fox
Alicia M. Pickrell
Rita M. Cowell

Dissertation Defense
December 8, 2023
Blacksburg, VA

Keywords: astrocyte, glia, CD38, Parkinson's disease, mitochondria, bioenergetics, neurodegeneration

Parkinson's disease risk gene, *CD38*, as it relates to glial function: dysregulation of astrocyte genes and bioenergetics as a result of CD38 deficiency

Raymundo D Hernandez

ABSTRACT

Parkinson's disease (PD) is the second most prevalent age-related neurodegenerative disease and currently affects over 8 million people worldwide. The primary features of PD include cognitive, behavioral, and motor function deficits induced primarily by the progressive loss of dopaminergic neurons within the substantia nigra of the basal ganglia (BG). Motor coordination becomes severely affected over the course of the disease, causing patients to experience tremors at rest, bradykinesia, and body rigidity. The availability of treatment options has increased the quality of life for patients experiencing the early stages of PD; however, there exists no cure and treatment options are limited for those experiencing severe, advanced disease symptoms.

Genetic studies in PD patients have led to the identification of causative genes, but revealed that less than 20% of cases can be attributed to monogenic variations. Evidence strongly indicates that the majority of PD cases are idiopathic and likely driven due to gene by environmental interactions. Reflective of this idea, recent research efforts have turned to genome-wide association studies (GWAS) to provide indications of gene variations, that while not causative of PD, incur increased risk within patient populations. GWAS findings play a particularly crucial role in neurodegenerative interventions, as early identification of patient risk may allow for preventative therapeutics to delay disease onset or reduce symptom severity.

Amongst the many gene variants identified as incurring increased PD risk, single-nucleotide polymorphisms (SNPs) in the loci for *CD38* that cause reduced gene expression are consistently identified as increasing risk. The cluster of differentiation 38 (CD38) protein serves two major roles: one as a receptor for immunological response and a second as an ectoenzyme that modulates bioenergetic functions. The particular functions of CD38 are highly relevant to neurodegenerative contexts, as changes in central nervous system (CNS) inflammatory status and means of cellular energy production typically precede pathological indications. In the brain, CD38 expression is most enriched in astrocytes in BG regions, including substantia nigra, midbrain, and striatum. However, it is not known how *CD38* deficiency may contribute to astrocytic dysfunction and neuropathological features of PD.

This dissertation describes how CD38 influences astrocytic gene expression and cellular bioenergetics. Astrocyte RNA was sequenced from the BG of one-year old male $Cd38^{+/+}$, $Cd38^{+/-}$, and $Cd38^{-/-}$ mice by magnetic-activated cell sorting (MACS) to acquire astrocyte isolates. Numerous differentially expressed genes (DEGs) were identified in *Cd38* $Cd38^{+/-}$ and $Cd38^{-/-}$ astrocytes that relate to regulation of cellular health, responses to stress, and bioenergetic functions. GO analysis further suggested mitochondrial dysfunction in both $Cd38^{+/-}$ and $Cd38^{-/-}$ astrocytes. In a subsequent set of experiments evaluating mitochondrial function by Seahorse XF96 platform, $Cd38^{+/-}$ and $Cd38^{-/-}$ astrocytes displayed altered bioenergetic function.

The results herein demonstrate that astrocytic *Cd38* expression regulates cellular function and implicates transcriptional changes associated with the hallmarks of neurodegeneration. These findings serve to provide future direction for studies evaluating the relationship between CD38 function and astrocytes as it relates to neurodegenerative PD risk.

Parkinson's disease risk gene, *CD38*, as it relates to glial function: dysregulation of astrocyte genes and bioenergetics as a result of CD38 deficiency

Raymundo D Hernandez

GENERAL AUDIENCE ABSTRACT

Parkinson's disease (PD) is the second most common age-related neurodegenerative disease and currently affects over 8 million people worldwide. The primary features of PD include cognitive, behavioral, and motor function deficits induced primarily by the progressive loss of specialized neurons within the substantia nigra of the basal ganglia (BG) brain region. Motor coordination becomes severely affected over the course of the disease, causing patients to experience body tremors, slowness, and rigidity. The availability of treatment options has increased the quality of life for patients experiencing the early stages of PD; however, there exists no cure and little treatment options for those experiencing severe, advanced disease symptoms.

Genetic studies in PD patients have led to the identification of causative genes, but revealed that less than 20% of cases can be attributed to specific, individual variations. Evidence strongly indicates that the majority of PD cases are likely caused by small gene changes that interact with environmental factors. Recent research efforts have turned to genome-wide association studies (GWAS) to identify these small changes, that while not causative of PD, may increase risk within patient populations. GWAS findings play a particularly crucial role in treating neurodegenerative diseases, as early identification of patient risk may allow for preventative therapeutics to slow disease onset or reduce symptom severity.

Amongst the many small gene changes identified as increasing PD risk, changes in the gene *CD38* that cause reduced gene expression are consistently identified as increasing risk. The cluster of differentiation 38 (CD38) protein serves two major roles: one as a receptor for immune responses and a second as an enzyme that impacts how cells produce energy. The functions of CD38 are highly relevant to neurodegenerative contexts, as changes in central nervous system (CNS) inflammatory status and means of cellular energy production typically precede disease pathology. In the brain, *CD38* expression is most enriched in astrocytes, specialized brain cells that supports neurons, in regions affected by PD. However, it is not known how *CD38* deficiency may contribute to astrocytic dysfunction and neuropathological features of PD.

This dissertation describes how CD38 influences astrocytic gene expression and cellular bioenergetics. Astrocyte RNA was sequenced from the BG of one-year old male $Cd38^{+/+}$, $Cd38^{+/-}$ (50% CD38 loss), and $Cd38^{-/-}$ (100% CD38 loss) mice by magnetic-activated cell sorting (MACS) to acquire astrocytes. Numerous changes in gene expression were identified in *Cd38* $Cd38^{+/-}$ and $Cd38^{-/-}$ astrocytes that relate to regulation of cellular health, responses to stress, and energy functions. Further analysis looking at functions, suggested mitochondrial abnormalities in both $Cd38^{+/-}$ and $Cd38^{-/-}$ astrocytes. In a subsequent set of experiments evaluating mitochondrial function by Seahorse XF96 platform, $Cd38^{+/-}$ and $Cd38^{-/-}$ astrocytes displayed altered energetic function.

The results herein demonstrate that astrocytic *Cd38* expression regulates cellular function and implicates transcriptional changes associated with the hallmarks of neurodegeneration. These findings serve to provide future direction for studies evaluating the relationship between CD38 function and astrocytes as it relates to neurodegenerative PD risk.

ACKNOWLEDGEMENTS

First and foremost, I thank Dr. Michelle Olsen for her exemplary mentorship. Thank you for helping me reach my dream of being an astrocyte researcher. Your expertise helped shape my excitable, naïve mind into a directional purpose. You taught me the value of pushing through when things are hardest and supported me throughout this entire journey. I also want to thank you for hearing my struggles and making space and opportunities for me when I was at my lowest. Michelle, you will always be my ideal in mentorship and humanity.

I also extend my thanks to former and current committee members. To Dr. Lucas Pozzo-Miller, thank you for helping me sharpen my scientific approaches. I also thank former member. Dr. Stefanie Robel for demonstrating how leadership principles make us all better scientists. I give a special thanks to Dr. Michael Fox for being a wealth of experience and knowledge when discussing ideas for experiments. I thank Dr. Alicia Pickrell for being willing to train me on confocal equipment and teach me about mitochondrial methods. Finally, I extend my thanks to Dr. Rita Cowell, for being so incredibly welcoming to me as a new collaborator.

Of course, I must extend the greatest thanks to my parents, Raymundo and Leticia Hernandez. Throughout all of my life, you have both continued to love and support me in ways that were not always easy, but were absolutely necessary. Thank you for holding my hand throughout life and keeping me in your prayers as I embarked on this wild, wild journey. To my Dad, thank you for teaching me persistence and humility. To my Madre, thank you for always hearing me, especially when I didn't know how to be heard. You have both given me the world and I can never thank you enough.

To my siblings Kassandra, Julian, and Arianna, thank you for hearing my out when I struggled and finding ways to make me laugh along the way. Being your big brother has shaped me into the person that I am. To my boys Omar, Michael, and Adrian, you are the brothers that carried me across every finish line since our days out of T-town. I won't ever forget our late-night talks and shenanigans. I'm proud of how far we've come and look forward to all that we will do.

To my Nana, my star, gracias por todos los años de amor y dedicación. Gracias por orar por nosotros cuando luchamos y celebrarnos con cada pequeño éxito. Gracias por darme tanto de tu vida y amor. Gracias por el dinero del helado y las hermosas palabras de sabiduría. Siempre serás mi inspiración. I love you, I love you, I love you.

To Christina, my love, thank you for being the steel that hones me into a better person. Thank you for seeing me through the most difficult parts of my life and helping me find myself when I was lost. Thank you for listening to my rantings and ravings of my work and supporting me when I couldn't support myself. Thank you for showing me how to love selflessly, even in the midst of the harshest struggles. You always are, and always will be, my person.

To my kids, Raymund, Mac, and Layel, thank you for all the joy you've brought into my life. I had always wanted to be a scientist, but you all showed me that I was made for so much more. My happiest moments have been spent with all of you and I can't wait for our next adventure.

TABLE OF CONTENTS

List of Tables

List of Figures

Abbreviations

PD – Parkinson's disease
DA – Dopaminergic
BG – Basal ganglia
SN – Substantia nigra
SNc – Substantia nigra pars compacta
VAMP – Vesicle associated membrane protein
GWAS – Genome-wide association study
ATP – Adenosine triphosphate
TCA – Tricarboxylic acid cycle
NAD – Nicotinamide adenine dinucleotide
NADH – Nicotinamide adenine dinucleotide (+hydrogen)
$FADH_2$ – Flavin adenine dinucleotide
MAO-B – Monoamine oxidase B
CD38 – Cluster of differentiation 38
ADPR – Adenosine diphosphate-ribose
cADPR – Cyclic Adenosine diphosphate-ribose
NAM – Nicotinamide
Ca^{2+} – Calcium
PAP – Peripheral astrocyte process
GFAP – Glial fibrillary acidic protein
MACS – Magnetic activated cell sorting
FACS – Fluorescence-activated cell sorting
FCX – frontal cortex
PCX – parietal cortex
TCX – temporal cortex
LIM – limbic cortex
IN - insular cortex
OCX – occipital cortex
BF – basal forebrain
CLA – claustrum
AMY – amygdala
HIP – hippocampus
STR – striatum
GP – globus pallidus
DI – diencephalon
MID – midbrain
PON – pons
MED – medulla
SC – spinal cord
CB – cerebellum
RNA-seq – RNA sequencing
cDNA – Complementary DNA
PCR – Polymerase chain reaction
OCR – Oxygen consumption rate

ECAR – Extracellular acidification rate
FCCP – Phenylhydrazone
KO – Knockout
KD – Knockdown
SNP – Single-nucleotide polymorphism
FISH – Fluorescence *in situ* hybridization
RT-PCR – Reverse transcription-polymerase chain reaction
^{1}H NMR – Proton nuclear magnetic resonance
DEG – Differentially expressed gene
GO – Gene ontology
ETC – Electron transport chain
PDH – Pyruvate dehydrogenase
TCA – Tricarboxylic acid cycle
CS – Citrate synthase
UMI – Unique molecular identifier
FC – Fold change
BCA – Bicinchoninic acid assay
ROS – Reactive oxygen species
NDD – Neurodegenerative disease

Chapter 1: Introduction

1.1 Parkinson's disease

Parkinson's disease (PD) is the second most common age-related neurodegenerative disease (Tolosa et al., 2021) , affecting an estimated 8.5 million people worldwide (World Health Organization, 2023) and costing over $50 billion dollars in economic burden within the United States alone (Yang et al., 2020). The features of PD symptoms remain similar to those first described by British physician James Parkinson in 1817 (Parkinson, 2002), namely resting tremors, bradykinesia, and rigidity of the limbs. Today, it is recognized that PD is also associated with cognitive deficits, behavioral changes, and the onset of dementia. The most common risk factor in PD development is age, with people over the age of 60 having a 1% prevalence rate(Tysnes & Storstein, 2017) which escalates to 3% prevalence by age 85 (Sontheimer, 2021).

The root cause of PD is due to the progressive cell death of dopaminergic (DA) neurons within the substantia nigra (SN, Fig. 1a, (Poewe et al., 2017)) of the basal ganglia (BG), a region containing neuronal populations that act as major regulators of motor function. Similar to other neurodegenerative diseases, PD has been demonstrated to have a prodromal phase characterized by physiological disturbances unrelated to the core of motor dysfunction. Namely, these pre-motor symptoms include changes in bowel movements, cognitive flexibility, sleep behavior, and olfaction (Fullard et al., 2017; Roos et al., 2022). As DA neurons degenerate, patients progress through early PD stages indicated by the hallmarks of rigidity, tremors at rest, and bradykinesia. The early symptoms can be treated by administration of levodopa, a dopamine substitute that allows for conversion of additional dopamine to regulate motor regions. Eventually, levodopa treatments become less effective during the moderate stage of DA cell loss and dyskinesia often appears as an additional symptom. The severe stage of symptoms, characterized by significant

posture instability, gait cessation, dysphagia, and neuropsychiatric illness (Kalia & Lang, 2015), is caused by further loss of DA neurons within the SN (Fig. 1b-d) that induce dysfunction of brainstem and cortical pathways. Moderate and late stages may be treated by invasive means, such as deep brain stimulation of BG systems; however, current treatments offer no cure.

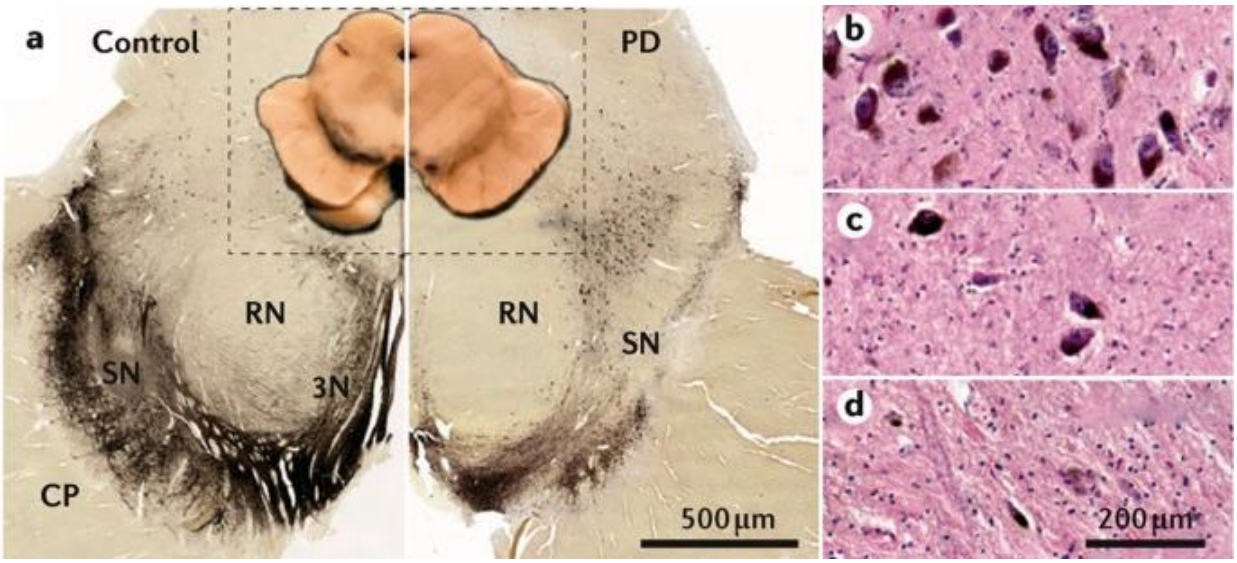

Figure 1. Progressive loss of dopaminergic neurons is a pathological hallmark of PD. Immunohistochemical staining of tyrosine hydroxylase, an essential enzyme in dopamine generation, in the SN of human control (a, right) and PD patient (a, left) demonstrate a loss of dopaminergic neurons. Severity of symptoms is often associated with the degree of cell loss, indicted by hematoxylin and eosin staining, highlighting SN neurons (dark purple) in asymptomatic (b), mildly symptomatic (c), and severely symptomatic (d) patient samples (Poewe et al., 2017).

All PD treatments aim to reduce dysfunction of the BG systems, the series of coordinated regions that requires DA neuronal inputs to integrate motor function signals (Fig. 2A). The BG are a collection of distinct nuclei including the striatum (putamen, caudate nucleus), nucleus accumbens, globus pallidus, subthalamic nucleus, and substantia nigra. At its core, motor function requires a balance between the initiation of a motor response and an inhibition of antagonistic responses in order to facilitate smooth, continuous movement. This is achieved

within the BG through utilization of DA neuronal inputs to drive an excitatory direct pathway and inhibitory indirect pathway. DA neuronal inputs of the SN pars compacta (SNc) are crucial for both initiating motor drive and regulating compensatory inhibition via dopamine release in the striatum along the nigrostriatal pathway. SNc projections into the striatum activate resident medium spiny neurons differentially dependent upon dopamine receptor subtype (D1, D2) activation. In the simplest of terms, D1-type receptor stimulates the direct pathway for initiation of movement while D2-type receptors drive suppressing of motor responses. Loss of DA neurons of the SNc decreases activity of the excitatory direct pathway and shifts the balance in favor of motor inhibition, resulting the cardinal symptom of bradykinesia (Fig. 2B).

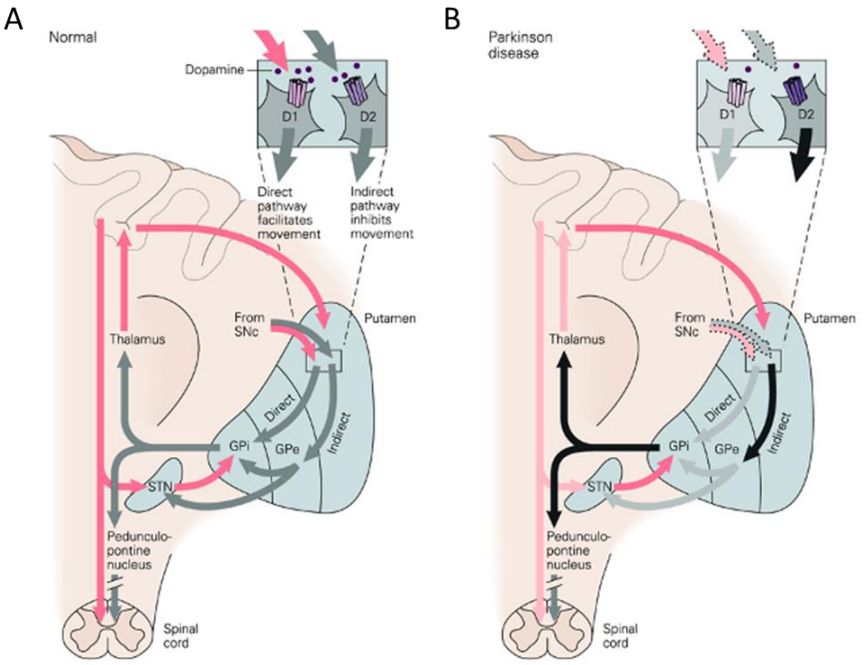

Figure 2. Schematic of PD effect on BG direct and indirect motor pathways. BG motor control relies on a series of excitatory (pink) and inhibitory (grey) pathways. (A) DA neurons of the SN pars compacta (SNc) act on D1 receptor cells to excite them along the direct pathway to initiate motor behaviors and D2 containing cells to cause inhibition of competing motor tasks. (B) In PD, DA loss results shifts balance towards the inhibitory indirect pathway, resulting in bradykinesia. Globus pallidus internus (GPi) and externus (Gpe), subthalamic nucleus (SN) (Kandel et al., 2014).

Currently, it is believed that there are numerous pathological, genetic, and environmental factors that contribute to the loss of DA cells in PD patients. The pathological accumulation of α-synuclein in the brain is a common feature correlated with disease severity, however. In healthy contexts, α-synuclein is believed to serve as a molecular chaperone to vesicle-associated membrane proteins (VAMPs) within the synapse to modulate vesicular binding and release (Burré et al., 2010; Meade et al., 2019). It has been consistently observed in PD patient tissues that α-synuclein presence is increased and aggregates into cytotoxic plaques termed Lewy bodies (Braak et al., 2003). While identification of α-synuclein as a disease contributor has helped us understand how DA neurodegeneration may occur, the association between Lewy bodies and cell death was largely determined from patient tissues with familial forms of PD including gene mutations associated with α-synuclein production, post-translation modification, and degradation (Meade et al., 2019). In its entirety, however, familial PD caused by a single-gene variant accounts for less than 20% of all cases (Balestrino & Schapira, 2020; Sellbach et al., 2006). While relatively small to the total PD population, research surrounding these rare genetic instances have proven crucial to our understanding which factors contribute to the progressive loss of DA neurons of the SN.

1.2 Genetics and Parkinson's

While the medical understanding of pathological and symptomatic features of PD are well established, the disease etiology remains fairly elusive. Studies evaluating PD-causative genes, however, have provided a stronger understanding of the biological mechanisms that underlie DA neuronal susceptibility to degeneration. Within the last three decades, advances in our ability to evaluate genomic variations have allowed for the identification of over 20 single-gene mutations

that are causative of PD (Blauwendraat et al., 2020; Ye et al., 2023). Additional studies evaluating PD family history further demonstrates a strong genetic component, with up to 25% of patients also having a family member with a diagnoses (Noyce et al., 2012; Sellbach et al., 2006). Importantly, some gene mutations have demonstrably high disease penetrance (*SNCA*, *PINK1*, *PARK7*, *PRKN*), while other are more variable (*LRRK2*, *GBA1*) dependent on the specific variant type (Table 1). Regardless of the degree of penetrance, identification of causative genes of monogenic PD demonstrates that many of the genes implicated in DA neuronal death converge on the regulation of specific cellular features, namely mitochondrial and lysosomal function. These determinations allow for potential development of novel treatments that help to better regulate pathways disrupted while simultaneously providing information that may help us understand functions relating to PD cases unrelated to familial monogenic cause.

	Gene (HGNC Approved Name)	Alternative Gene Names	Inheritance	Pathogenicity	PD Phenotype	Function
High penetrance	*SNCA*	*PARK1, PARK4, NCAP*	AD	Pathogenic	Early-onset	Uncertain (encodes α-synuclein)
	VPS35	*PARK17, MEM3*	AD	Pathogenic	Typical	Retromer and endosomal trafficking
	PINK1	*PARK6*	AR	Pathogenic	Early-onset	Mitochondrial
	PARK7	*DJ-1*	AR	Pathogenic	Early-onset	
	PRKN	*PARK2, PARKIN*	AR	Pathogenic	Early-onset	
	PLA2G6	*PARK14, IPLA2*	AR	Pathogenic	Early-onset, atypical	Cell membrane
	ATP13A2	*PARK9*	AR	Pathogenic	Early-onset, atypical	Lysosomal
	FBXO7	*PARK15, FBX7*	AR	Pathogenic	Early-onset, atypical	Mitochondrial
	POLG	*POLG1, POLGA*	AD	Pathogenic	Early-onset, atypical	Mitochondrial DNA maintenance
	DNAJC6	*PARK19, DJC6*	AR	Likely pathogenic	Early-onset	Synaptic vesicle formation and trafficking
	DNAJC13	*PARK21, RME8*	AD	Conflicting reports	Typical	
	TMEM230	*C20ORF30*	AD	Conflicting reports	Typical	
	SYNJ1	*PARK20*	AR	Pathogenic	Early-onset, atypical	
	VPS13C	*PARK23*	AR	Pathogenic	Early-onset	Mitochondrial
	CHCHD2	-	AD	Pathogenic	Typical	Uncertain
	DCTN1	-	AD	Pathogenic	Atypical	Microtubule
Variable penetrance	*LRRK2*	*PARK8, DARDARIN*	AD	Pathogenic	Typical	Lysosomal, mitochondrial, microtubule
	GBA	*GBA1*	AD	Pathogenic	Typical	Lysosomal
Associated with PD but unlikely to be pathogenic	*HTRA2*	-	AD	Uncertain/likely benign	-	Mitochondrial
	UCHL1	*PARK5*	AD	Uncertain/likely benign	-	Ubiquitin-proteasome
	GIGYF2	*PARK11*	AD	Uncertain/likely benign	-	Uncertain
	EIF4G1	-	AD	Benign	-	mRNA translation
	LRP10	*LRP9*	AD [1]	Uncertain	-	Uncertain

[1] AD = autosomal dominant, AR = autosomal recessive, HNGC = HUGO Gene Nomenclature Committee.

Table 1. Monogenic gene variants associated with PD risk organized by penetrance. Though monogenic variants are rare, they provide valuable information relating to functional changes that strongly influence PD pathogenicity (Day & Mullin, 2021).

The identification of pathogenic mutations is critical for understanding specific PD risk; however, these monogenic causes do not make up the majority of cases. Strictly speaking, it is believed that single-gene based PD cases make up less than 20% of diagnoses (Blauwendraat et al., 2020; Ye et al., 2023). Idiopathic cases make up the greatest majority of cases, leading research efforts to focus on genetic factors that, while not directly causative, pose increased risk

of pathogenicity. Genome-wide association studies (GWAS) are a method by which one may assess genetic variations within a given population to derive genomic regions and changes associated with the features of the group evaluated. In the field of PD research, GWAS datasets have provided volumes of information used for additional meta-analyses for determinations of risk genes associated with patient risk. For example, a recent GWAS meta-analysis utilizing nearly 1.5 million samples from across 17 datasets identified over 300 total PD candidate genes and 90 risk-associated loci, of which 38 were identified as novel (Nalls et al., 2019). Continued efforts in understanding how small genetic variances interact with environmental and aging factors is viewed as crucial to identifying patterns for better identification, prevention, and treatment of patients at risk of PD.

1.3 Bioenergetics and Parkinson's

Cellular energy production is a biological imperative for all forms of life. In mammalian eukaryotic cells, mitochondria are the primary facilitators of energy production in the form of adenosine trisphosphate (ATP). In humans, food is broken down to derive glucose, which is then enzymatically processed by enzymes within the mitochondrial matrix to produce substates necessary for maximizing ATP production. This process, termed the tricarboxylic acid cycle (TCA), generates essential metabolites such as pyruvate, nicotinamide adenine dinucleotide (NADH), and flavin adenine dinucleotide ($FADH_2$) for utilization as energy transfer substrates. In essence, these substrates are reduced in a process known as oxidative phosphorylation and then used to pass electrons through protein complexes within the inner mitochondrial membrane, where they form an electrochemical gradient. The gradient created allows for controlled, directional flow of protons in order to drive the molecular turbine, ATP-synthase, and generate

ATP. All essential cellular functions, from gene transcription to protein regulation, require ATP. Without ATP, the cessation of these functions will lead to the death of cells.

Mitochondrial dysfunction is a common cellular feature implicated in across PD cases. The association between energy insufficiency and PD was made clear in 1982, when a group of young individuals used a contaminated source of synthetic heroin and developed parkinsonian symptoms (Nonnekes et al., 2018). The heroin-derivative was identified to have been contaminated with MPTP, a precursor molecule of the mitochondrial toxin MPP^+. Later work identified that MPP^+ was selectively deleterious for DA neurons within the substantia nigra, as the conversion from MPTP to MPP^+ required the presence monoamine oxidase B (MAO-B) enzymes within astrocytes of the SN (Ransom et al., 1987). “The case of the frozen addicts” established a crucial link between DA neuron susceptibility to energy collapse and our understanding of motor symptoms associated with PD.

Today, monogenic PD findings and GWAS meta-analyses similarly identify genes associated with mitochondrial function to be linked to PD risk (Borsche et al., 2021). *PINK1* causal mutations, for instance, impair the mitophagy process responsible for removal of damaged mitochondria (Pickrell & Youle, 2015). Similarly, genes with variable disease penetrance, such as *LRRK2* mutations, affect mitochondrial oxygen consumption, responses to oxidative stress, and trafficking within cells (Singh et al., 2019). Mitochondrial impairments from PD-associated genes are harmful to all cellular processes within patients, but especially so for the CNS, as it is the largest consumer of ATP (Dunn & Grider, 2020). DA neurons fire depolarizing action potentials as often as 5-10 times per second, required large amounts of ATP to reestablish ionic concentrations necessary to maintain their membrane potentials and continue operating (Ni &

Ernst, 2022; Sheng, 2014). Altogether, converging evidence from environmental and genetic studies strongly implicates mitochondrial bioenergetic dysfunction as a PD feature (Fig. 3).

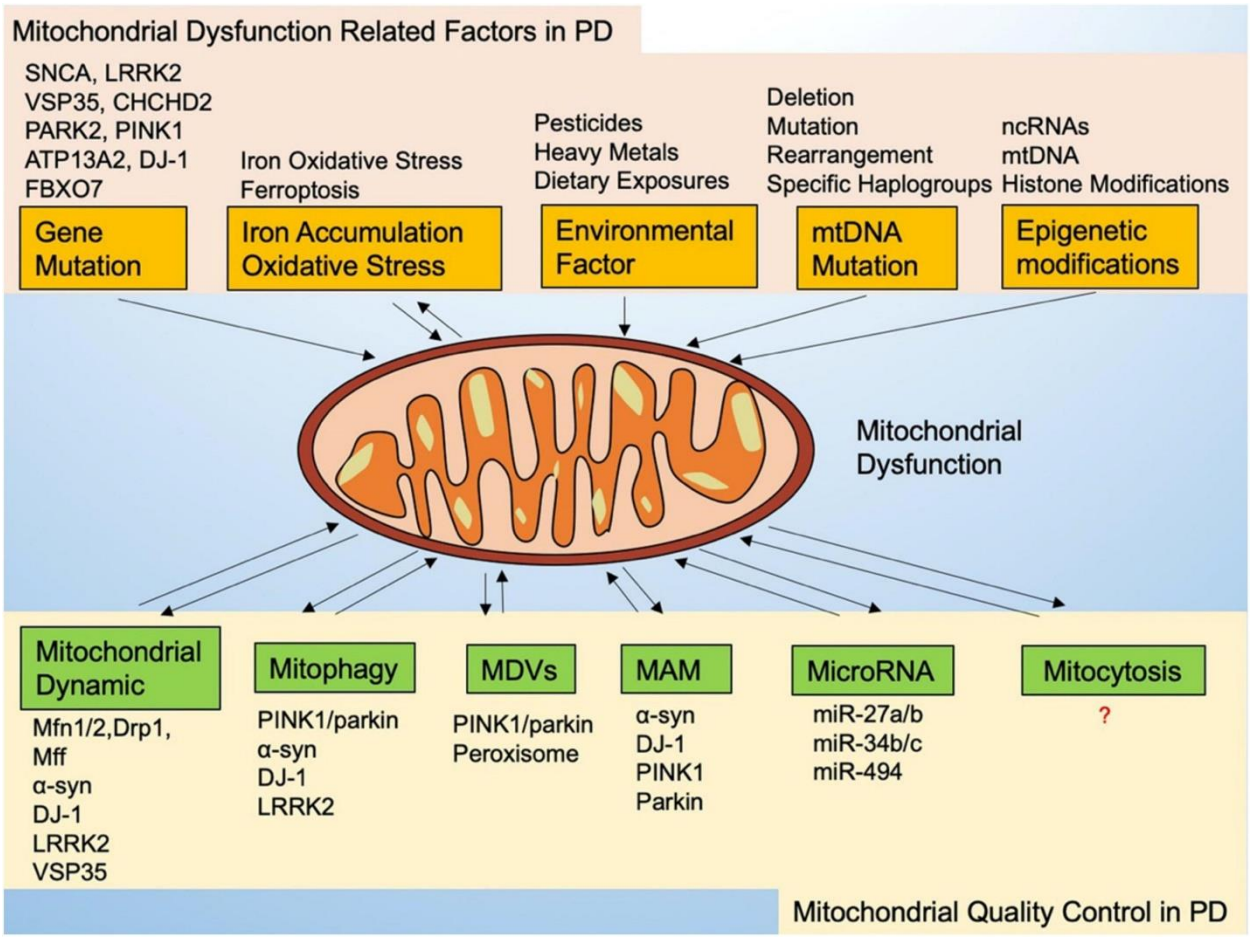

Figure 3. Changes in mitochondrial function and quality are strongly associated with PD. Genetic factors and accumulated environmentally incurred damage have been demonstrated to increase the risk of PD. Similarly, dysfunction of processes involved in maintaining mitochondrial health and integrity increase PD risk (Gao et al., 2022).

The identification of mitochondrial dysfunction as a common PD feature has led to a growing interest in therapeutic interventions that help improve bioenergetic function. Antioxidants, mitochondrial enhancers, and senolytics are various strategies of current interest given their ability to help improve mitochondrial function directly or indirectly (Borsche et al., 2021;

Deledda et al., 2022; Thomas & Beal, 2010). Identification of effective strategies, however, are dependent upon identification and study of how candidate genes affect biological processes.

1.4 *CD38*

GWAS identification of PD-risk genes have helped identify potential therapeutic targets that relate to bioenergetics. *CD38* is a relevant gene of interest as variations in its genomic region increase PD risk odds (Chen et al., 2014; J. Li et al., 2019; Sharma et al., 2012). Even further, the cluster of differentiation 38 (CD38) protein regulates bioenergetic substrate balance and demonstrates age-related changes in expression (Camacho-Pereira et al., 2016; Guerreiro et al., 2020). While *CD38* expression is most associated with immune cells and tissues of the immune system, brain expression is detectable at a physiologically relevant level (Piedra-Quintero et al., 2020). Amongst CNS cell populations, the glial cells, namely astrocytes, oligodendrocytes, and microglia, are the highest *CD38* expressing cells, in respective order (Kelley et al., 2018; Saunders et al., 2018). Astrocytes in particular serve numerous support roles within the CNS (see Chapter 1.5).

CD38 function is unique, as it operates as an extracellular enzyme and receptor (Fig. 4). As an ectoenzyme, CD38 acts as an NADase and consumes the bioenergetic substrate NAD^+, converting it into adenosine diphosphate-ribose (ADPR)/cyclic ADPR (cADPR) and nicotinamide (NAM) (Grozio et al., 2013; Malavasi et al., 2008). Importantly, ADPR/cADPR mediates the release of intracellular calcium (Ca^{2+}) to serve as a second messengers and regulate numerous cellular functions, including metabolism, gene expression, and cell survival (Bagur & Hajnóczky, 2017). NAM products can translocate from the extracellular to intracellular space, where it can be repurposed into NAD^+ via the salvage pathways for later use in mitochondrial

ATP production (Khaidizar et al., 2021). As a receptor, CD38 can interact with other cluster of differentiation proteins to transduce signals relating to immunological function, similarly driving Ca^{2+} release in order to modulate inflammatory responses (Morandi et al., 2019).

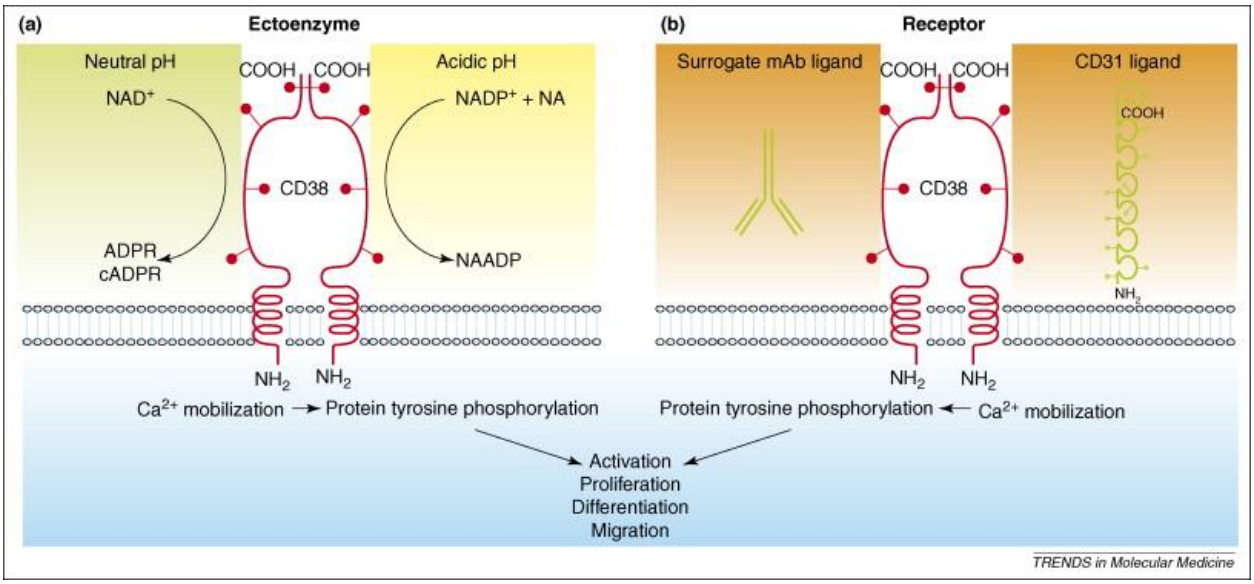

Figure 4. CD38 operates as an ectoenzyme and receptor. (a) CD38 function facilitates signaling via indirect pathways as an ectoenzyme that modulates bioenergetic substrate bioavailability. (b) As a receptor, CD38 can interact with other immunomodulatory molecules to facilitate direct signaling most associated with immune responses and cell migration (Deaglio et al., 2008).

The convergence of CD38 amongst age-related changes, mitochondrial function, immune regulation, and PD-risk association in CD38 studies has strongly implicated its function within neurodegenerative contexts. The aging process can be conceptually simplified as the accruement of damage across lifespan interacting with failing cellular systems. This concept, termed inflammaging, relates to the observations of increased inflammatory states across tissues observed in advanced age (Franceschi et al., 2018). During this time, CD38 expression across tissues increases whilst NAD levels decrease (Camacho-Pereira et al., 2016). A particularly striking observation is that NAD levels are further reduced in PD patients relative to age-

matched controls (Wakade et al., 2014). Furthermore, decreased NAD and increased ADPR/cADPR as a result of CD38 function have been identified as contributing to pro-inflammatory states (Camacho-Pereira et al., 2016; Wei et al., 2014; World Health Organization, 2023). For these reasons, some have argued that CD38 inhibition or supplementation of NAD precursors may be of benefit for age-related disease (Fig. 5).

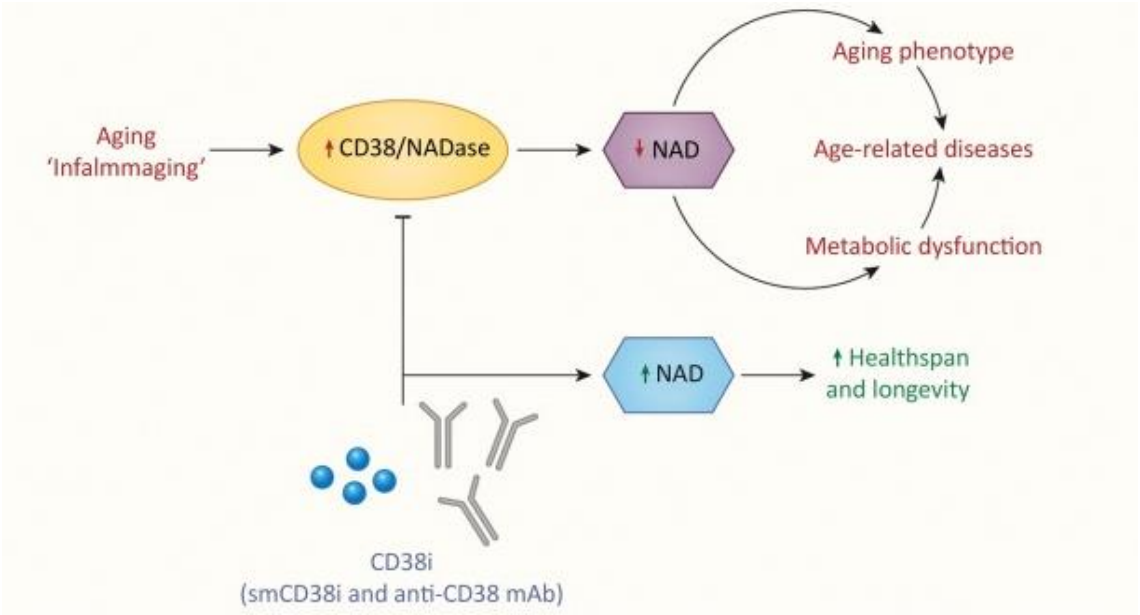

Figure 5. Age-related changes alter CD38 expression and function. Advanced age elicits an increase in CD38 protein expression alongside a decrease in NAD presence. Therapeutic approaches aim to modulate CD38 function to increase NAD and reduce aging phenotypes (Chini et al., 2018).

There exists an incongruity with CD38-based interventions as they relate to PD, however. While inhibition of CD38 function has become a therapeutic topic of interest, human SNP variants that induce decreased *CD38* expression have been identified as increasing risk odds for PD diagnosis (Chen et al., 2014; J. Li et al., 2019; Sharma et al., 2012). A gap currently exists within our understanding of the contexts in which manipulations of CD38 function induce impairment and benefit, requiring further research efforts to establish appropriate scenarios to

targeting CD38 function. Furthermore, we have limited information as to how glia, especially *CD38*-enriched astrocytes, of the brain respond to manipulations of CD38.

1.5 Astrocytes

Astrocytes represent the largest population of CNS glial cells and are intimately tied to the regulation of brain function. The astrocyte does not function as a neuron, but instead supports the functions that allow neuronal activity and health to be maintained. Astrocytic hallmarks include a highly ramified morphology comprised of structures termed peripheral astrocyte processes (PAPs), which are utilized to interact with the microenvironments of synapses, vascular networks, and neighboring glia (Schiweck et al., 2018). At the synapse, astrocytes regulate ionic homeostasis to allow maintain the parameters in which neurons require to fire action potentials. Neuronal activity stimulates astrocytic responses typically in the form of intracellular Ca^{2+} release, which serves as a second messenger to a host of intracellular signaling cascades (Nedergaard et al., 2003). Astrocytes also play a dynamic role in provisions of growth factors and energy metabolites, such as ATP, to neurons in order to meet the large energy demanded to sustain action potentials (Savtchouk & Volterra, 2018). The myriad of responses and roles that astrocytes have demonstrated has been reviewed at great depth (Sofroniew & Vinters, 2010) with a summary of primary astrocytic functions provided here (Fig. 6, left).

Typical astrocyte function can be perturbed by CNS injury, inflammation, and disease. Astrocytes can assume a reactive form, indicated by transcriptional and protein expression changes whereby astrocytes reduce typical homeostatic-related functions and become hypertrophic via increased expression of glial fibrillary acidic protein (GFAP). This reactive astrocytic state is associated with release of cytokines to mount inflammatory and anti-

inflammatory responses (Phatnani & Maniatis, 2015). Relevant to the discussions herein, neurodegenerative disease is strongly associated with changes in astrocytic states and functions, with some indications that reactive astrocytic phenotypes exacerbate neurodegenerative diseases (NDDs, Fig. 6, right). In fact, pro-inflammatory, reactive astrocytes are identified across neurodegenerative diseases in patient tissues (K. Li et al., 2019). The association between reactive astrocytes and neurodegenerative contexts likely arise from responses to disease pathology (e.g. α-synuclein), neuronal dysfunction (e.g. bioenergetic stress), and inflammatory signals that influence neuron to glia interaction (Adamczyk, 2023). In PD, astrocyte-to-neuron dysfunction has also been demonstrated to instigate disease states (Miyazaki & Asanuma, 2020). In MPTP-induced PD, astrocytes are the first to take up the compound, followed by the subsequent conversion and release of neurotoxic MPP^+. MPTP application in experimental animal models induces a pro-inflammatory state characterized by induction of reactive astrocytes and cytokine release (Michalovicz et al., 2019). Furthermore, when reactive astrocytic states are pharmacologically inhibited, MPTP-mediated inflammation and DA neuronal death is reduced (Yang et al., 2009). In PD pathology, α-synuclein aggregates in neurons can be taken up by astrocytes (Rannikko et al., 2015). However, increased α-synuclein uptake in astrocytes has been shown to reduce homeostatic-related functions and induce reactive phenotypes (Rannikko et al., 2015). Though neurodegenerative disease is most typically associated with neuron dysfunction or death, astrocytes and other glia clearly have a contributing role.

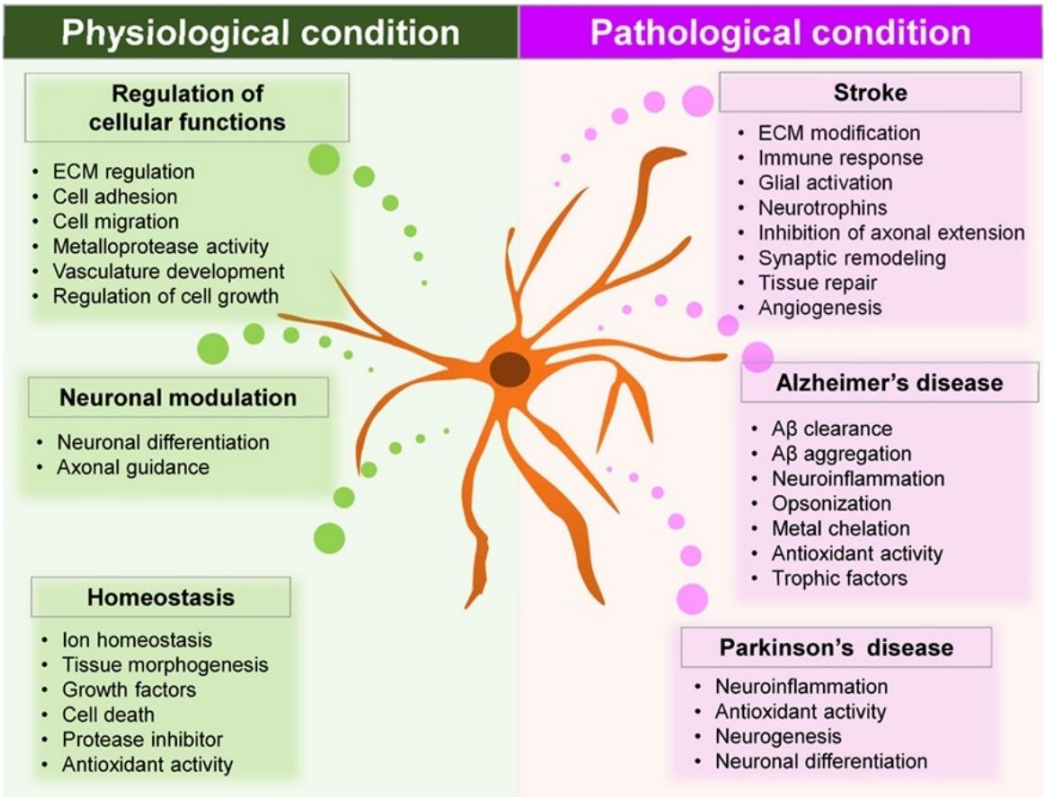

Figure 6. Astrocytes as regulators of function and their implications in disease. Astrocytes hold numerous support roles within the CNS. Their significance as support cells to neuronal function, response to injury, and maintenance of microenvironmental conditions places them in a precarious position as disease modifiers when dysfunctional or perturbed (Jha et al., 2018).

Astrocytes also express many of the genes associated with genetically-linked PD (Booth et al., 2017). *LRRK2* mutations associated with familial PD, for instance, have been shown to disrupt astrocytic lysosomal function (Henry et al., 2015). In patient-derived *LRRK2* variant astrocytes cell culture experiments, it was found that patient astrocytes had autophagy dysfunction and contributed to α-synuclein aggregation in neurons (di Domenico et al., 2019). In mice, it was determined that astrocyte-specific *Snca* overexpression was sufficient to induce neurological dysfunction across motor tasks and contribute to reductions in glutamate transporters , damage to blood-brain barrier integrity, and increased inflammation. Altogether, understanding astrocytic

contributions in NDDs is paramount to determining how disease states arise and may be mitigated.

1.6 MACS isolation

Research and technological developments over the last few decades have revealed numerous ways in which we can distinguish one cell type from another. Importantly, it has become apparent that studying the contributing role of particular cell types within the context of health and disease is critical to our understanding of development and pathology. Within Dr. Michelle Olsen's lab, we utilize a magnetic activated cell sorting (MACS) technique that allows for specific, sequential isolation of CNS cells of interest (Holt, Hernandez, et al., 2019; Holt & Olsen, 2016; Holt, Stoyanof, & Olsen, 2019). The premise of MACS isolation relies upon identification of cell-specific surface markers that can be labeled with specialized antibody beads that contain metallic ions (Fig. 7). Cells tagged with metallic-antibody beads are then run through a specialized ferromagnetic column in the presence of a powerful magnetic force. Labeled cells are then trapped within the ferromagnetic matrix while the remaining, unlabeled cells pass through for further processing or collection. In this way, once may positively select a cell population of interest or remove contaminating cells for a negative selection of the remaining column flowthrough.

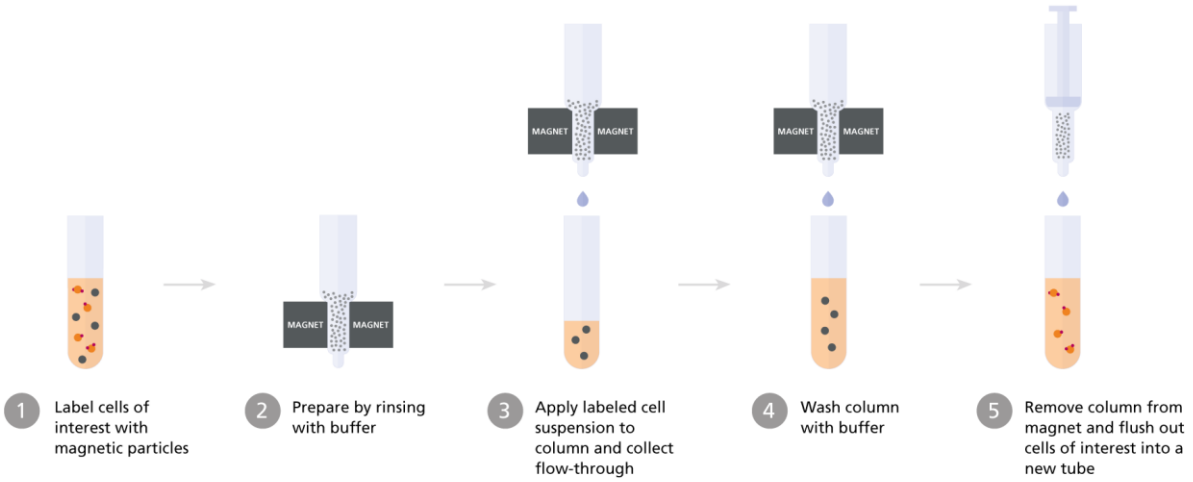

Figure 7. Magnetic activated cell sorting premise. Simplified diagram illustrating essential steps of MACS protocols (Technologies, 2023).

A major benefit of the MACS approach is the ability to isolate highly purified cellular fractions from whole tissues that retain much of their former morphological features (Fig. 8). Neurons and astrocytes in particular have highly complex morphological features that can often be damaged and lost in similar isolation methods, such as in the case of fluorescence-activated cell sorting (FACS). The retention of the information contained within astrocytic processes is highly relevant for the field of glial biology in particular, as these astrocyte PAPs are the way by which they interact with neuronal synapses and other microenvironments within the CNS (Baldwin et al., 2023). Furthermore, PAPs have been shown to play a role in the translational and bioenergetic regulation of astrocytes (Derouiche et al., 2015; Sakers et al., 2017). The evaluation of largely intact astrocytes provides a clearer vantage point of cellular processes relevant to neuron-glia communication.

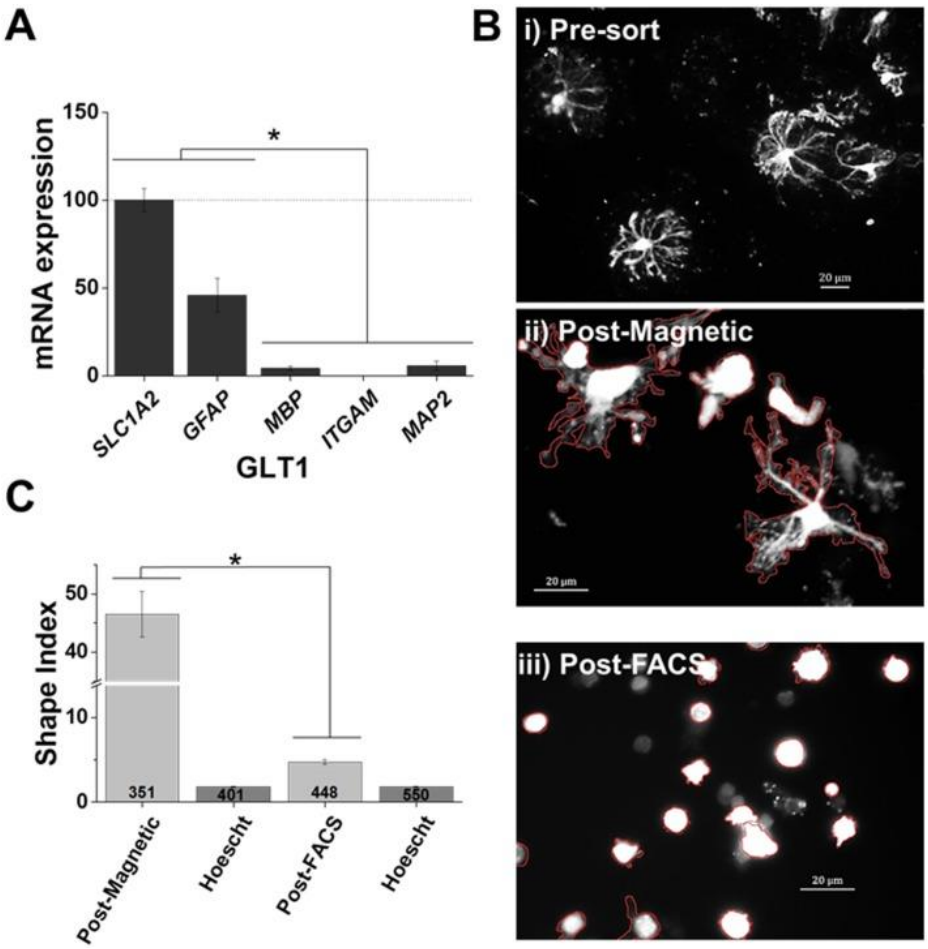

Figure 8. MACS isolations provide pure, morphologically intact astrocytes. (A) RT-PCR verification of cortical mouse astrocyte fractions showing enrichment of astrocytic genes (*Slc1a2*, *Gfap*) and depletion of oligodendrocyte (*MBP*), microglia (*Itgam*), and neuronal markers (*Map2*). (B) Cortical mouse astrocytes have a complex, bushy appearance prior to any sorting methods (i) and largely retain complex morphological states after MACS isolations (ii), but are largely reduced to only soma compartments during FACS isolations (iii). (C) Evaluations of shape index from mouse astrocyte indicate significant morphological retention in MACS to FACS comparisons (Holt & Olsen, 2016). *$p < 0.001$

1.7 RNA-sequencing

Within the broad field of biology, the central dogma is a core concept that explains that genomic DNA is the source by which all proteins within an organism are generated. While understanding the final protein created from DNA is incredibly valuable information, proteomic approaches often rely on highly specialized equipment and incur high operating costs relative to

transcriptomic approaches (Houfani & Foster, 2022; Sidoli et al., 2017). Transcriptomics operate to help us understand the RNA intermediates between a DNA source and the potential protein product. Developments in transcriptomics has given research powerful tools to better understand how gene activity in response to environmental stimulus give rise to cellular pathways and processes.

RNA-sequencing (RNA-seq) is a powerful method by which one can evaluate the molecular changes that arise in cells across development, disease, and within the context of specific genetic changes (Lowe et al., 2017). Briefly, RNA-seq methods begin with acquisition of RNA isolates from cells or tissues. Crude samples are typically purified through RNA isolation protocols or kits to reduce the potential of error in downstream processes. The purified RNA samples must then be placed through a library preparation processes that allows for sequencing to take place. First, RNA is fragmented and reversed transcribed into a more stable double-stranded complementary DNA (cDNA) form that reflects the genomic exon regions responsible for creation of the original RNA fragment. Oligonucleotides adapters with a known sequence are then ligated to the generated cDNA to allow for polymerase chain reaction (PCR) amplification of the cDNA-adapter construct. The amplification process is a series of heating and cooling steps to denature the double stranded cDNA, allow for primers to anneal to each individual strand, then begin extension of a new complementary stand. Next-generation sequencing platforms measure this amplification reaction via dyes or fluorescent tags associated with nucleotide bases to detect each nucleotide extension event to generate data representing the code of each transcript strand. Once the data has been generated, it must be further processed to remove sequencing artifacts by adapter trimming and removal of low-quality transcript reads (Fig. 9).

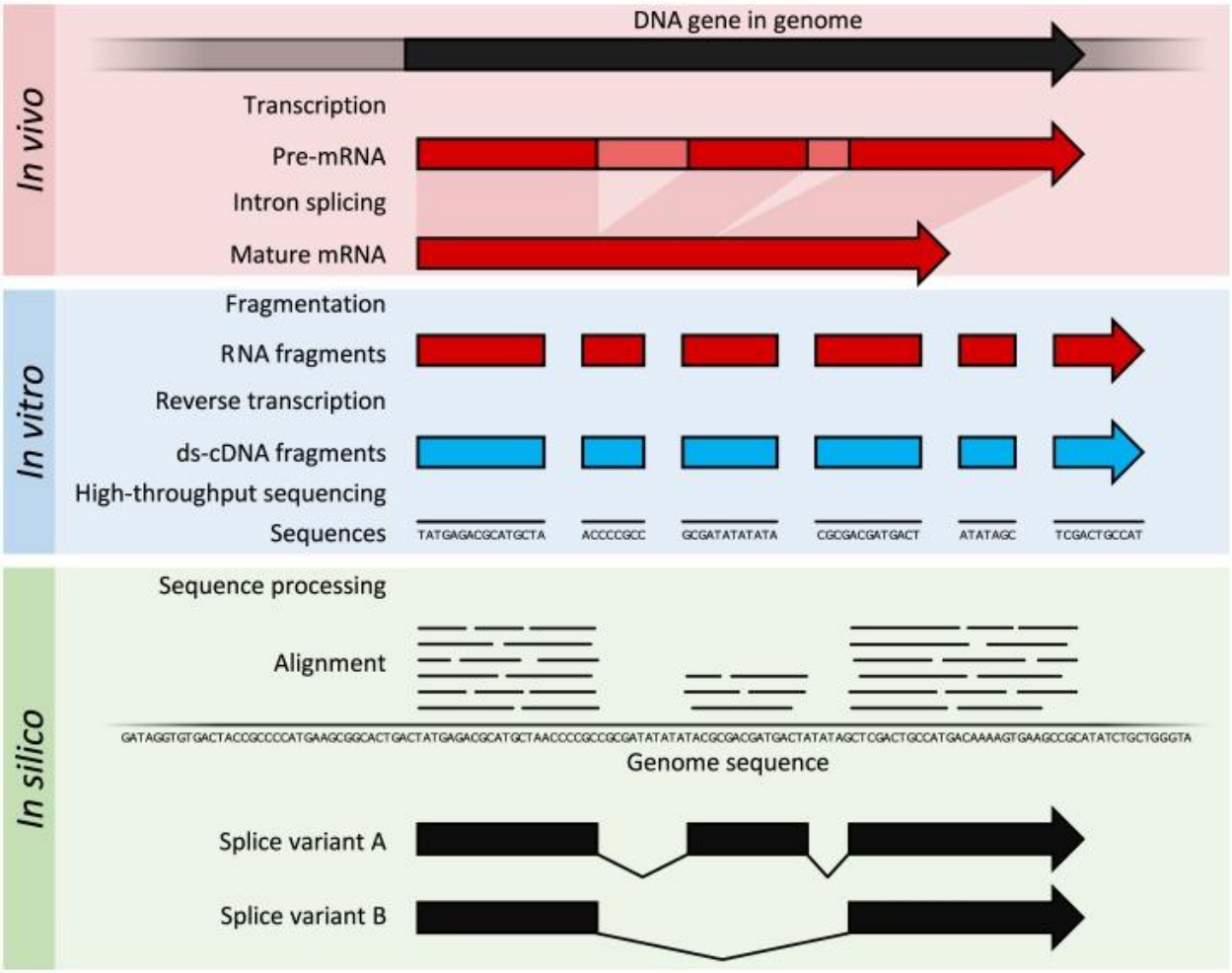

Figure 9. RNA-sequencing workflow. Diagram illustrating how genomic DNA gives rise to RNA in living organism (top), which is then extracted and fragmented to generate RNA-seq samples (middle), followed by reorganizing the sequencing data and determine genes expressed (Lowe et al., 2017).

1.8 Agilent Seahorse XF96

The Agilent Seahorse platform (Santa Clara, California) is an apparatus that allows for real-time observations mitochondrial bioenergetics (Caines et al., 2022; Wu et al., 2007). Changes in mitochondrial function are associated with disease states; however, functional measures of bioenergetic function are often limited to secondary methods via fluorescent reporters of activity or damage (Connolly et al., 2018). Seahorse assays allow for discrete observation of

mitochondrial function by measuring the oxygen consumption rate (OCR) and extracellular acidification rate (ECAR) of cells or isolated mitochondria *in vitro* (Horan et al., 2012). OCR and ECAR data are reflective of mitochondrial oxidative phosphorylation and glycolysis. Numerous kits are commercially available to evaluate particular aspects of mitochondrial function ranging from ATP rate, oxidative stress, and metabolic profiling. Of relevance to the work presented herein, the Mito Stress Test has become a recent gold standard for evaluations of mitochondrial respiration.

The Seahorse SF Mito Stress Test assay allows for real-time, live observations of OCR and ECAR measures through the utilization of mitochondrial toxins to drive particular mitochondrial responses (Fig. 10A). Cells or isolated mitochondria are first placed within 24 or 96 well plates and prepped according to the particular needs of the experiment. Once prepped, the plate is placed within the Seahorse XF analyzer to establish and measure basal respiration (3 times, over the course of 5-8 minutes, Fig. 10B). Oligomycin is then added to each well through an injector port, ceasing function of ATP synthase (complex V). The drop in OCR is measured and reflects changes in ATP production and uncoupled basal respiration attributed to proton leaks along the mitochondrial membrane. Addition of phenylhydrazone (FCCP) is an uncoupling agent used to collapse the proton gradient across mitochondrial membranes, causing complex IV to reach its maximal respiration as electron flow remains uninhibited. The spare respiratory capacity, or ability for mitochondria to respond to changes in ATP demand, can be derived from the difference between maximal and basal respiration. Finally, rotenone and antimycin A are added to inhibit complex I and III, respectively. Altogether, the combinatorial effect of toxins ceases mitochondrial function and allows measures to evaluate respiration that persists outside of the mitochondrial space.

While OCR responses are the typical measure for the Mito Stress Test and reflect mitochondrial oxidative phosphorylation, ECAR recordings during the same series of events serve as measures of glycolytic function (Sonntag et al., 2017) (Fig. 10C). Similar to OCR measures, the period of basal respiration is measured as basal glycolysis. The period between oligomycin and FCCP application is reflective of glycolytic capacity. Glycolytic reserve can then be extrapolated from the difference between glycolytic capacity and basal glycolysis. However, it is important to note that glycolytic measures during the Mito Stress Test may not be entirely reflective of cellular glycolysis. Specifically, the Mito Stress Test does not provide an injection of glucose to more accurately assess cellular utilization of the substrate. Instead, it is recommended to use the Glycolysis Stress Test to provide a more accurate portrait of cellular glycolysis. Taken together with OCR data, one is able to better understand how experimental manipulations by genes, treatments, or environmental hazards may influence specific mitochondrial functions.

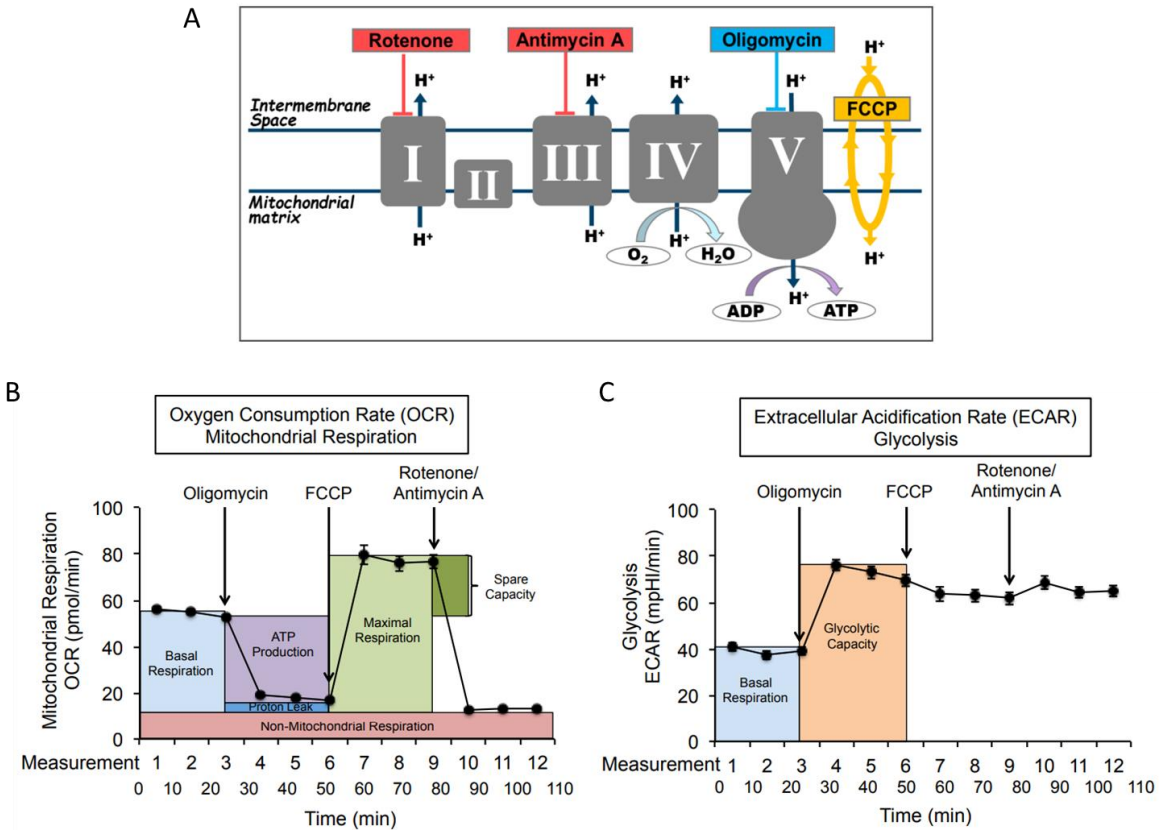

Figure 10. Agilent Seahorse XF principals. (A) Utilization of specific mitochondrial toxins allows for functional interference of complex proteins that facilitate ATP energy production. Oligomycin decreases OCR and ATP production by inhibition of the complex IV ATP synthase, FCCP disrupts membrane potential and induces maximal respiration to restore the collapsed proton gradient, while rotenone/antimycin A together further inhibit complex I and III, respectively, to cease mitochondrial function. (B) The changes induced can be measured in a typified change in oxygen consumption, reflective of oxidative phosphorylation. (C) Similarly, glycolytic function can be assessed as measured by extracellular acidification of wells (Sonntag et al., 2017).

Chapter 2: Review of Literature

2.1 CD38 in cellular function, bioenergetics, and age-related changes

CD38 has become a topic of interest due to its functional relationship with immune function, bioenergetics, and aging. CD38 was first discovered in 1980 (Deaglio et al., 2001) as a lymphocyte cell marker. In the following decades, CD38 research was largely focused understanding its function as a mediator of immune cell differentiation, activity, and inflammatory signaling (Piedra-Quintero et al., 2020). It was also during this time that CD38 was determined to act as an NADase that generates cADPR and ADPR molecules from NAD to serve as mobilizers of intracellular Ca^{2+} (Howard et al., 1993). This initial revealing of the association between CD38 and bioenergetic substrate modulation eventually collided with the field of aging, where it was determined that NAD levels decrease as humans (Massudi et al., 2012) and rodents (Braidy et al., 2011) advance in age. It was only as recent as 2016, that the relationship between CD38 expression and age-related NAD decline was experimentally evaluated. Using aged mice, Camacho-Pereira et al. found that during aging (5-32 months), animals had increased CD38 protein content in liver, adipose, spleen, and skeletal muscle tissue (Camacho-Pereira et al., 2016). Alongside increased protein content within these tissues, it was also determined that CD38 NADase activity was increased and reduced mitochondrial oxygen consumption by up to 70% in 24-month-old animal samples. Importantly, evaluations of the remaining NADase family members, PARP1 and SIRT1, did not show similar increases in protein content, suggesting that NAD decline was most associated with CD38-related changes. Altogether, these findings helped set the stage for further examination of the role of CD38 expression as it relates to cellular states, bioenergetics, and relationship to age-related disease.

2.2 CD38 as a contributor to neuronal, astrocytic, and glial function

Human CNS cell data indicates that glial cells are the primary *CD38* expressing cells (Kelley et al., 2018). Astrocyte, oligodendrocytes, microglia and neurons all have demonstratable expression in the human brain in the respective rank order. *CD38* in human and rodent also demonstrates differences in expression across regions and is most associated with cells within the basal ganglia (Kelley et al., 2018; Mizuguchi et al., 1995; Sjöstedt et al., 2020; Yamada et al., 1997). Currently, experimental human data relating to CD38 in the CNS is limited to the aforementioned histological studies evaluating expression. *Cd38* knockout model animals, however, have been useful in determining how its typical expression promotes CNS cell health and function.

In neurons, for example, $Cd38^{-/-}$ mice were found to have impaired dendritic organization in the hippocampus and visual cortex (Nelissen et al., 2018). Similar to findings in immune cells studies, CD38 production of cADPR was found to activate ryanodine receptor, initiate intracellular Ca^{2+} release, and stimulate neurotransmitter and oxytocin release (Higashida et al., 2007; Higashida et al., 2012; Jin et al., 2007). Furthermore, $Cd38^{-/-}$ have cognitive deficits as indicated by impairments in hippocampal-dependent learning and memory (Morris water maze), social recognition (3-chamber task), and novel object recognition when compared to cage-matched, $CD38^{+/+}$ peers (Kim et al., 2016).

It is important to note that the majority of neuron-based studies utilize global knockout (KO) of *Cd38*, a gene largely expressed by glia. Recently, one group utilized an astrocyte-specific, tamoxifen-inducible $Cd38^{flox/flox}$, $GLAST^{CreERT2}$ animal model, finding that the reported deficits in social memory were recapitulated in mice with astrocytic *Cd38* knockdown (Hattori et al., 2023). The impaired social memory phenotype was dependent upon the timing of *Cd38* knockdown

(KD), as deficits were only significant in animals with KD prior to the postnatal maturation period (approximately P14-30 in mice, P10-14 KD) and not when in animals with adulthood KD (P42 KD). Additionally, cell autonomous and non-cell autonomous changes were reported in astrocytic *Cd38* postnatal KD animals. KD astrocytes had reductions in canonical astrocytic genes, *Gfap, s100β,* and *Cx43*, while proteomic analysis of *Cd38*$^{-/-}$ astrocyte primary mouse cultures found reductions in the excitatory-synapse promoting protein SPARCL1 (Gan & Südhof, 2020). Postnatal astrocytic loss of CD38 also altered neuronal dendritic structures and reduced colocalization of synaptic markers (VGLUT1/PSD95) within pyramidal neurons of the prefrontal cortex, indicating decreased presence of functional synapses (Hattori et al., 2023). These recent findings reflect some of the strongest evidence for the significance of glial expression of CD38, as they represent the first instance of cell-specific manipulations *in vivo*. Interestingly, other *in vivo* findings concerning astrocytes have determined that CD38 function facilitates mitochondrial transfer (Wang et al., 2020), a feature recapitulated *in vitro* using human astrocytes (Sun et al., 2019). Similarly, previous glial-centric evaluations regarding the biological significance of CD38, however, paved the way for current research efforts. Altogether, astrocyte-based findings implicate CD38 function as a facilitator of neuron-glia interaction that impart benefit with expression and detriment in loss.

CD38 function in the brain is still a developing topic, with the majority of research discoveries having been published within the last decade. It is largely unknown how CD38 contributes to oligodendrocyte function; however, findings indicate that astrocytic expression of *CD38* facilitates oligodendrocyte cell differentiation in development (Hattori et al., 2017) and influences oligodendrogliopathy in models of metabolic dysfunction (Langley et al., 2021). In microglia, CD38 function has been found to be largely similar to that of peripheral immune cells;

namely, that CD38 expression is associated with inflammatory events and induce phenotypes associated with cytokine production (Wang et al., 2017). Figure 11 summarizes recent findings regarding how CD38 functionally contributes to major CNS subtypes. Given the limited information regarding CD38 as it relates to CNS cells, it is imperative that research efforts evaluate cell specific processes regulated by its expression.

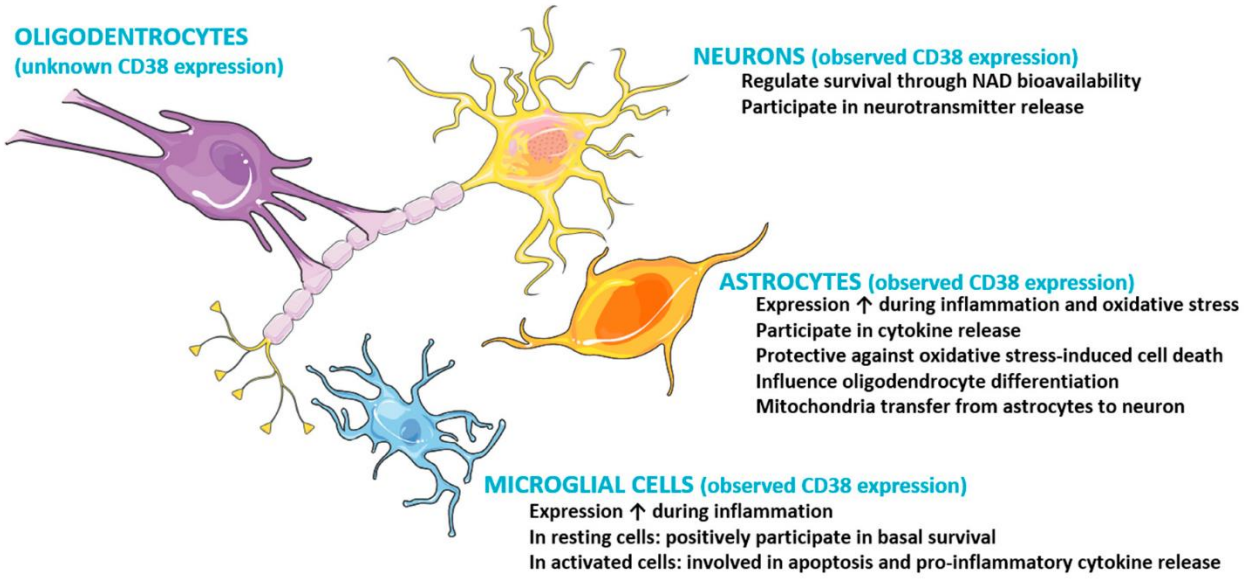

Figure 11. Summary of CD38-related findings in CNS cells. Recent evidence has helped elucidate how CD38 expression plays specific roles within neurons and major glial cell populations. Astrocytes in particular have been the most recent focus given their relatively high *CD38* expression (Guerreiro et al., 2020).

2.3 CD38 deficiency as it relates to Parkinson's disease

Recently, a meta-analysis of human brain and blood sample proteomic datasets was used to identify potential mediators of NDDs (Ge et al., 2023). The authors found increased CD38 in the brain correlated to decreased PD risk. This determination complements genome- and transcriptome-wide association studies (GWAS, TWAS) meta-analysis findings identifying

increased PD risk for individuals with SNPs that cause decreases in *CD38* expression (Chen et al., 2014; Kia et al., 2021; J. Li et al., 2019; Sharma et al., 2012; Zhou et al., 2023). Importantly, these recent risk-association studies utilize various methods and datasets and continue to identify reductions in *CD38* as a risk factor in the development of PD. In humans, single-nucleotide polymorphism (SNP) rs11724635 within the *CD38* locus has been implicated PD susceptibility in some populations (Chen et al., 2014; Hayete et al., 2017; Sharma et al., 2012). Our laboratory group has a standing collaboration with Dr. Rita Cowell, who determined via meta-analysis of publicly available data, that rs11724635 is associated an approximate 50% downregulation of *CD38* in basal ganglia regions associated with PD pathology (Fig. 12). These preliminary findings indicate that SNP rs11724635 resides in the locus shared by three genes (*FAM200B, BST1*, *CD38*), however only *CD38* expression changes are associated with the SNP (Fig. 12A). Furthermore, rs11724635 is associated with an estimated 50% reduction in *CD38* expression, preferentially in the BG brain region (Fig. 12B). These preliminary data serve as the foundation by which we further sought to interrogate the role of CD38 within models that recapitulate observable changes in humans as they relate to PD risk.

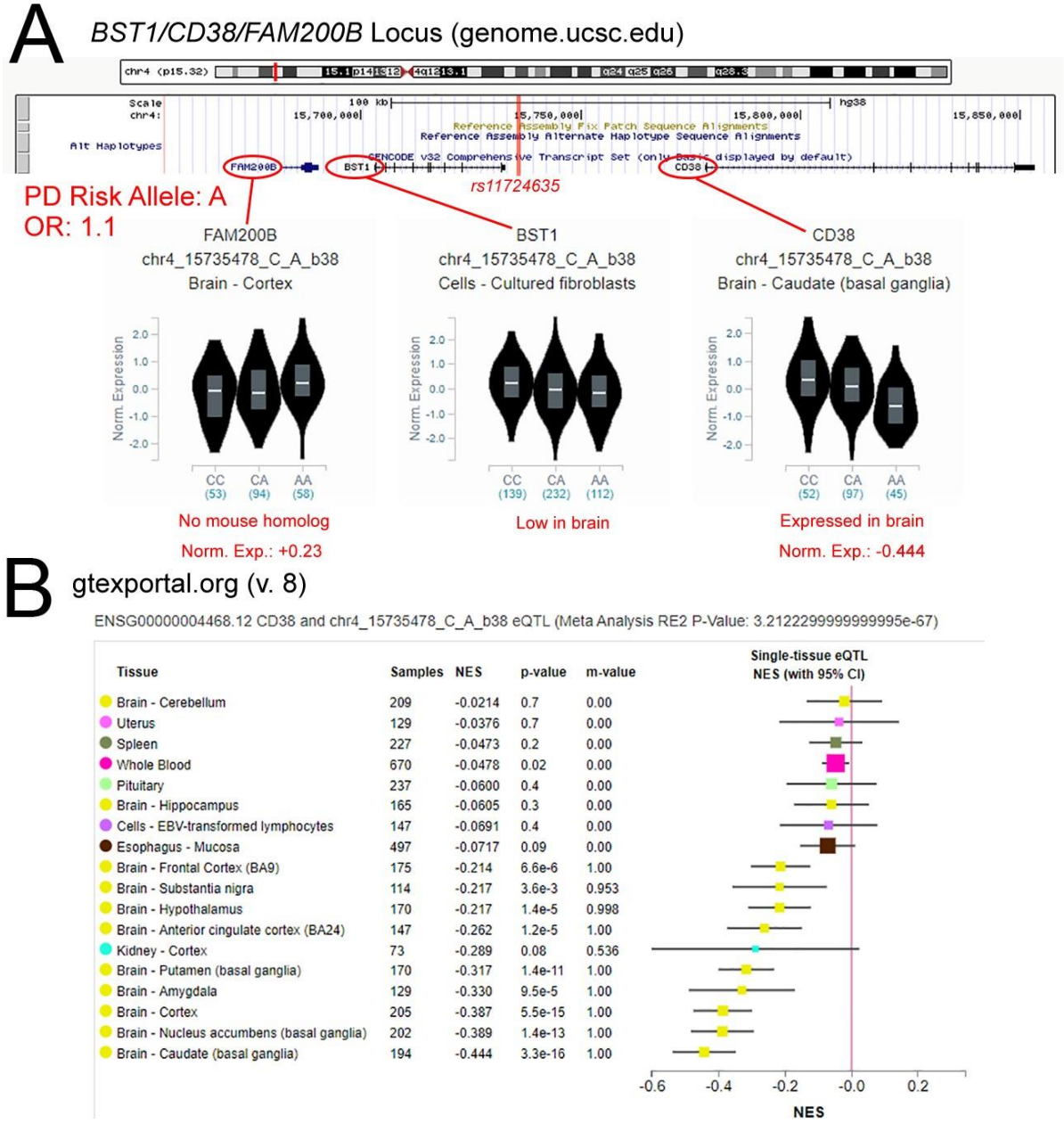

Tissue	Samples	NES	p-value	m-value
Brain - Cerebellum	209	-0.0214	0.7	0.00
Uterus	129	-0.0376	0.7	0.00
Spleen	227	-0.0473	0.2	0.00
Whole Blood	670	-0.0478	0.02	0.00
Pituitary	237	-0.0600	0.4	0.00
Brain - Hippocampus	165	-0.0605	0.3	0.00
Cells - EBV-transformed lymphocytes	147	-0.0691	0.4	0.00
Esophagus - Mucosa	497	-0.0717	0.09	0.00
Brain - Frontal Cortex (BA9)	175	-0.214	6.6e-6	1.00
Brain - Substantia nigra	114	-0.217	3.6e-3	0.953
Brain - Hypothalamus	170	-0.217	1.4e-5	0.998
Brain - Anterior cingulate cortex (BA24)	147	-0.262	1.2e-5	1.00
Kidney - Cortex	73	-0.289	0.08	0.536
Brain - Putamen (basal ganglia)	170	-0.317	1.4e-11	1.00
Brain - Amygdala	129	-0.330	9.5e-5	1.00
Brain - Cortex	205	-0.387	5.5e-15	1.00
Brain - Nucleus accumbens (basal ganglia)	202	-0.389	1.4e-13	1.00
Brain - Caudate (basal ganglia)	194	-0.444	3.3e-16	1.00

Figure 12. Parkinson's associated SNP rs11724635 in the *FAM200B/BST1/CD38* locus reduces *CD38* expression. (A) Identified PD-risk SNP rs11724635 is associated with decreased *CD38* expression, but leaves nearby genes *FAM200B* and *BST1* unaffected (Kent et al., 2002). (B) Regional changes in *CD38* expression as induced by rs11724635 indicate that brain regions impacted by PD pathology have reduced mRNA expression (GTEx Consortium, 2020).

2.4 Gaps in Knowledge

Human GWAS-based studies have provided valuable information relating to risk genes that contribute to the manifestation of PD, with recent findings consistently indicating that reductions in CD38 are associated with increased PD risk (Yao et al., 2021; Zhou et al., 2023). Interestingly, CD38 fits within our understanding of what induces greatest risk of PD, namely age-related changes that affect cellular bioenergetics. Within the brain, astrocytes are the primary *CD38* expressing cells, yet few papers have evaluated the functional relevance within astrocytes. Studies published thus far typically utilize complete knockout models to investigate the biological consequence of CD38 loss; however, these models do not recapitulate human health and somewhat lack in translational relevance as it relates to disease risk. To more strongly evaluate the translational relevance of CD38, we sought to examine astrocytic gene expression and function within the context of CD38-deficient model that recapitulates human SNP variants relating to PD risk. In this way, we aim to enhance knowledge as it pertains to astrocytic contributions to PD risk in the context of the risk gene, *CD38*.

Chapter 3: Experimental Design

3.1 Experiment 1: Identification of *Cd38* expression cell-type specificity

Our initial experiments set out to confirm *Cd38* enrichment within astrocytes of murine origin. Human data evaluating the expression profiles of CNS cells supports the notion of *CD38* glial enrichment (Fig. 13, (Kelley et al., 2018). We sought to confirm this within our own animal models, first by analysis of publicly available datasets, and second by way of immunofluorescence-based methods. DropViz is a readily available dataset containing transcriptional profiling of murine CNS cells (Saunders et al., 2018). Utilizing available datasets, a meta-analysis was performed to evaluate the mouse *Cd38* expression by cell type and region. Confirmatory evaluations of meta-analysis results were made using $Cd38^{+/+}$ wild-type mice compared to $Cd38^{-/-}$ knockouts. To achieve this, a fluorescence *in situ* hybridization (FISH) approach was used to determine if astrocytes within basal ganglia regions had enrichment of *Cd38* transcriptional markers that colocalized with astrocytic indicators. Additionally, confirmations were made using reverse-transcription polymerase chain reaction (RT-PCR) methods to evaluate tissues from $Cd38^{+/+}$ and $Cd38^{-/-}$ samples.

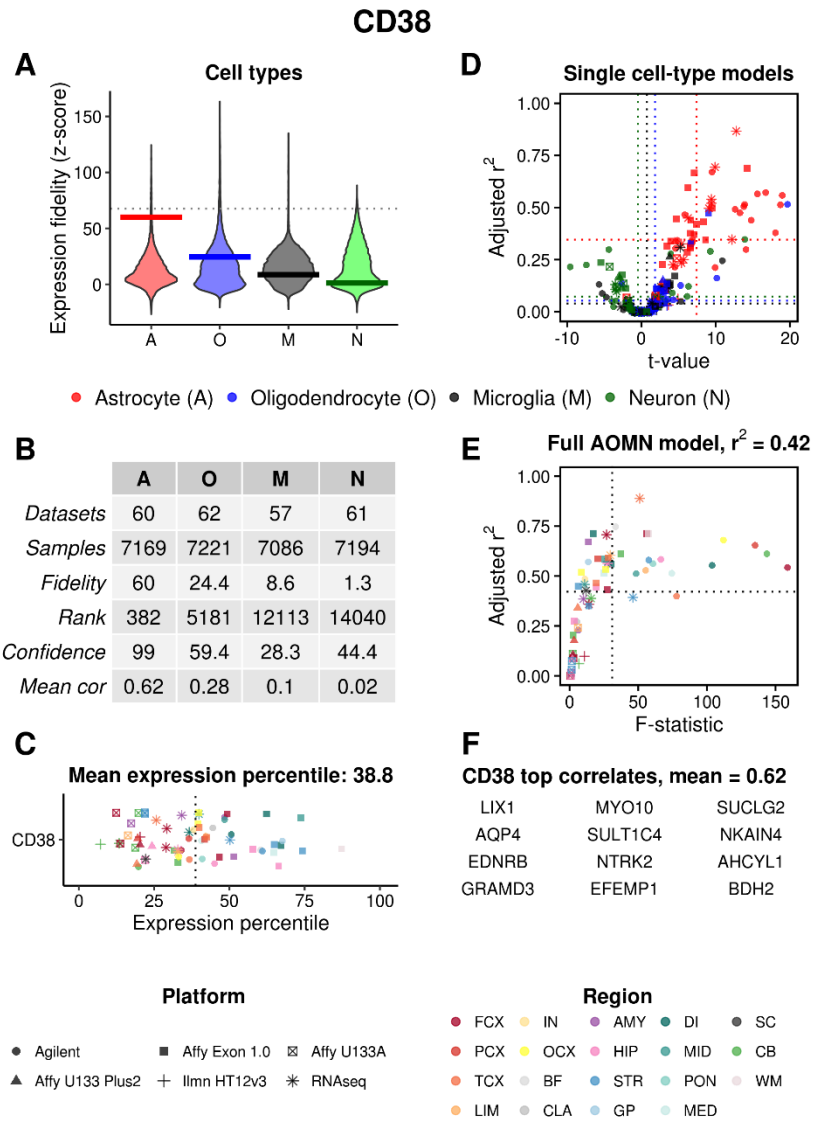

Figure 13. *CD38* is most enriched in astrocytes and the midbrain. (A) Genome-wide distributions of expression fidelity for CNS cells over all analyzed samples. The horizontal line denotes the expression fidelity of the *CD38* for each cell type. The dashed horizontal line indicates the threshold above which all fidelity scores had Confidence = 100. (B) Table containing information on data used to produce the distributions in (A). (C) Mean expression percentile ranks of the *CD38* in all analyzed datasets. Platform is indicated by shape (bottom left) and CNS region by color (bottom right). (D) Modeling results for expression levels of *CD38* as a function of variation in the inferred abundance of individual cell types. Simple linear regression is used to predict gene expression levels as a function of estimated CNS cell type abundance in all human regional datasets containing the *CD38*. (E) Modeling results for expression levels of *CD38* as a function of variation in the inferred abundance of all cell types. Multiple linear regression is used to predict gene expression levels as a function of CNS cell type abundance in all human CNS regional datasets containing the *CD38*. (F) The top 12 genes ranked by their aggregate correlation to *CD38* expression levels over all analyzed samples (Kelley et al., 2018).

3.2 Experiment 2: Evaluation of NAD and NAM content in CD38-deficent mice

Given that CD38 protein function specifically modulates NAD/NAM balance in tissues, we sought to explore how deficiency may alter the presence of these crucial bioenergetic substrates. To explore this, late-adulthood mouse (12 months) brains were microdissected for isolation of striatum and midbrain tissues and prepared for proton nuclear magnetic resonance (^{1}H NMR) analysis. ^{1}H NMR allows for separation, detection, and quantification of sample contents by evaluation of the chromatic signatures of compounds within the sample (Fig. 14). For our purposes, tissue samples were isolated and homogenized in a chloroform-based solvent. Samples were spun down, and the upper liquid supernatant layer containing NAD and NAM were taken for ^{1}H NMR applications. Spectral readings were taken for detection of NAD and NAM for each sample run to indicate if there were particular shifts in these bioenergetic substrates across genotypes. Finally, an NAD/NAM ratio was generated from acquired readings to provide information relating to shifts in substrate balance amongst *Cd38*$^{+/+}$, *Cd38*$^{+/-}$, and *Cd38*$^{-/-}$ animals.

CD38 protein function also modulates NAD/NAM balance in tissues, therefore, we sought to explore how deficiency may alter the presence of these crucial bioenergetic substrates. To explore this, late-adulthood mouse (12 months) brains were microdissected for isolation of striatum and midbrain tissues and prepared for proton nuclear magnetic resonance (^{1}H NMR) spectroscopy. NMR methods allow for detection of specific electromagnetic signatures within samples to identify molecular compounds from one another (Fig. 14). In the simplest terms, radio frequency is applied to samples while the frequency absorption is detected to identify differences in nuclear resonance, indicative of particular chemical compositions. ^{1}H NMR relies upon detection of hydrogen protons within biological functional groups to record spectra and allow for determinations of structural composition. For our purposes, tissue samples were

isolated and homogenized in a chloroform-based solvent. Samples were spun down, and the upper liquid supernatant layer containing NAD and NAM were taken for ^{1}H NMR applications. Spectrum readings were taken for detection of NAD and NAM for each sample run to indicate if there were particular shifts in these bioenergetic substrates across genotypes. Finally, an NAD/NAM ratio was generated from acquired readings to provide information relating to shifts in substrate balance amongst *Cd38*$^{+/+}$, *Cd38*$^{+/-}$, and *Cd38*$^{-/-}$ animals.

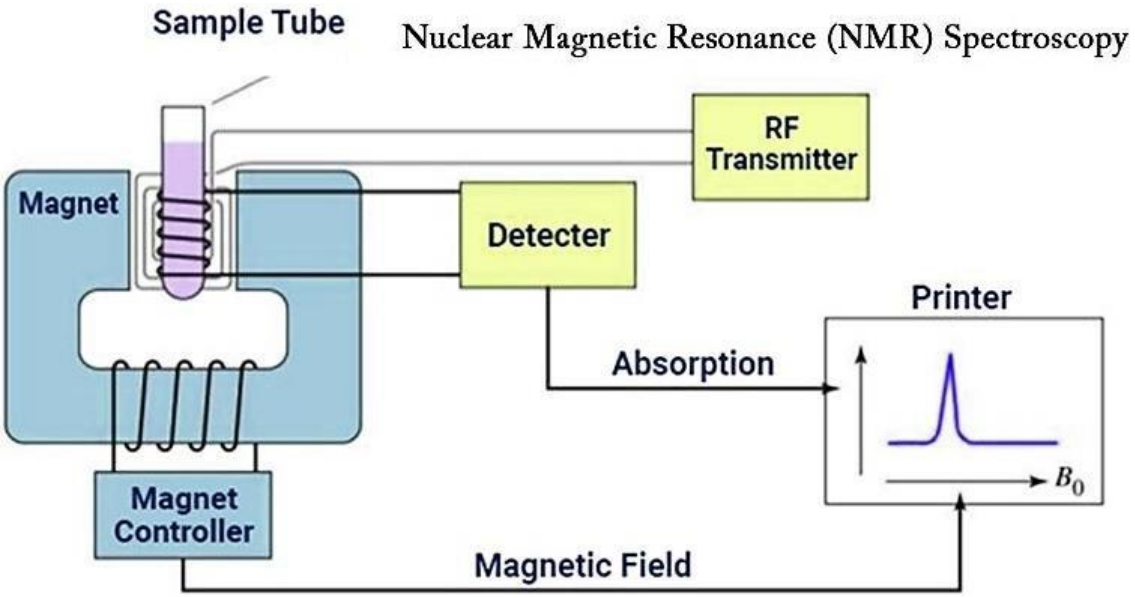

Figure 14. General ^{1}H NMR workflow. Generally, samples are placed within a magnetic apparatus containing a radio frequency (RF) transmitter and detector. Magnetic force is applied alongside RF transmission, where absorption data is measured and transferred to a computer for interpretation with software programs (Patel & Chudasama, 2021).

3.3 Experiment 3: Determination of CD38-deficient astrocytes expression profiles

Currently, evidence suggests that a relationship exists between human SNPs that reduce *CD38* expression and the modulation of PD risk (Yao et al., 2021; Zhou et al., 2023). Additional

works also indicate that astrocytes display the highest *CD38* expression in the CNS (Saunders et al., 2018) and are particularly transcriptionally and functionally affected by changes in its expression (Hattori et al., 2017; Hayakawa et al., 2016). Utilizing a cell-specific isolation approach paired alongside next-generation RNA-sequencing, the following experiment sought to examine how changes *Cd38* expression in mice models alters astrocytic gene expression may reflect changes in neurodegenerative risk. Late-adulthood mice were used to represent the prodromal period believed to precipitate cellular changes associated with later PD diagnosis (Mahlknecht et al., 2022). Late-adulthood $Cd38^{+/+}$, $Cd38^{+/-}$, and $Cd38^{-/-}$ mice (approximately 12 months of age) basal ganglia were collected for MACS isolation of astrocytic populations. RNA was extracted and RNA-seq libraries were prepared from samples for Nova-seq 6000 next-generation sequencing. From the acquired dataset, differentially expressed gene (DEG) were identified from $Cd38^{+/+}$ to $Cd38^{+/-}$ and $Cd38^{+/+}$ to $Cd38^{-/-}$ pairwise comparisons. DEGs were used in additional gene ontology (GO) pathway analyses to find functionally relevant pathways that may further be examined (Fig. 15).

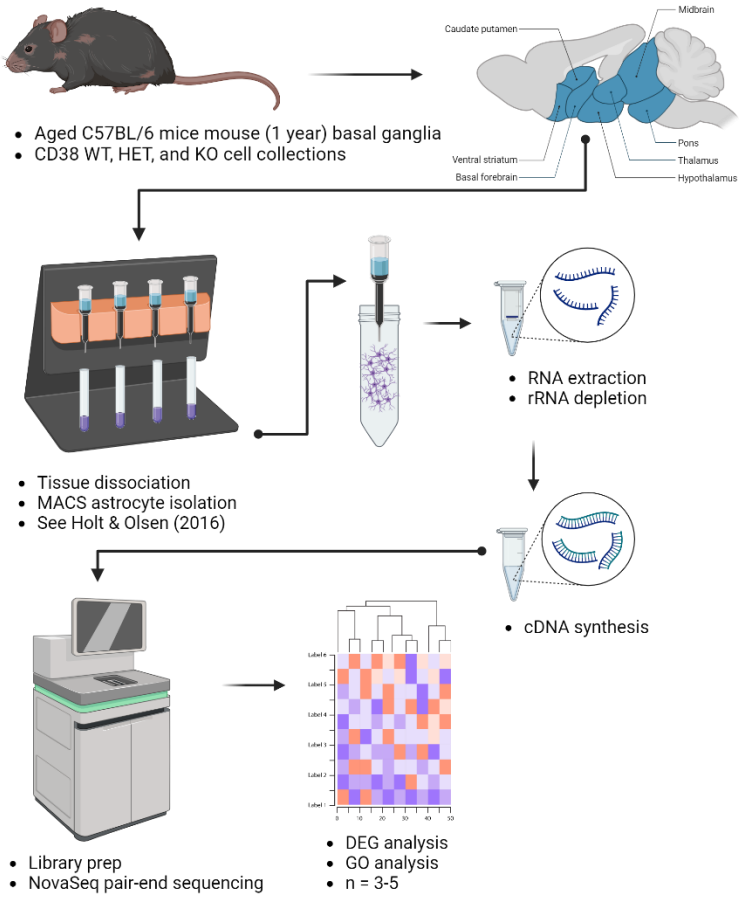

Figure 15. RNA-sequencing as it relates to the research presented herein. Diagram illustrating RNA-seq workflow relevant to data within this dissertation (Biorender, 2023).

3.4 Experiment 4: Evaluation of mitochondrial-related changes in basal ganglia

Mitochondrial dysfunction often lies at the heart of neurodegenerative phenotypes, so we chose to utilize a series of assays to explore basal ganglia mitochondrial function. Based on the relationship between CD38 enzymatic activity and bioenergetics, we selected three checkpoint enzymes of interest to evaluate if changes exist within specific mitochondrial events (Fig. 16) between *Cd38*$^{+/+}$, *Cd38*$^{+/-}$, and *Cd38*$^{-/-}$ animals. Cytochrome *c* oxidase (COX) activity was measured as an indication of electron transport chain (ETC) function. Also known as complex IV along the ETC within the inner mitochondrial membrane, COX plays a crucial role in

maintaining the electrochemical gradient that allows H^+ proton flow to drive ATP production. Pyruvate dehydrogenase (PDH) enzymatic activity measures were taken to assess the state of the tricarboxylic acid cycle (TCA). PDH catalyzes the conversion of pyruvate into acetyl-CoA for downstream generation of NADH, $FADH_2$, and ATP from the TCA cycle. Lastly, we took measures of citrate synthase (CS) as an indicative measure of intact mitochondria within samples (Larsen et al., 2012).

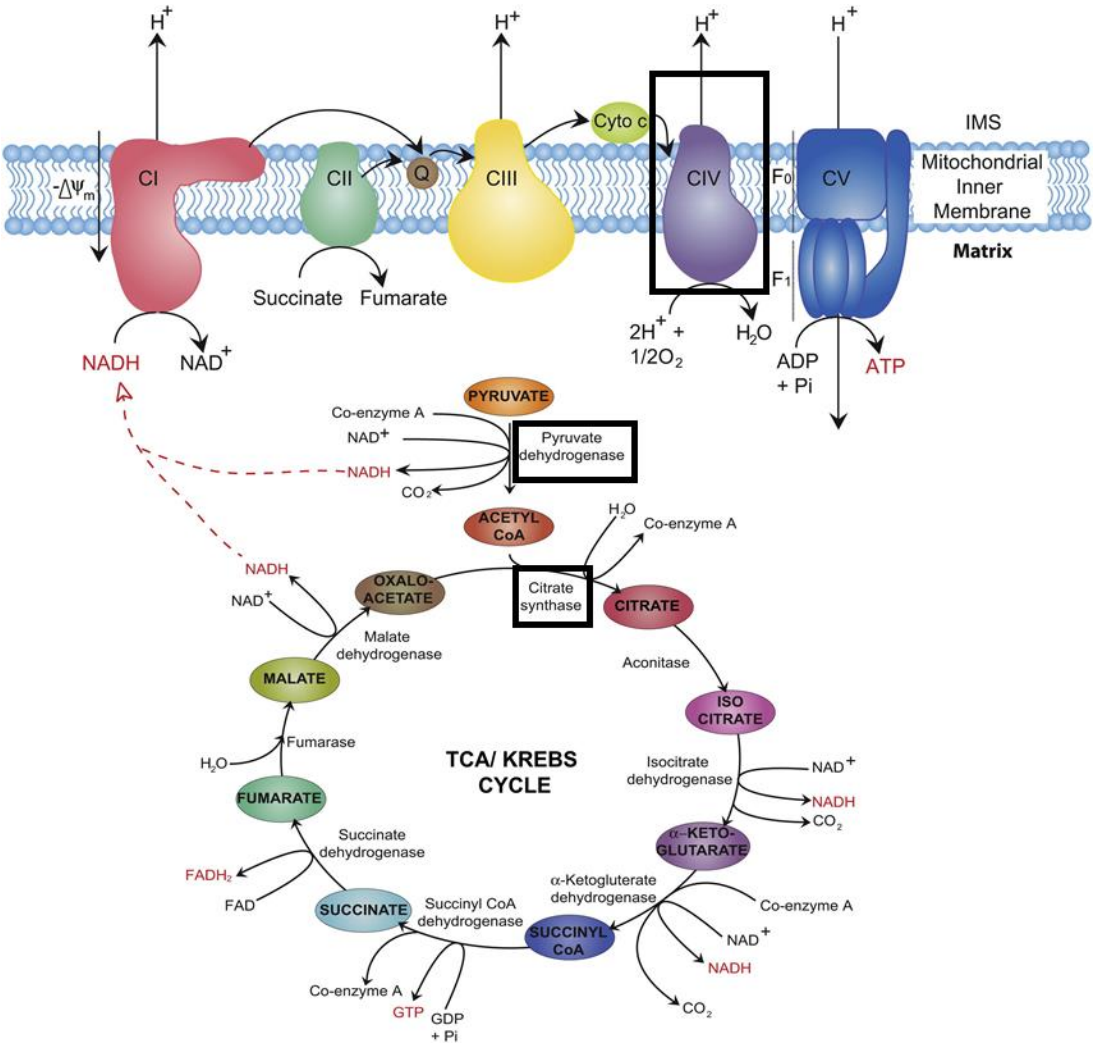

Figure 16. Major enzymes of interest for mitochondrial determinations. We selected three checkpoint enzymes of interest to evaluate if changes exist within specific mitochondrial events. Cytochrome C oxidase, also known as complex IV (top box), is essential for mitochondrial inner membrane ETC-mediated ATP production. Pyruvate dehydrogenase (middle box) activity is amongst the most important enzymes within the TCA cycle, allowing for production of acetyl-CoA, NADH, and $FADH_2$ within the mitochondrial matrix for later use in ETC-ATP production. Citrate synthase (bottom box) is another enzyme important to TCA cycle function and often serves as a measure of mitochondrial content (Osellame et al., 2012).

3.5 Experiment 5: Assessing bioenergetic function of CD38-deficient astrocytes

We further assessed the relationship between bioenergetic function and *Cd38* expression by inclusion of Agilent Seahorse XF96 Mito Stress Test measures. As previously described (see Chapter 1.8), the Seahorse platform allows for evaluation of oxygen consumption and

extracellular acidification rates to indicate changes in oxidative phosphorylation and glycolytic function, respectively. Astrocytes were evaluated given that they display the highest *CD38* expression profile in the CNS. We sought to understand if CD38 deficiencies had a particular effect on astrocytic bioenergetic function by utilizing an *in vitro* model Mito Stress Test paradigm. In short, $Cd38^{+/+}$, $Cd38^{+/-}$, and $Cd38^{-/-}$ pups were used to generate primary astrocyte cultures and then grown to a matured phenotypic state (Schildge et al., 2013). Primary astrocytes were then prepped for Seahorse XF96 Mito Stress Test evaluations of mitochondrial function. Once the paradigm was completed, culture dish protein content was assessed by bicinchoninic acid assay for final normalizations of data. Data was sorted and organized according to Agilent parameters and similar to methods used by others (Sonntag et al., 2017; Wu et al., 2007).

Chapter 4: Methods

4.1 Animals

All animals were maintained in accordance with Virginia Tech and University of Alabama at Birmingham veterinary and IACUC protocols respective to each institution. Mice were housed in facilities on 12-hour reverse light/dark cycle with ambient temperature and humidity maintained at all times across experiments. Mice had access to purified water and standard chow *ad libitum*. Animal health was monitored daily by veterinary staff with all efforts taken to minimize pain and distress. All mice used were bred from the C57BL/6 strain. *Cd38* knockout mice (B6.129P2-Cd38tm1Lnd/J, The Jackson Laboratory) have a global disruption in exons 2-3 of the Cd38tm1Lnd allele, resulting in heterozygous mice ($Cd38^{+/-}$) with an approximate 50% decrease in CD38 presence and knockout animals ($Cd38^{-/-}$) having nearly no *Cd38* transcript and CD38 protein (Cockayne et al., 1998). Animal breeding utilized pairs of $Cd38^{-/-}$ male and female mice to generate animals for experiments . All animal comparisons were made against litter and/or peer matched controls. Samples were blinded for analysis to reduce potential biases.

4.2 Data Curation

Single-nucleotide polymorphism *rs11724635* (chr4:15737101), in the region of *BST1/FAM200B/CD38* localized to chromosome 4 (Kent et al., 2002), was previously identified as statistically significantly associated with PD risk (Nalls et al., 2019). Relative expression profiles for *BST1*, *FAM200B*, and *CD38* mRNA in human tissues were explored by genotype at that locus using GTExPortal version 8 (GTEx Consortium, 2020). Cell type-specific expression data for human cortex was explored using the Human Protein Atlas database single cell database (Karlsson et al., 2021), the Allen Brain Atlas (Allen brain atlas, 2006) or the Oldham Brain

Expression Correlates database (Kelley et al., 2018). Cell type and region-specific transcriptional data for mouse was downloaded from Dropviz.org; data were normalized to the total unique molecular identifier (UMI) hits for each cell subcluster and multiplied by 100,000 similar to the browser tool. Cell types were categorized based on criteria described in by others (Saunders et al., 2018).

4.3 ^{1}H NMR Analysis

Striatum and midbrain samples from *Cd38*$^{+/+}$, *Cd38*$^{+/-}$, and *Cd38*$^{-/-}$ mice were microdissected then pooled into 1.5 mL microcentrifuge tubes, snap frozen in liquid nitrogen, and stored at -80 ºC. Tissues were placed in 15 mL tubes and 4 mL of 80% ice-cold methanol per gram tissue was added. Tissues were homogenized using homogenizer pestles, followed by grinding for 30 s. 2 mL chloroform per gram tissue was then added to each sample, followed by homogenization for 30 s. An additional 2 mL of chloroform and 2 mL HPLC grade water per gram tissue was added to each sample. Samples were incubated on ice for 30 min and centrifuged at 4,000g at 4 ºC for 30 min. The upper aqueous layer of the supernatant containing metabolites was extracted for NMR analysis. Samples were dried using a heat block at 42ºC followed by lyophilization using a freeze dry system. Samples were then dissolved in 0.6 mL D_2O (99.96% D) and transferred to NMR tubes. Tetramethylsilane (0 ppm) was added as reference.

Experiments were conducted at 25ºC using a Bruker Avance III-HD spectrometer (^{1}H, 600 or 850 MHz) equipped with cryogenic triple-resonance probes. Data were processed and analyzed with TopSpin (v. 4.2). ^{1}H spectra were recorded with 32k complex points, acquisition time of 1.6 s, recovery delay of 2.0 s, and pre-saturation of the residual HDO signal. A 0.5 Hz exponential apodization was applied and data size doubled by zero-filling before Fourier transformation.

Each spectrum was phased manually, and automatic baseline correction was achieved using 2nd order polynomial in the region 0.5–9.5 ppm. Integral intensities were scaled identically for all spectra within each series. Final integration values for metabolites were the average of integration values obtained for a set of five samples.

The High-Field NMR facility at the University of Alabama at Birmingham was established through the NIH (1S10RR026478) and is supported by the UAB Comprehensive Cancer Center (NCI grant P30 CA013148).

4.4 MACS Astrocyte Isolation

Astrocytes were isolated from *Cd38*$^{+/+}$, *Cd38*$^{+/-}$, and *Cd38*$^{-/-}$ late-adulthood male mice after 1 year of age (12-14 months, $\bar{x}$ = 13.5 months) utilizing a MACS approach (Holt & Olsen, 2016; Holt, Stoyanof, & Olsen, 2019). BG regions associated with Parkinson's disease pathology (striatum, thalamus, and substantia nigra) were microdissected from brain tissue for cell-specific isolation. Tissue dissociation was performed as previously described (Holt & Olsen, 2016; Holt, Stoyanof, & Olsen, 2019), whereby regions of interest were utilized for MACS. All dissections were performed in modified artificial cerebral spinal fluid (120 mM NaCl, 3 mM KCl, 6 mM $2NaHCO_3$, 11 mM glucose, 5 mM HEPES, 200 µM CaCl, 1 mM MgCl) containing neuronal activity inhibitors (20 µM CNQX, 20 µM D-AP5, 295-299 mOsm) to reduce glutamate excitotoxicity. Briefly, BG tissues were removed then sectioned into 1mm pieces, followed by papain dissociation (Worthington Biochemical Corporation, cat. LK003150). A series of centrifugation (4°C, 300 RCF, 3-5 minutes, Eppendorf cat. 58048R) and PBS wash steps were performed to retain cell containing tissue pellets. Supernatants were discarded and pellets were resuspended in 0.5% w/v bovine serum albumin (Millipore Sigma, cat. A7030) in PBS for

filtration (70 µm, Fisher Scientific cat. 22-363-548) and attainment of BG cellular fractions. Cell fractions were then treated with Miltenyi Biotec Microbeads to remove contaminating endothelial cells (cat. 130-097-418) and myelin/oligodendrocytes (cat. 130-096-433). Samples were incubated in microbeads for 10 minutes at 4°C followed by filtering through Miltenyi LS columns (cat. 130-042-401). Samples were then treated with anti-CD31 microbeads (cat. 130-092-263) for 10 minutes at 4°C to selectively isolate microglia by elution of magnetically captured cells for collection. Finally, astrocytes were positively selected using the Miltenyi ACSA-II microbead kit (cat. 130-097-679). Samples were first incubated with an FcR blocking reagent for 10 minutes at 4°C immediately followed by an additional 10-minute incubation at 4°C with anti-ACSA-2 microbeads. After LS column filtration and elution, collected cells were stored in 300 µL Trizol (ThermoFisher Scientific, cat. 15596026) and snap frozen before being placed in storage at -80°C.

4.5 RNA-sequencing

Isolated BG astrocytes were gently lysed by syringe for preparation of RNA isolation (Zymo Research, cat. R2062). RNA was extracted according to the Direct-zol RNA Microprep protocols, including DNA-degradation with DNase I. Total RNA was eluted in 10µL of DNAse/RNAse free water. Samples were submitted to Medgenome for rRNA depletion, quality verifications, library construction, and ultra-low input RNA-sequencing. RNA integrity was determined by Qubit fluorometric quantitation and tapestation bioanalyzer analysis. Collected RNA was then converted to cDNA samples by using the Takara SMART-Seq v4Ultra low Input RNA kit. Generated cDNA was checked for quality utilizing Quibit and tapestation measures,

whereby libraries with marginal pass and higher quality for were used for pair-ended sequencing on the NovaSeq 6000 platform.

4.6 Sequencing Analysis

After RNA-seq data acquisition, bases with quality scores less than 30 were removed and adapters were trimmed from raw sequencing reads by Trim Galore (v 0.6.4). After trimming, only reads with length greater than 30bp were mapped to mm10 by STAR (v 2.7.1a). Raw counts and normalized counts for each gene were outputted by RSEM (v1.2.28). The raw counts were used to identify differentially expressed genes by DESeq2 program (v 1.36.0). Genes with an average TPM greater than 5 in at least one group and a q-value of less than 0.05 were considered as differentially expressed genes. Differentially expressed genes ±1.2 fold-change (FC) were used for GO enrichment with R package clusterProfiler (v4.4.4) and org.Mm.eg.db (v3.15.0) (Yu et al., 2012). DEGs were further evaluated relative to available datasets representation PD risk association studies (Kia et al., 2021; Yao et al., 2021; Zhou et al., 2023), genes involved in reactive oxygen species (ROS) pathways (Rouillard et al., 2016), and mitochondrial function (Rath et al., 2021).

GO chord plots were generated with R package GOplot (v1.0.2) (Walter et al., 2015). GO enrichment terms were then hand-curated into groups relevant to the hallmarks of neurodegenerative diseases (Wilson et al., 2023) and organized by largest fold-change to generate related figures.

4.7 Metabolic Assays

Functional metabolic assays were performed on late-adulthood aged *Cd38*$^{+/+}$, *Cd38*$^{+/-}$, and *Cd38*$^{-/-}$ mice from a convenience sample of male and female BG (8-12 months, $\bar{x}$ = 10.34 months). Whole BG were removed via microdissection and snap-frozen for protein-based applications. Samples were brought to the Virginia Tech Metabolism Core for functional measures of mitochondrial bioenergetics. Measures of pyruvate dehydrogenase, citrate synthase, and cytochrome c oxidase enzymatic activity were assayed utilizing specialized kits (see below). Midbrain samples were homogenized in SET buffer (250 mM sucrose, 1 mM EDTA, 10 mM Tris-HCL, and 1 mM ATP, 7.4 pH) then distributed across assays. Data was normalized to total protein content per sample.

Pyruvate dehydrogenase activity assessed by measuring $^{14}CO_2$ production from [1-^{13}C]-pyruvic acid (Perkin Elmer, Waltham, MA). Samples were first incubated in 0.35 uCi/mL of [1-^{14}C]-pyruvic acid for 1 hour. Next, the media was acidified by 45% perchloric acid for 1 hour to release $^{14}CO_2$ for capture in a tube containing 1M NaOH. After $^{14}CO_2$ capture, the NaOH was transferred to a scintillation vial with 5 mL of scintillation fluid. A scintillation counter (LS 4500, Beckman Coulter) was then used to measure $^{14}CO_2$ presence.

Citrate synthase function was determined by measuring the reduction of DTNB by, a process downstream of citrate synthase's catalyzation of citrate and CoASH from acetyl-coA and oxaloacetate. Homogenized midbrain samples were added in duplicate to 170 µL solution containing Tris buffer (0.1M, pH 8.3), DNTB (1mM, in 0.1M in Tris buffer) and oxaloacetate (0.01M, in 0.1M Tris buffer) at a 1:5 ratio of sample to buffer, respectively. Spectrophotometer (SPECTRAmax ME, Molecular Devices Corporation, Sunnyvale California) readings were taken

after background subtraction. To initiate the reaction, 30 µL of 3mM acetyl-CoA per sample and kept at 37°C. Absorbance (405nm) was measured every 12 seconds for a total of 7 minutes.

Cytochrome *c* oxidase activity was evaluated by measuring the oxidation of rate of ferrocytochrome *c* to ferricytochrome *c* by cytochrome *c* oxidase. Homogenized samples (5 µL) were added to a solution (290 µL) containing 2 mg/mL reduced cytochrome c and 10 mg/mL sodium dithionite dissolved in a 0.1M potassium phosphate buffer. Absorbance measures (550nm) were taken every 10 seconds for 5 minutes to measure the oxidation rate of reduced cytochrome c by cytochrome c oxidase.

4.8 Primary Astrocyte Cell Culture

Primary *Cd38*$^{+/+}$, *Cd38*$^{+/-}$, and *Cd38*$^{-/-}$ astrocyte cultures were generated from BG of postnatal day 3-5 pups. Astrocyte isolations were similarly prepared via MACS method as described in previous sections (see "Astrocyte Isolation"). Agilent Seahorse XF24 24-well cell culture microplates (cat. 100777-004) were treated with 0.1 mg/mL poly-ornithine (Millipore Sigma, cat. P3655) and 1 µg/cm^2 laminin (Millipore Sigma, cat. L2020). After MACS astrocyte isolation, cells were suspended in serum-free defined astrocyte media (neurobasal plus medium (Thermo Fisher Scientific, cat. A3582901), 1x B27 plus, 1x Glutamax (Thermo Fisher Scientific, cat. 35050061), 1 mM sodium pyruvate, 625 U/mL penicillin/streptomycin (Thermo Fisher Scientific, cat. 15070063)). Cells were seeded at 30K cells per well in 250 µL serum-free astrocyte media. Plates were housed at 37°C with 5% CO_2 for the duration of experiments. Half-volume media changes took place every 5 days until 21DIV, when cells were prepared for immunocytochemistry and Agilent Seahorse XF Mito Stress experiments (see section 4.7).

4.9 Agilent Seahorse XF96 Mito Stress Test

At 21 DIV, BG primary astrocyte culture plates (see section 4.6) were prepared for Agilent Seahorse XF96 Mito Stress Test assessment (cat. 103015-100) to measure mitochondrial oxidative phosphorylation function. Extensive protocol details can be found in published citations (Anderson et al., 2014). In brief, one day prior to running the experiment, injection plates were calibrated in 1 mL Agilent calibration solution. On the day of the experiment run, serum-free defined astrocyte media was removed from all wells. Wells were then washed 3 times with Agilent DMEM. After the final wash, all wells were brought to a final volume of 675 µL DMEM and left to incubate at 37°C, without CO_2, for 1 hour. During this time, mitochondrial stress test reagents oligomycin (5 µM), FCCP (6 µM), and rotenone (10 µM) stocks were prepared and loaded into the injection cartridge. The calibration cartridge is then used to calibrate settings prior to each run. After 1 hour of incubation, plates were run according to standard Agilent Mito Stress Test protocols.

The mitochondrial stress test is performed in phases, during which, OCR is evaluated in each well and normalized to total protein content as measured by bicinchoninic acid assay (BCA, ThermoFisher cat. 23225). First, basal respiration is measured as a baseline series of observations. Following basal respiration measures, oligomycin is administration into each well to measure proton leakage. Next, FCCP is administered in order to evaluate maximal respiration. Differences between the OCR rise after FCCP administration and the reduced OCR during proton leak measures serves as an indicator of ATP-linked respiration. Mitochondrial spare capacity can be derived by measuring the OCR difference between maximal respiration and basal respiration following FCCP administration. Finally, antimycin A and rotenone are added to measure non-mitochondrial respiration. Following each run, all wells were washed 2 times in

PBS followed by addition of 50 µL RIPA lysis buffer to each well. Plates were then stored in -20°C overnight, followed by protein collection and assessment of protein content by BCA (Thermo Fisher Scientific, cat. 23225) the following day.

Mitochondrial glycolytic function can also be evaluated during the Mito Stress Test paradigm, similar to methods described for measures of oxidative phosphorylation. The Agilent Seahorse XF96 simultaneously measures ECAR in each well alongside OCR measures. ECAR measures during the basal respiration period serve as measures of basal glycolysis. ECAR values between oligomycin and FCCP administration are indicative of glycolytic capacity. The difference in ECAR values between glycolytic capacity and basal glycolysis indicates glycolytic reserve. As previously stated for OCR measures, all ECAR data is normalized to total protein per well as determined by BCA.

4.10 Statistics and Software

R studio (Posit, PBC) was used to analyze RNA-seq datasets and generate GO pathway analysis figures. Prism software (GraphPad) was used to generate DEG and bioenergetic-related figures Kruskal-Wallis ANOVA analyses and post-hoc tests were also performed with Prism software. For all statistical tests, alpha was set to $\alpha \leq 0.05$.

Chapter 5: Results

5.1 *Cd38* expression is most enriched in astrocytes of the substantia nigra

When evaluating *Cd38* expression by cell type, single-cell sequencing datasets reveal that astrocytes have the highest expression followed by oligodendrocytes, microglia, and neurons, respectively (Fig. 17A, left). *Cd38* was also identified to be enriched in astrocytes of the midbrain (Fig. 17A, center) amongst other basal ganglia regions (Fig. 17A, right). We utilized fluorescence *in situ* hybridization (FISH) to further evaluate *CD38* expression in wild-type ($Cd38^{+/+}$) and *Cd38* knockout ($Cd38^{-/-}$) mouse substantia nigra parc compacta (SNc, finding that *Cd38* expression is colocalized to astrocytic marker, *Gja1*, in $Cd38^{+/+}$ mice (Fig. 17B). Furthermore, *Cd38* was not found to colocalize with dopaminergic cell markers, *Th*, in either $Cd38^{+/+}$ or $Cd38^{-/-}$ mice (Fig. 17C). Similar to curated data findings (Fig. 17A), SNc *Cd38* FISH pixel intensity was found to be increased in astrocytes of the SNc relative to striatal astrocytes (Fig. 17D). Using reverse-transcription PCR to quantify relative differences in *Cd38* expression amongst genotypes, it was further confirmed that *Cd38* depletion was induced in knockout models (Fig. 17E).

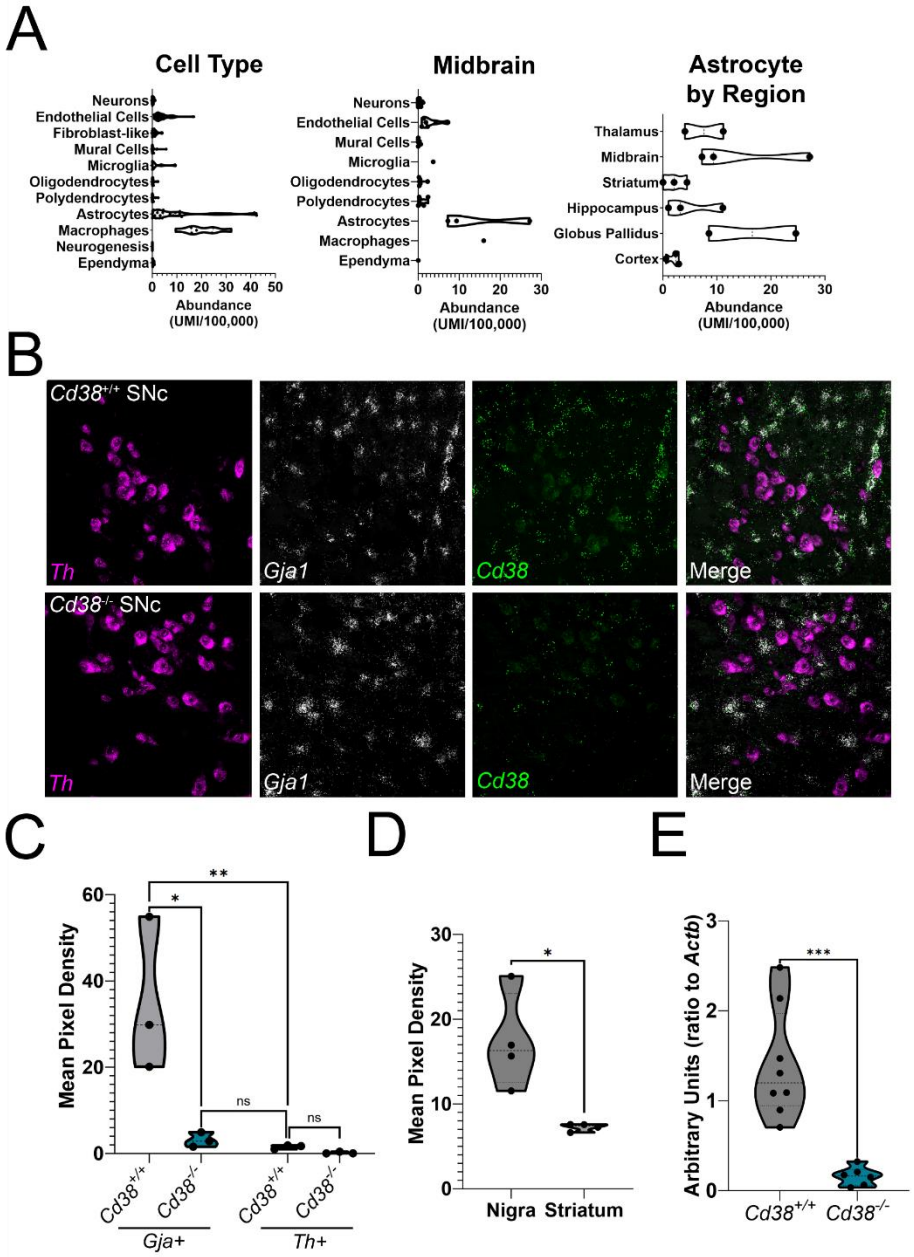

Figure 17. Determinations of *CD38* specificity in astrocytes. (A) A DropViz (Saunders et al., 2018) meta-analysis reveals that astrocytes have high *Cd38* abundance relative to other cells (left), especially so in midbrain regions (middle). Furthermore, basal ganglia-related populations show high abundance (right). (B) Representative FISH images of $Cd38^{+/+}$ (top) and $Cd38^{-/-}$ (bottom) for tyrosine hydroxylase (*Th*), connexin-43 (*Gja1*), and Cd38 in the SNc. (C) Astrocytic marker *Gja1* colocalizes with *Cd38*, not DA neuronal markers (*Th*) in $Cd38^{+/+}$ animals. $Cd38^{-/-}$ animals show significant decrease of colocalization. (D) Relative to striatum, substantia nigra has significantly increased *Cd38* in $Cd38^{+/+}$ animals. (E) rt-PCR measures of *Cd38* indicate that that $Cd38^{-/-}$ have significantly reduced transcripts relative to $Cd38^{+/+}$ animals. Significance attributions are as follows: $p < 0.05$ (*), $p < 0.01$ (**), $p < 0.001$ (***).

Importantly, astrocytic enrichment of *CD38* is relevant to understanding how glial may play a contributing role in PD pathogenesis. The *CD38* gene is located in chr4_15735476_C_A_b38 in humans, a region containing other genes of importance (Chapter 2.4, Fig.12A). GWASs have identified numerous SNPs that modulate PD risk to exist within this region (Chen et al., 2014; J. Li et al., 2019; Sharma et al., 2012). Amongst these studies, SNP variant rs11724635 repeatedly has been found to increase risk odds of PD development. This particular variant specifically results in decreased *CD38* expression without altering expression of *FAM200b* or *BST1* (Chapter 2.4, Fig. 12A). Furthermore, rs11724635 is associated with decreased *CD38* expression across brain regions associated with motor function (Chapter 2.4, Fig.12B). Based upon our determinations of astrocytic enrichment of *CD38*, we sought to further evaluate how a clinically-relevant disruption of *CD38* expression may impact astrocytic functions.

5.2 *Cd38*$^{-/-}$ have elevated NAD and depreciated NAM within basal ganglia

The canonical activity of CD38 is to enzymatically function as an NADase and ADP-ribosyl cyclase, whereby NAD is degraded to generate ADPR/cADPR and NAM (Aksoy et al., 2006; Howard et al., 1993). It has also been previously demonstrated that *CD38*$^{-/-}$ animals have increased NAD content across peripheral tissues (Camacho-Pereira et al., 2016). Given initial findings regarding SNP rs11724635 and the associated decrease in *CD38* expression (Fig. 12), we sought to explore the relationship in a translationally relevant heterozygous knockout (*Cd38*$^{+/-}$) that recapitulates the approximately 50% decrease in *CD*38 expression. 12-month-old *Cd38*$^{+/+}$, *Cd38*$^{+/-}$, and *Cd38*$^{-/-}$ mouse striatum and midbrain tissues were isolated for ^{1}H NMR analysis of NAD and NAM content. Spectra recordings indicated that *Cd38*$^{-/-}$ mice have elevated NAD and reduced NAM (Fig. 18A). Upon analysis, it was confirmed that *Cd38*$^{-/-}$striatal and

midbrain samples had increased NAD and reduced NAM relative to *Cd38*$^{+/+}$ peer-matched controls (Fig.18B-C). Interestingly, *Cd38*$^{-/-}$ midbrain tissue had elevated NAD relative to *Cd38*$^{+/-}$ animals, but not in the striatum. In regards to NAM, *Cd38*$^{-/-}$ also had significantly reduced content relative to *Cd38*$^{+/-}$ samples in both midbrain and striatum. The ratio between NAD/NAM content was calculated, revealing that *Cd38*$^{-/-}$ significantly shifted upwards towards NAD abundance relative to NAM levels in both striatum and midbrain when compared to *Cd38*$^{+/+}$ and *Cd38*$^{+/-}$ animals (Fig. 18D). These findings are in line with previous literature evaluating the effects of CD38 deficiency on NAD balance within *Cd38*$^{-/-}$ animals (Aksoy et al., 2006; Braidy et al., 2014). However, these are the first instances in which NAD/NAM evaluations have been experimentally determined in brain regions that are translationally relevant to PD.

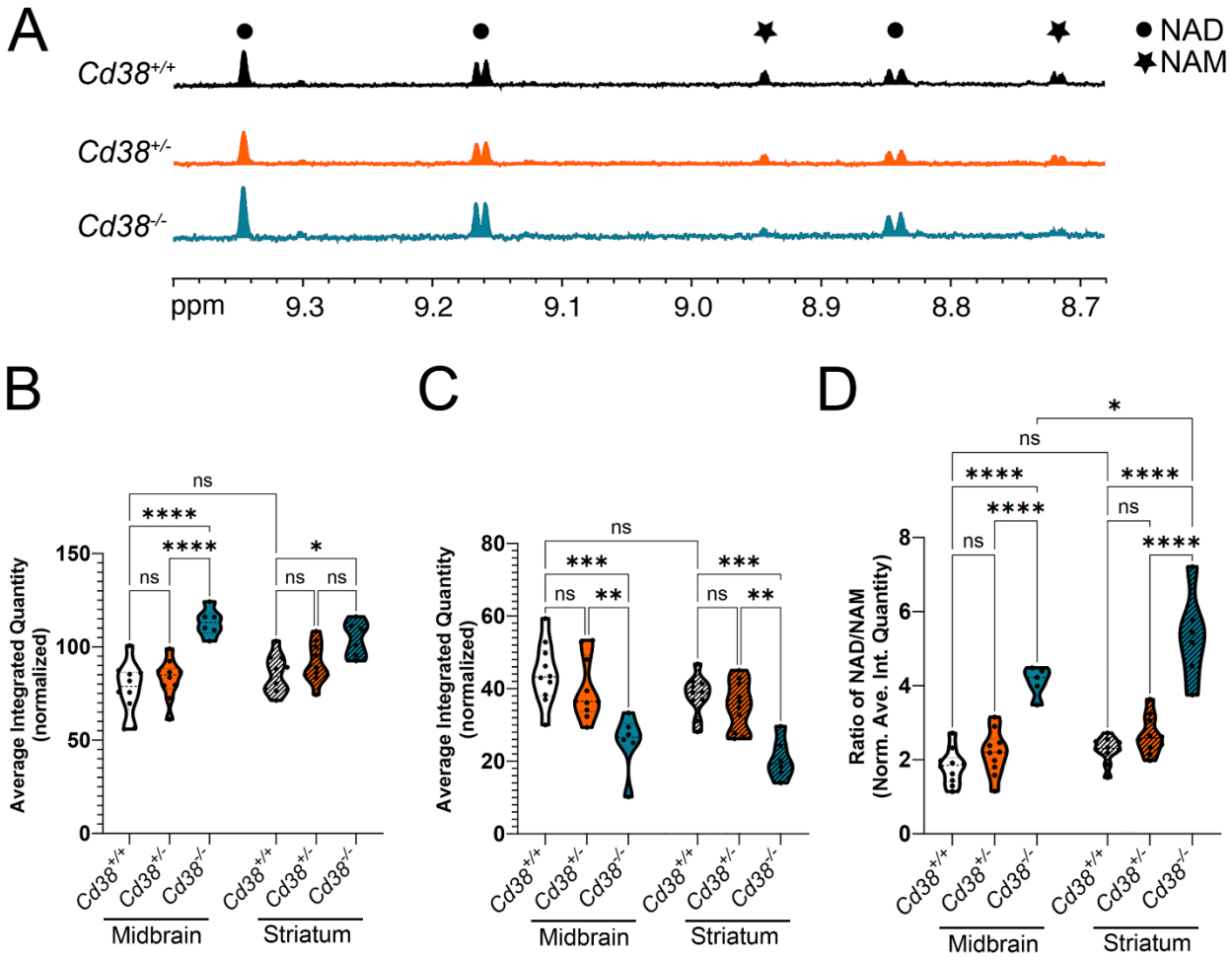

Figure 18. NAD and NAM levels are altered in *Cd38*$^{-/-}$ mice. (A) ^{1}H NMR spectra of three representative midbrain tissue samples containing NAD and NAM. Plots showing quantifications of NAD (B) and NAM (C) as average integrals of the ^{1}H NMR signals. NAD levels are elevated in *Cd38*$^{-/-}$ animals while NAM is decreased across basal ganglia regions. (D) NAD/NAM ratio comparisons show a significant shift in NAD relative to NAM content in *Cd38*$^{-/-}$ mice. $p < 0.05$ (*), $p < 0.01$ (**), $p < 0.001$ (***), $p < 0.0001$ (****).

5.3 *Cd38* depletion dysregulates astrocyte gene expression

CD38 expression has been shown to influence astrocyte development and mediate functions that manifest in behavioral deficits (Hattori et al., 2023; Hattori et al., 2017). These studies, however, did not transcriptionally evaluate astrocytes *in vivo* or in the context of advanced age. We sought to fill this gap in knowledge by using RNA-sequencing in aged animals to better identify how *Cd38* may transcriptionally regulate astrocytes beyond postnatal periods. Cell-

specific MACS isolation protocols were utilized to collect 12-month-old (12-14 months, $\bar{x}$ = 13.5 months) basal ganglia (globus pallidus, putamen, thalamus, substantia nigra) astrocytes in *Cd38*$^{+/+}$, *Cd38*$^{+/-}$, *and Cd38*$^{-/-}$ for next-generation RNA-seq applications. Pairwise comparisons between *Cd38*$^{+/-}$ to *Cd38*$^{+/+}$ and *Cd38*$^{-/-}$ to *Cd38*$^{+/+}$ were performed to identify DEGs, followed by a GO pathway analysis. RNA principal component analysis did not reveal any particular grouping patterns between genotypes (Fig.19A). Transcript correlations between groups also indicates similarity in astrocytic cellular identity (Fig.19B).

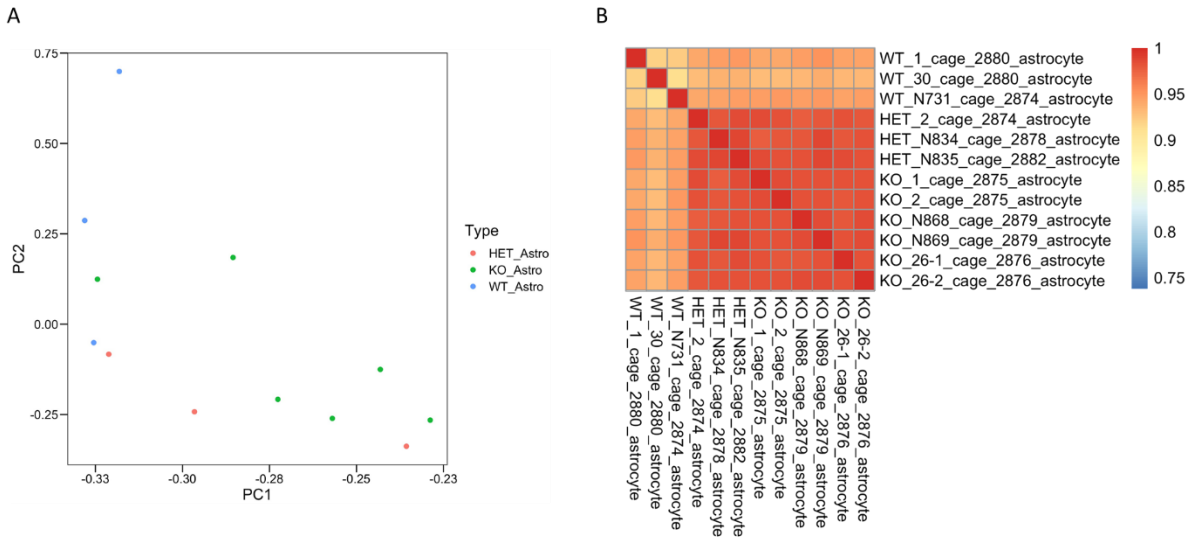

Figure 19. PCA and transcript similarity by heatmap. (A) Principal component analysis showing spread of samples from RNA-seq. (B) Heatmap organized by r^2 value showing correlation amongst sample transcripts.

We were able to identify 349 significant DEGs in *Cd38*$^{+/-}$ to *Cd38*$^{+/+}$ comparisons (Fig. 20A-B, Table 2). Of these, 90 DEGs are unique to the *Cd38*$^{+/-}$ to *Cd38*$^{+/+}$ comparison while 260 DEGs identified are shared were also found in *Cd38*$^{-/-}$ to *Cd38*$^{+/+}$ comparisons. Altogether, approximately 75% of DEGs identified in *Cd38*$^{+/-}$ were identified in *Cd38*$^{-/-}$ comparisons. In terms of expression directionality, there was a total of 183 upregulated DEGs and 166

downregulated DEGs in *Cd38*$^{+/-}$ comparisons, indicating no particular directional change towards upregulation nor down regulation of genes. When increasing FC stringency to ±1.2, we found that the number of upregulated and downregulated genes remained unchanged. Further scrutiny at FC ±1.5 identified that the great majority of genes (322) remained differentially expressed.

A total of 1,480 significant DEGs were identified in *Cd38*$^{-/-}$ to *Cd38*$^{+/+}$ comparisons (Fig. 20A-B, Table 2). We found that 1,220 DEGs were unique to *Cd38*$^{-/-}$ comparisons, with the remaining 260 DEGs also found in *Cd38*$^{+/-}$ to *Cd38*$^{+/+}$ comparisons as previously stated. The unique set of *Cd38*$^{-/-}$ DEGs compromise approximately 82% of comparisons. Of the total number of significant DEGs identified, 718 were upregulated while 762 were downregulated. Increasing FC cutoff to ±1.2-fold change results in identification of 716 upregulated and 760 downregulated DEGs. Applying the more stringent ±1.5-fold expression cutoff left a remaining 591 upregulated DEGs and 517 downregulated DEGs.

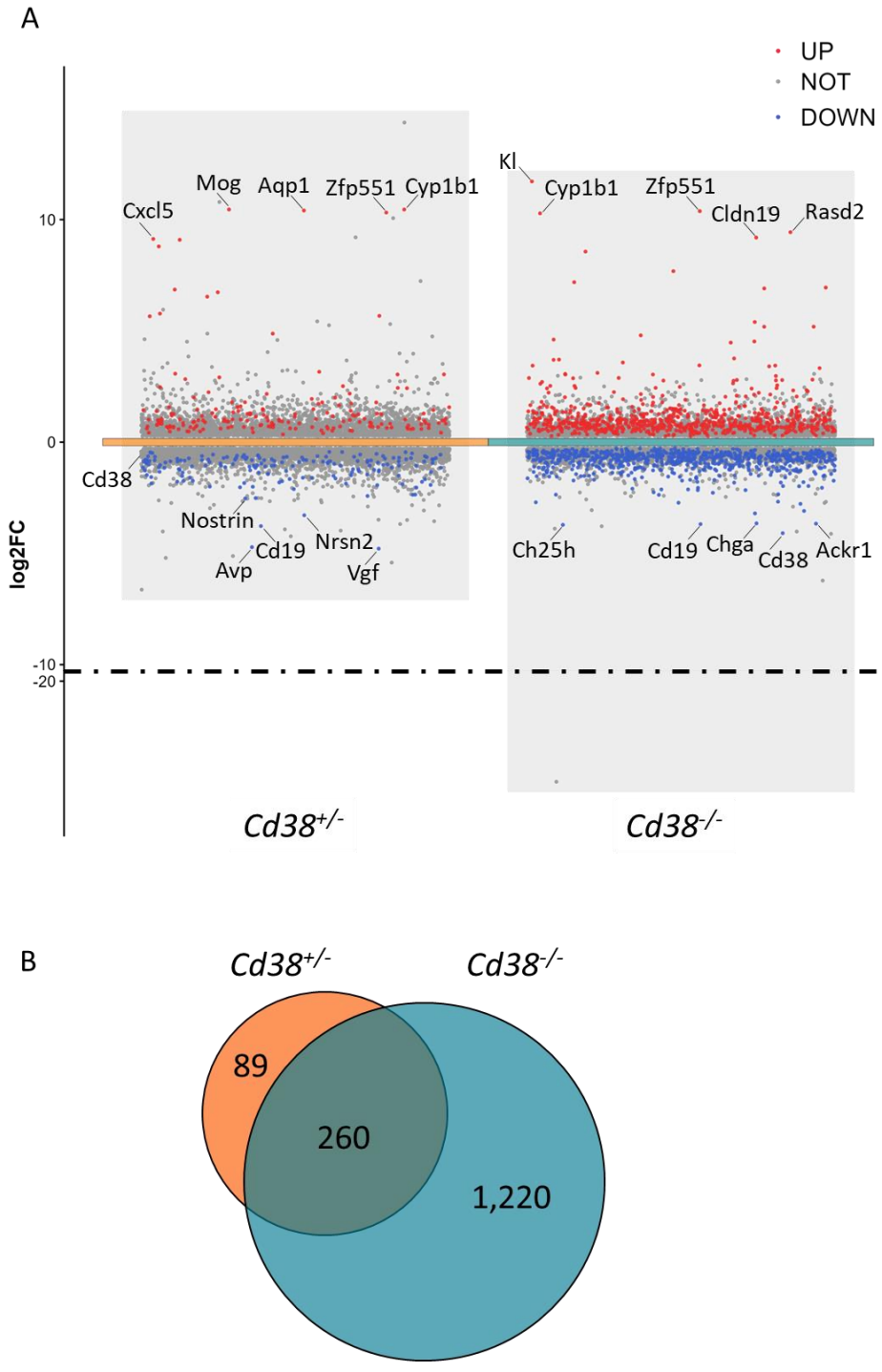

Figure 20. CD38-deficient astrocytes have numerous differentially regulated genes. (A) Volcano plot from *Cd38*$^{+/-}$ to *Cd38*$^{+/+}$ astrocyte comparisons (orange) and *Cd38*$^{-/-}$ vs. *Cd38*$^{+/+}$ comparisons (teal) showing all upregulated (red), downregulated (blue), and unchanged (gray) DEGs. Highlighted are the 5 most upregulated and downregulated DEGs organized by fold-change (log2FC). (B) Venn diagram demonstrating unique and shared DEGs from *Cd38*$^{+/-}$ and *Cd38*$^{-/-}$ comparisons to *Cd38*$^{+/+}$.

Sig. DEGs (q < 0.05)	Astrocyte	
	Cd38+/-	Cd38-/-
Total DEGs	349	1,480
Upregulated DEGs	183	718
Downregulated DEG	166	762
Expression FC +/-1.2 (q < 0.05)	Astrocyte	
	Cd38+/-	Cd38-/-
Total DEGs	349	1,476
Upregulated DEGs	183	716
Downregulated DEG	166	760
Expression FC +/-1.5 (q < 0.05)	Astrocyte	
	Cd38+/-	Cd38-/-
Total DEGs	322	1,108
Upregulated DEGs	167	591
Downregulated DEG	155	517

Table 2. Significant DEGs by expression directionality and fold-change cutoff. All significant DEGs identified in comparisons (top) and DEGs remaining after increasing fold-change stringency to ±1.2 (middle) and ±1.5 (bottom). Significance set to $q \leq 0.05$ for all displayed data.

Within the overlapping DEGs identified from pair-wise comparisons, we identified that classical genes that regulate water homeostasis (*Aqp4*) and cytoskeletal architecture (*Gfap*) are upregulated in *Cd38*$^{+/-}$ and *Cd38*$^{-/-}$ astrocytes. *Gfap* is of particular interest as its upregulation suggests elevation in reactive astrogliosis (Lawrence et al., 2023). Astrocytes are also capable of responding to immune system signals and responding as immune effectors (Dong & Benveniste, 2001). In our overlapped DEGs dataset, we identified upregulation in immune function genes that regulate cytokine-induced responses (*Cxcl5*) and compliment system activity (*C4b*) in CD38-deficient astrocytes. Relevant to the hallmarks of neurodegenerative disease, CD38-

deficient astrocytes also had disruptions to genes that regulate DNA/RNA functions (*Trex1*), protein homeostasis (*Ubb*), and cellular bioenergetics (*Cox10*). Dysregulation of groups of genes that regulate RhoGTPase activity (*Arhgap27, Arhgdia, Arhgef16*), Krüppel-like factors (*Klf2, Klf6*), solute carriers (*Slc12a6, Slc38a5*), transmembrane proteins (*Tmem161b, Tmem204*), and zinc finger proteins (*Zfp251, Zfp407, Zfp551*) are amongst the many DEGs identified within the overlapping dataset. It is important to note, that thin the overlapped DEGs group, directionality was shared between $Cd38^{+/-}$ to $Cd38^{+/+}$ and $Cd38^{-/-}$ to $Cd38^{+/+}$pairwise comparisons (Fig. 21). Altogether, dysregulation of essential biological processes is suggested by induction of CD38 deficiency.

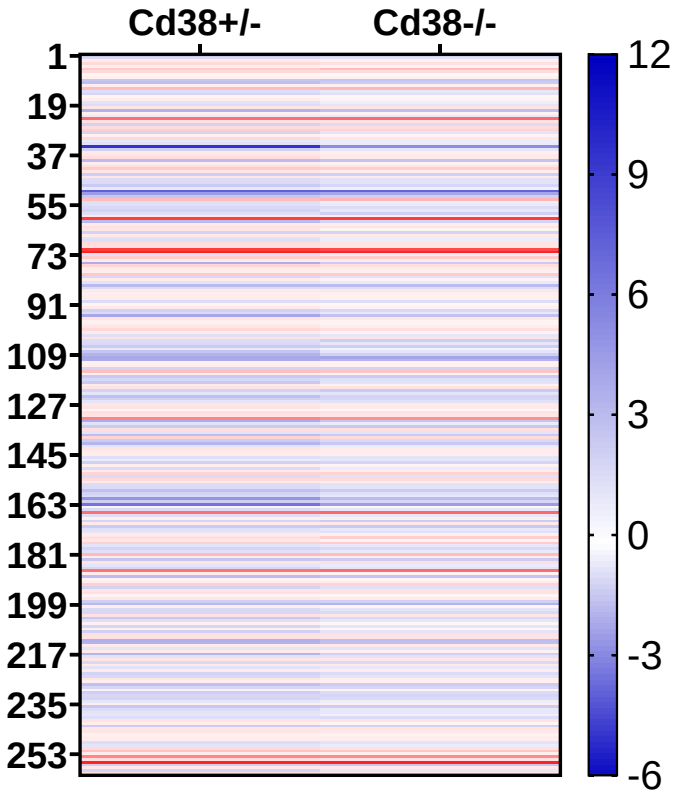

Figure 21. Heatmap of overlap in *Cd38*$^{+/-}$ and *Cd38*$^{-/-}$ pairwise comparisons. Heatmap organized alphabetically and placed in numerical order to highlight consistency within overlapped DEGs. Color corresponds to $\log_2$FC value. All data meets statistical significance ($q < 0.05$).

Given that CD38 function is implicated in PD (Zhou et al., 2023) cADPR-induced inflammation (Wei et al., 2014), and NAD-related bioenergetics (Lautrup et al., 2019), we sought to cross reference our DEG findings with available datasets. First, we examined our pairwise comparisons relative to PD TWAS, GWAS, and PWAS datasets (Kia et al., 2021; Yao et al., 2021; Zhou et al., 2023). Numerous astrocytic DEGs were matched to genes implicated in PD risk (Fig. 22A). *CD38*$^{+/-}$ comparisons had 11 matches while we identified 32 *CD38*$^{-/-}$ DEG matches. Most interestingly, both *Cd38*$^{+/-}$ and *Cd38*$^{-/-}$ astrocytes show increased expression of *Lrrk2*, a gene responsible for the majority of autosomal dominant PD cases in humans (Usmani et al., 2021). *Cd38*$^{-/-}$ astrocytes also have upregulation in *Prkn*, another gene implicated in high penetrance PD. These results suggest that reductions in *Cd38* are sufficient to induce changes amongst numerous genes implicated in PD.

We next evaluated our comparisons to genes implicated in reactive oxygen species (ROS) pathways (Rouillard et al., 2016). In this cross-comparison, there were 22 *CD38*$^{+/-}$ and 74 in *CD38*$^{-/-}$ ROS-related DEGs. Of note, *Apoe* was identified as downregulated in both comparisons (Fig. 22B). This finding is interesting as *Apoe* is implicated in astrocytic regulation of neuronal excitability (Konings et al., 2021) as well as in neurodegenerative disease (Fernández-Calle et al., 2022). *Sod3* downregulation has also been implicated in human PD risk (Ilyechova et al., 2018) and was also found to be downregulated in *Cd38*$^{+/-}$ and *Cd38*$^{-/-}$comparisons (Fig. 22B). Regulation of ROS is paramount, as free radicals are able to intercept electrons and damage cellular DNA, proteins, and membranes. Additionally, increased cellular ROS accumulation incurs mitochondrial damage and can contribute to bioenergetic dysfunction (Nissanka & Moraes, 2018).

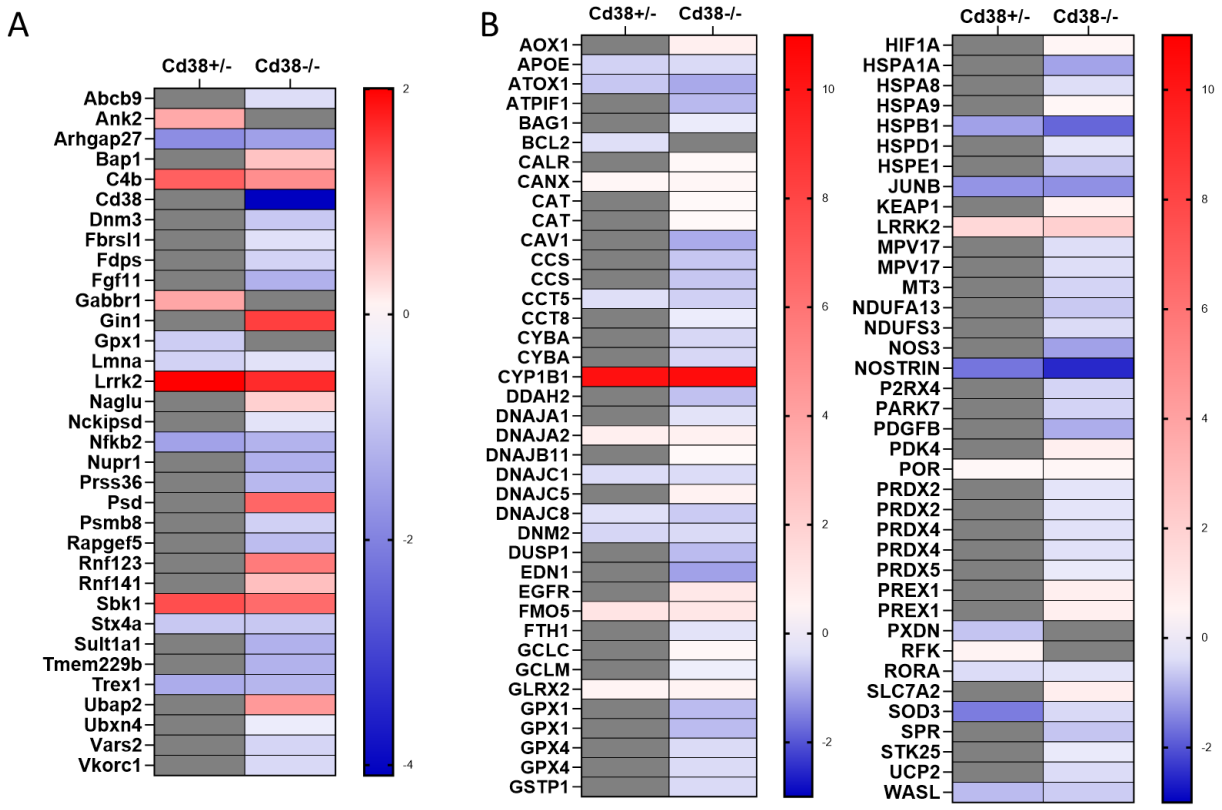

Figure 22. Identified DEGs in *Cd38*-defient astrocytes relative to PD and ROS datasets. (A) Heatmap for comparisons against available TWAS, GWAS, and PWAS datasets of PD-risk implicated genes. (B) Heatmap of ROS genes dataset comparisons, organized in alphabetical order and placed side-by-side. Color corresponds to $\log_2$FC value. All data meets statistical significance ($q < 0.05$).

Mitochondrial dysfunction is highly associated with NDDs and PD, therefore, we sought to determine if our datasets indicate mitochondrial perturbations. Utilizing the MitoCarta 3.0 database (Rath et al., 2021), we evaluated our DEGs against those established to be directly involved with mitochondrial function. *Cd38*$^{+/-}$ and *Cd38*$^{-/-}$comparisons indicated that 18 and 114 DEGs, respectively, are implicated in mitochondrial function (Fig. 23). Shared amongst identified genes are those that mediate fatty acid synthesis (*Acacb*), complex IV activity (*Cox10*), protein synthesis (Mrpl41), complex I activity (*Ndufb7*), and DNA regulation (*Top1mt*). Dysregulation of

complex I and IV genes are directly tied to mitochondrial ATP-production, implicating mitochondrial bioenergetics may be perturbed.

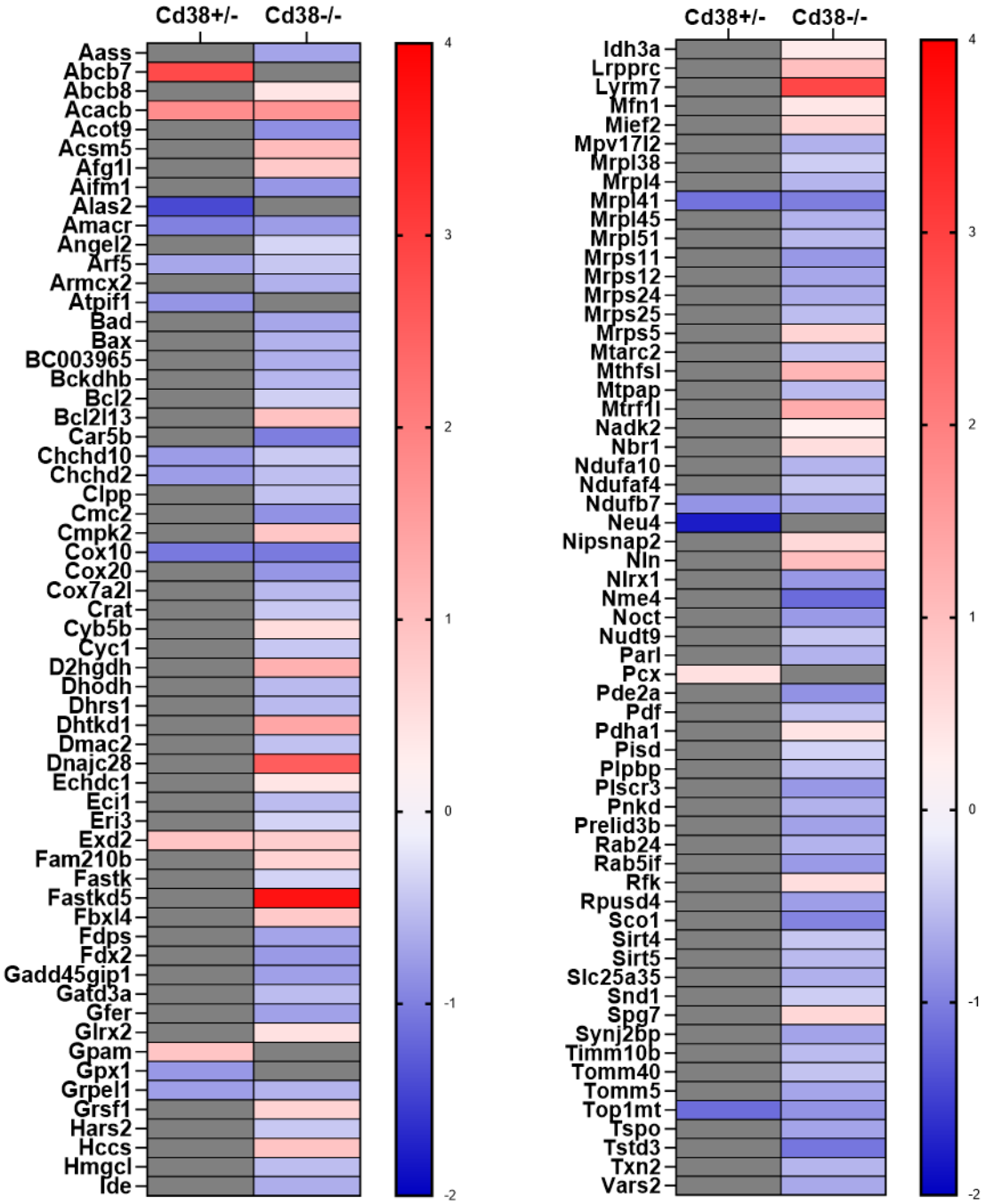

Figure 23. Mitochondrial DEGs identified in *Cd38*$^{+/-}$ to *Cd38*$^{-/-}$ comparisons. Heatmap for comparisons against known functionally relevant mitochondrial genes (Rath et al., 2021) organized alphabetically organized. Color indicates $\log_2$FC associated with pair-wise comparisons. All data meets statistical significance ($q < 0.05$).

5.4 Dysregulation by CD38-deficiency implicates hallmarks of neurodegeneration

Following DEG identification, we performed a GO pathway analysis to evaluate if any biological processes were dysregulated as a result of CD38-deficiency. GO analysis was performed with significant DEGs with an expression fold change of ±1.2. In *Cd38*$^{+/-}$ to *Cd38*$^{+/+}$ comparisons, we identified 563 significant GO terms in total. Further evaluations of directionality by upregulated DEGs found 181 significant GO groups with downregulated DEG input finding 23 GO terms.

Given the translational relevance of *CD38* reductions and the associated increase in PD risk, we sorted biological process GO terms by groups associated with the hallmarks of NDDs (Wilson et al., 2023) using GO terms identified from total (upregulated and downregulated) DEG input. GO groups were identified for all major hallmarks relating to the major features of PD, namely cell death, protein regulation, CNS cell function, and bioenergetics then sorted by total gene count involved per GO term to identify genes of interest (Fig. 24A). While all ND relevant hallmarks were identified, no group had larger than 20 DEGs counted within a term. DEG and GO indications both suggest that major hallmarks of PD, namely bioenergetic (Fig. 24B) and CNS cell function (Fig.24C), are dysregulated. Out of all GO terms, bioenergetic groups represented approximately 7% of the dataset, while CNS cell function represented approximately 6% of all terms.

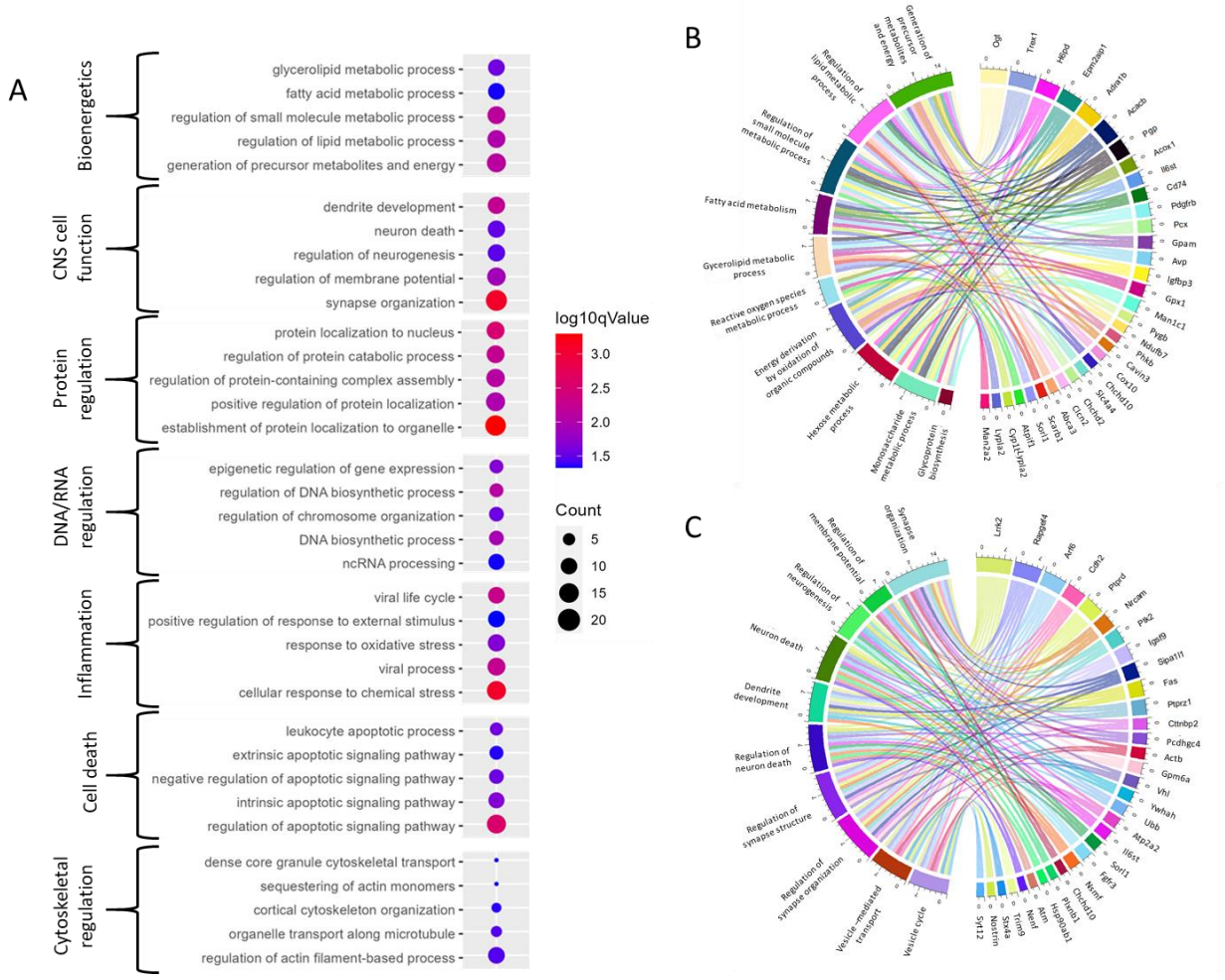

Figure 24: GO pathway analysis of *Cd38*$^{+/-}$ astrocytes reveal familiar hallmarks of neurodegeneration. (A) GO bubble plot is organized based on neurodegeneration hallmarks. The top 5 biological process (BP) GO terms by gene count per term are displayed for each group. Bubble color indicates the log10 q-value while the circle size indicates gene count per term. (B) GO chord plot of top 10 bioenergetics-related genes by total gene count highlights genes of interest common to indicated terms. (C) GO chord plot of top 10 CNS cell function-related genes by total gene count highlights genes of interest common to indicated terms.

GO pathway analysis of DEGs identified in *Cd38*$^{-/-}$ to *Cd38*$^{+/+}$ comparisons were also performed utilizing significant DEGs with a minimum fold change of ±1.2. Utilizing these thresholds, we revealed 723 total significant GO terms. Inputting solely upregulated DEGs into

the GO analysis revealed 181 terms, while inputting downregulated DEGs resulted in finding 288 GO group terms. Similar to *Cd38*$^{+/-}$ to *Cd38*$^{+/+}$ comparisons, further evaluation of GO terms identified from total DEGs analyses resulted in identification of GO groups associated with the hallmarks of ND (Fig. 25A). Relative to *Cd38*$^{+/-}$ comparisons, *Cd38*$^{-/-}$ engaged more DEGs per group, with counts in some groups reached as high as 56 genes involved (Fig. 25A). Bioenergetic GO pathways (Fig. 25B) and CNS cell process (Fig. 25C) are highlighted again, as they strongly relate to human PD and functional disruptions previously indicated by others. In *Cd38*$^{-/-}$ comparisons, bioenergetics accounted for approximately 5% of total GO pathways while CNS cell function represented an additional 4%.

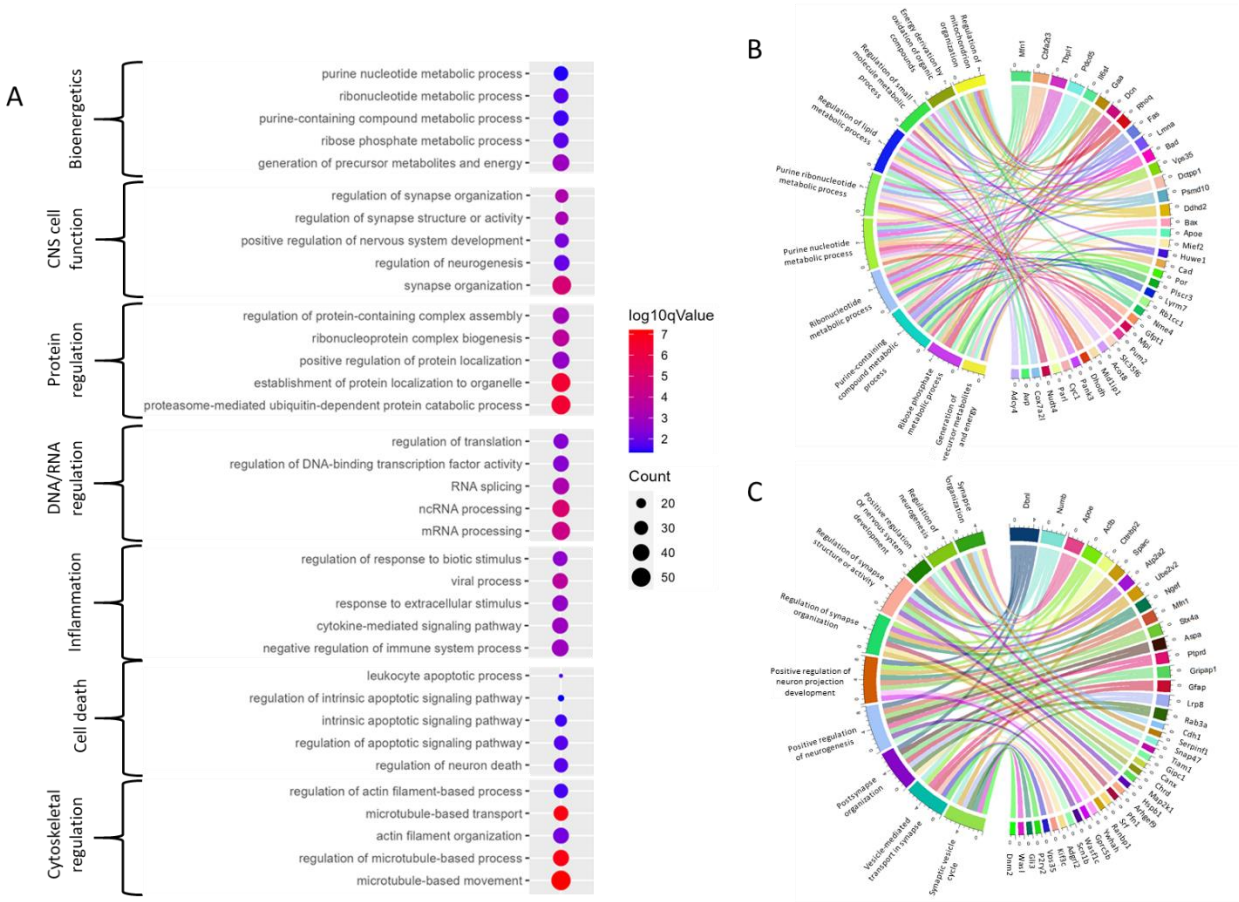

Figure 25. GO pathway analysis of *Cd38*$^{-/-}$ astrocytes similarly reveal familiar hallmarks of neurodegeneration. (A) GO bubble plot is organized based on neurodegeneration hallmarks. The top 5 biological process (BP) GO terms by gene count per term are displayed for each group. Bubble color indicates the log10 q-value while the circle size indicates gene count per term. (B) GO chord plot of top 10 bioenergetics-related genes by total gene count highlights genes of interest common to indicated terms. (C) GO chord plot of top 10 CNS cell function-related genes by total gene count highlights genes of interest common to indicated terms.

5.5 Reductions in *Cd38* alter bioenergetics

We next sought to better understand if CD38 deficiency has discernable effects on mitochondrial function in midbrain tissues from late-adulthood CD38 *Cd38*$^{+/+}$, *Cd38*$^{+/-}$, and *Cd38*$^{-/-}$ animals (8-12 months, $\bar{x}$ = 10.34 months). Measures of pyruvate dehydrogenase and cytochrome c oxidase activity were of interest given our RNA-sequencing dataset showing differential regulation of genes involved with these functions. Importantly, pyruvate dehydrogenase and cytochrome c are crucial for ATP synthesis via oxidative phosphorylation. While citrate synthase genes did not show differential expression in our dataset, functional measures of activity serve as a representation of mitochondrial content. We found that there were no differences between genotypes in measures of pyruvate oxidation and cytochrome c oxidase activity (Fig. 26A-B). There was, however, increased citrate synthase activity in *Cd38*$^{-/-}$ to *Cd38*$^{+/+}$ comparisons (Fig. 26C). While general mitochondrial function remains unchanged between groups, the increased citrate synthase activity of *Cd38*$^{-/-}$ samples suggests that there may be bioenergetic changes if further evaluated.

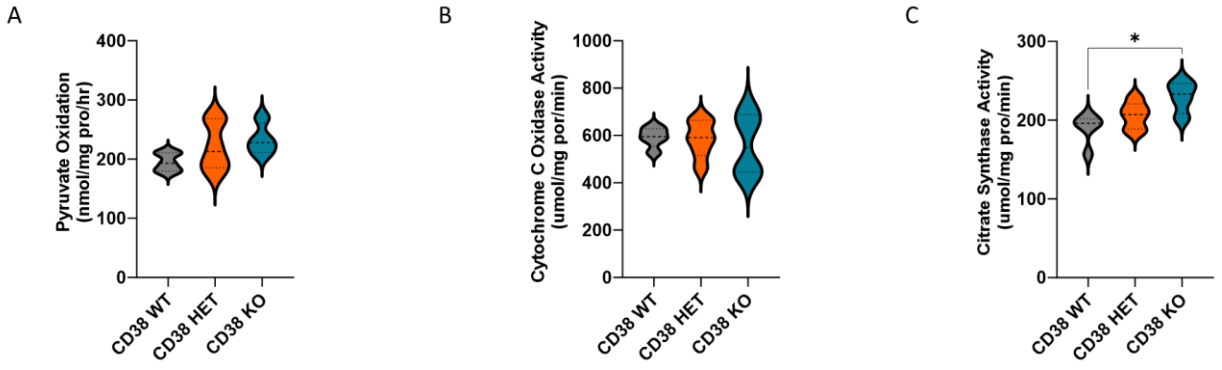

Figure 26. CD38 deficiency mildly alters global bioenergetics. (A) BG tissues from LA animals (8-12, $\bar{x}$= 10.34 months) did not show differences in pyruvate oxidation between groups. (B) LA animal tissue also did not differ in measures of cytochrome C oxidase activity. (C) However, *Cd38*$^{-/-}$ tissues show increased citrate synthase activity in compared to *Cd38*$^{+/+}$ ($f(2,14) = 5.018$, $p < 0.261$).

Based on the implication of altered mitochondria number in *Cd38*$^{-/-}$ conditions, we evaluated the bioenergetic capacity of isolated astrocytes. We generated an astrocyte culture by utilizing our previously described technique (Holt & Olsen, 2016; Holt, Stoyanof, & Olsen, 2019) and seeded cells within Seahorse XF 24-well plates in preparation. At DIV21, cells were prepared for Seahorse evaluations of oxygen consumption and acidification by glycolysis across a mitochondrial stress test paradigm. Analysis was performed similar to others (Anderson et al., 2014; Sonntag et al., 2017), where comparisons were made between measurable periods that signify basal respiration, ATP-linked respiration, proton leak, maximal respiration, spare respiratory capacity, non-mitochondrial use, and the coupling effect of oxygen consumption to ATP production. Glycolytic measures were derived from the observation period similarly to previous works (Sonntag et al., 2017).

Seahorse oxygen consumption rate (OCR) measures serve as indications of mitochondrial respiration. OCRs were significantly different in *Cd38*$^{+/-}$ to *Cd38*$^{+/+}$ comparisons for basal respiration and non-mitochondrial oxygen use (Fig. 27A-B), whereby *Cd38*$^{+/-}$ samples had higher an elevated OCR. Similarly, *Cd38*$^{-/-}$ to *Cd38*$^{+/+}$ comparisons revealed increased OCR in *Cd38*$^{-/-}$ samples during basal respiration, proton leak, and non-mitochondrial oxygen use (Fig. 27B). Altogether, the mitochondrial profile of *Cd38*$^{+/-}$ and *Cd38*$^{-/-}$ suggest that astrocytic expression of CD38 modulates mitochondrial function and membrane integrity.

The Seahorse platform allows for simultaneous measure of extracellular acidification rate (ECAR) during the length of the experiment and acts as an index of glycolysis. ECAR measures were used to evaluate basal glycolysis, glycolytic capacity, and glycolytic reserve. Compared to *Cd38*$^{+/+}$ samples, *Cd38*$^{+/-}$ astrocytes had increased ECAR during basal glycolysis (Fig. 27C-D). No significant differences were found during glycolytic capacity or reserve in *Cd38*$^{+/-}$ to *Cd38*$^{+/+}$

comparisons (Fig. 27D). *Cd38*$^{-/-}$ to *Cd38*$^{+/+}$ comparisons found increased *Cd38*$^{-/-}$ ECARs during basal glycolysis and glycolytic capacity measures (Fig. 27D). A reduced glycolytic reserve ECAR was also observed in *Cd38*$^{-/-}$ samples compared to *Cd38*$^{+/+}$ (Fig. 27D). Our glycolytic measures indicate that CD38 deficiency affects astrocyte glycolytic function alongside altered oxygen consumption. Astrocytes are largely glycolytic relative to other CNS cells (Rose et al., 2020), thus, perturbations within glycolytic function may have functional consequence beyond measures indicated here.

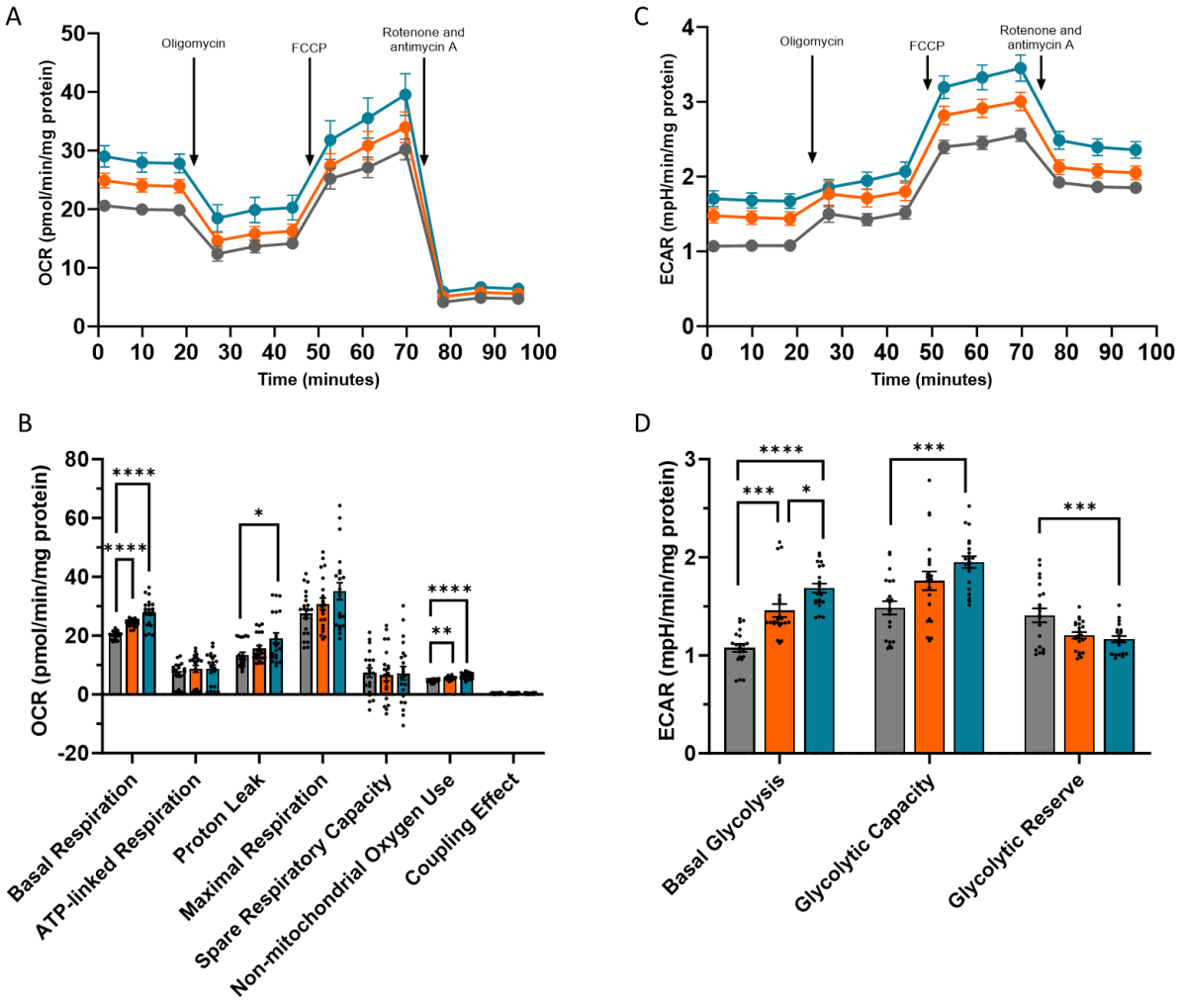

Figure 27. Seahorse XF96 analysis identifies mitochondrial dysfunction in CD38-deficient astrocytes. (A) Seahorse XF Mito Stress Test measures of oxygen consumption rate measures of *Cd38*$^{+/+}$, *Cd38*$^{+/-}$, and *Cd38*$^{-/-}$ across time suggest differences in mitochondrial function between groups. (B) Oxygen consumption between *Cd38*$^{+/+}$, *Cd38*$^{+/-}$, and *Cd38*$^{-/-}$ astrocytes differed during measures of basal respiration ($H(3)= 36.93$, $p < 0.0001$), proton-leak ($H(3)= 8.028$, $p = 0.0181$), and non-mitochondrial oxygen consumption ($H(3)= 29.89$, $p < 0.0001$). (C) Similarly, extracellular acidification rates appear different between groups and suggest glycolytic dysfunction. (D) Extracellular acidification between groups differed when evaluating basal glycolysis ($H(3)= 39.97$, $p < 0.0001$), glycolytic capacity ($H(3)= 16.78$, $p < 0.0002$), and glycolytic reserve ($H(3)= 8.157$, $p < 0.0169$). Significance attributions are as follows: $p < 0.05$ (*), $p < 0.01$ (**), $p < 0.001$ (***), $p < 0.0001$ (****)

Chapter 6: Discussion

6.1 *Cd38* and translational relevance

While the pathology of PD has been well documented, there still exists a large gap in our current understanding of genetic and environmental risks that precipitate dopaminergic cell loss (Skrahina et al., 2021; Vollstedt et al., 2023). The SNP variant rs11724635 has been implicated as a risk gene in multiple GWAS studies and meta-analyses (Chen et al., 2014; J. Li et al., 2019; Sharma et al., 2012). In humans, rs11724635 is associated with decreased *CD38* expression without alterations to nearby genes *FAM200b* and *BST* (Chapter 2.4, Fig. 12). *Cd38*$^{+/-}$ mice serve as a relevant analog to this mutation, while *Cd38*$^{-/-}$ animals allow us to better understand the biological contributions of *CD38* expression. This two-model approach has proven useful, as *Cd38*$^{+/-}$ and *Cd38*$^{-/-}$ mice show some similarities and differences in NAD/NAM balance, DEGs identified, GO pathways implicated, and mitochondrial function. Across all measures, *Cd38*$^{-/-}$ animals were notably more dysregulated than their *Cd38*$^{+/-}$ peers, an important distinction that allows for identification of targets that may be otherwise difficult to interpret simply from *Cd38*$^{+/-}$ to *Cd38*$^{+/+}$ comparisons. This distinction between levels of CD38 deficiency may prove useful in further evaluation of the interaction between rs11724635 risk and environmental contributions. Chinese and Taiwanese populations, for example, have an increased odds-risk-ratio of PD if identified with the rs11724635 SNP, whereas Japanese population studies did not find this association (Chen et al., 2014; Miyake et al., 2012; Zhu et al., 2017). While the genetic basis associated with rs11724635 is similar, environmental factors may differentially interact within these populations to confer risk. Similarly, the differences observed in our *Cd38*$^{+/-}$ and *Cd38*$^{-/-}$ models may allow us some insight into how rs11724635, environmental contributors, and aging may interact to confer specific risk to specific populations.

6.2 Astrocytic bioenergetic perturbations as a consequence of CD38 deficiency

The role of CD38 in relation to CNS health and function has been a growing topic of interest due, in part, to the therapeutic potential of boosting NAD levels in aged persons. In physiologically healthy contexts, CD38 function in the brain facilitates glial development (Hattori et al., 2017) and regulates NAD/NAM balance (Aksoy et al., 2006). During aging, this balance is disrupted in part due to increased expression and activity of CD38 across tissues (Camacho-Pereira et al., 2016; Guerreiro et al., 2020). Here, we demonstrate that astrocytes within the basal ganglia are most associated with *Cd38* expression (Fig. 17). We also show that NAD/NAM balance is shifted shifting in favor of NAD abundance in the context of severe CD38 deficiency (Fig. 18). These findings are relevant, as they corroborate the limited research currently available regarding bioenergetic alterations in relation to age-related changes within the context of novel PD risk-associated gene, *CD38*. Even further, these data provide further context to how global alterations of CD38 may perturb astrocytes

Modulation of mitochondrial function has also been linked to CD38 activity (Camacho-Pereira et al., 2016; Meyer et al., 2022). Bioenergetic dysfunction is well-established as a feature of neurodegenerative pathologies, including PD. Some reports have linked reductions in CD38 to increased mitochondrial function (Camacho-Pereira et al., 2016; Meyer et al., 2022), with our own transcriptional dataset and bioenergetic profiles similarly recapitulating these features in astrocytes (Fig. 23-27). There is a discrepancy herein, however, whereby reductions in CD38 drive increased mitochondrial activity while simultaneously conferring increased risk of PD risk. Additional evaluation of PD models (MPTP induced, *LRRK2*, *PRKN*, etc.) in addition to CD38-based mutant models or via pharmacological inhibition may help demystify how both events can

coexist. Further study of astrocytic, neuronal, and other CNS cell responses to CD38 modulation may further strengthen our understanding of these interactions.

6.3 Loss of CD38 as it relates to PD and age-related inflammation

Astrocytes themselves are integral to all aspects of CNS function as contributors to neuronal function, blood-brain barrier support, and responding to CNS insult amongst numerous other roles as major support cells (Patani et al., 2023). Unsurprisingly, dysfunctional astrocytes are implicated in nearly all neurodegenerative disorders as being directly or indirectly affected within the context of disease. Our sequencing dataset identifies dysregulated genes associated with PD, as well as a small number of astrocytic genes that regulate function and reactive astrogliosis (*Gfap)*. Overexpression of *Lrrk2*, for instance, modulates autophagy-lysosome functions (Kam et al., 2020) and is an established cause of PD we identified as upregulated in *Cd38*$^{+/-}$and *Cd38*$^{-/-}$ astrocytes relative to controls. *Cd38*$^{-/-}$astrocytes also had increased *Prkn* expression, which has a demonstrated role in modulating cellular stress (Singh et al., 2018). Importantly, our transcriptional DEG and GO pathway analyses indicate disruption of numerous paths relevant to NDDs.

The combinatory effect of dysregulation amongst ROS, mitochondrial, and neurodegenerative hallmark pathways is of important consideration, as manifestation of idiopathic PD is believed to manifest as a result of convergent, deleterious events that induce DA neuronal death. Generally, we found that ROS-related astrocyte DEGs had reduced expression, which may be reflective of reduced inflammatory states in CD38-deficient models similar to reports by others (Roboon et al., 2019). DEGs common to both *Cd3*$^{+/-}$ and *Cd38*$^{-/-}$ indicate that reductions in CD38 influence functions relating to metabolic oxygen utilization (*Cyp1b1*),

antioxidant defense (*Nostrin, Sod3*), and inflammatory signaling (*Junb, Rora*). Across the aging process, ROS inflammatory drive is increased and contributes to neurodegenerative disease pathology (Zhang et al., 2023). Likewise, increased ROS generation . Based upon the established relationship of inflammaging to PD development, one may suspect that reduced astrocytic inflammatory profiles by CD38 loss may be beneficial; however, this concept is not corroborated by human data (Ge et al., 2023; Yao et al., 2021; Zhou et al., 2023). While reductions in CD38 may appear to induce anti-inflammatory states in astrocytes, they may instead be indicative of a loss of immunocompetence. In models of the autoimmune disease lupus, for example, *Cd38* deletion resulted in accelerated disease progression, suggesting that the contributions of CD38 to inflammation may be beneficial (Viegas et al., 2011). Traumatic brain injury facilitates inflammatory signaling and ROS generation, and similar to lupus findings, *Cd38* deletion in closed-head injury mouse models were more severely impaired than controls (Levy et al., 2009). Altogether, the benefits and risks associated with changes in CD38 presence and activity may be contingent upon context and require further investigation.

Chapter 7: Summary and Future Directions

7.1 Summary

Parkinson's disease affects millions globally, yet despite an increasing case prevalence (Rajan & Kaas, 2022), we understand little regarding what specific events instigate PD pathology. This dissertation seeks to elucidate how the decreased expression of the PD risk gene, *CD38*, influences astrocytes. The work presented here demonstrates that deficiencies in CD38 modulates astrocyte gene expression, molecular pathways associated with the hallmarks of neurodegeneration, and mitochondrial bioenergetics. These findings further our understanding of how CD38 facilitates astrocyte function in the aging brain, while simultaneously providing evidence for how its dysregulation maybe tied to neurodegenerative features. Our dataset will be readily available for future researchers to further evaluate risk genes and pathways identified here for further evaluation of this intersection that lies between aging, gene risk, and cellular perturbation.

7.2 Future directions

Our findings suggest astrocyte dysfunction as a result of CD38 deficiency; however, there are additional layers of complexity before we can directly link our results to PD development. The most immediate of which is the evaluation of DA neurons within the SNc. Future work will aim to understand how decreased *Cd38* expression in translationally relevant *Cd38*$^{+/-}$ models affect DA neuronal gene expression, health, and function. Most immediately, our lab plans to utilize markers of DA cells (tyrosine hydroxylase, dopamine transporters) to conduct cell counts across various ages within the SNc to determine if PD pathology is present. Similarly, we plan to evaluate markers of PD pathology, such as alpha-synuclein and TUNEL staining to evaluate

indicators phenotypic of disease onset. In future experiments, it is important to explore how CD38 loss transcriptionally impacts neurons, similar to how we evaluated astrocytes here. Lastly, functional evaluations utilizing electrophysiology measures of DA neurons within the context of CD38 loss would further provide indications as to how PD risk is associated with SNP variant rs11724635.

As was previously stated, age-related changes are the leading risk for the development of NDD pathology in humans. The conclusions drawn from our work rely upon late-adult age animals (8-12 months), without inclusion of models of advanced age (18-24 months). Additional study of the interaction between aging and CD38 deficiency is warranted to help elucidate how age-related changes contribute to astrocytic states. It is also important for future experiments to consider environmental contexts that may be translationally relevant to what is experienced by industrialized populations determined to be most at risk of PD (De Miranda et al., 2022). Paradigms that cross genetically relevant models (*Cd38*$^{+/-}$) with environmental challenges such as high fat diet, chemical contaminants, or chronic inflammation may help establish better understanding of the intersectionality between gene risks that set the stage for further events to instigate disease. Inclusion of various ages would further help distinguish the role of each factor as a contributing force in PD pathogenicity. Furthermore, additional mitochondrial assays relating to glycolytic function and function within the context of inflammatory events, like lipopolysaccharide administration, may allow for a more comprehensive understanding of the relationship between astrocyte bioenergetics when meeting environmental challenges.

It is also important to note that while our findings implicate astrocyte dysfunction in relation to SNP rs11724635, it does not directly provide information as to how astrocytic expression of CD38 may be a driving force in our observed transcriptional and bioenergetic changes. An

approach utilizing Cre/lox systems or tamoxifen-inducible models would allow for specific *Cd38* deletion in cells of astrocytes for specific determinations of cell-autonomous and non-cell-autonomous effects. This has recently been accomplished by others to evaluate the role of *Cd38* as it relates to behavior (Hattori et al., 2023). An astrocyte-specific *Cd38* knockout model would allow for better understanding of the cell-autonomous changes relating to astrocyte gene expression, morphology, and function similar to what others have reported in global knockout models (Hattori et al., 2017). This proposed model would also be of great benefit to all of the studies discussed within this chapter.

Lastly, our RNA-seq dataset reveal numerous DEG and GO pathways related to the familiar hallmarks of neurodegeneration. The scope of this work primarily serves to provide additional understanding of the effect of CD38 deficiency on astrocytic gene expression and bioenergetics. We anticipate that others will utilize our dataset to evaluate genes and pathways related to dysfunctional aspect that we have not described in detail here. Altered gene expression in DNA/RNA regulation and altered inflammatory responses are examples of pathways associated with PD and other neurodegenerative diseases (Wilson et al., 2023) that we have identified within our sequencing data, but did not discuss in full detail here. Altogether, our results provide additional context to the relationship between CD38 deficiency, astrocyte function, and neurodegenerative risk. Our anticipate that our sequencing data provides a resource for others to further evaluate specific genes, pathways, and potentially therapeutic targets of interest that may be relevant in the context of human health and Parkinson's disease risk.

REFERENCES

Adamczyk, A. (2023). Glial-Neuronal Interactions in Neurological Disorders: Molecular Mechanisms and Potential Points for Intervention. *Int J Mol Sci*, *24*(7). https://doi.org/10.3390/ijms24076274

Aksoy, P., White, T. A., Thompson, M., & Chini, E. N. (2006). Regulation of intracellular levels of NAD: a novel role for CD38. *Biochem Biophys Res Commun*, *345*(4), 1386-1392. https://doi.org/10.1016/j.bbrc.2006.05.042

Allen brain atlas. (2006). *Developing Mouse Brain Atlus*. https://portal.brain-map.org/

Anderson, A. S., Roberts, P. C., Frisard, M. I., Hulver, M. W., & Schmelz, E. M. (2014). Ovarian tumor-initiating cells display a flexible metabolism. *Exp Cell Res*, *328*(1), 44-57. https://doi.org/10.1016/j.yexcr.2014.08.028

Bagur, R., & Hajnóczky, G. (2017). Intracellular Ca(2+) Sensing: Its Role in Calcium Homeostasis and Signaling. *Mol Cell*, *66*(6), 780-788. https://doi.org/10.1016/j.molcel.2017.05.028

Baldwin, K. T., Murai, K. K., & Khakh, B. S. (2023). Astrocyte morphology. *Trends in Cell Biology*.

Balestrino, R., & Schapira, A. H. V. (2020). Parkinson disease. *Eur J Neurol*, *27*(1), 27-42. https://doi.org/10.1111/ene.14108

Biorender. (2023, 2023). *Biorender.com*. Biorender.com. Retrieved 11/21/2023 from https://www.biorender.com/

Blauwendraat, C., Nalls, M. A., & Singleton, A. B. (2020). The genetic architecture of Parkinson's disease. *Lancet Neurol*, *19*(2), 170-178. https://doi.org/10.1016/s1474-4422(19)30287-x

Booth, H. D. E., Hirst, W. D., & Wade-Martins, R. (2017). The Role of Astrocyte Dysfunction in Parkinson's Disease Pathogenesis. *Trends Neurosci*, *40*(6), 358-370. https://doi.org/10.1016/j.tins.2017.04.001

Borsche, M., Pereira, S. L., Klein, C., & Grünewald, A. (2021). Mitochondria and Parkinson's Disease: Clinical, Molecular, and Translational Aspects. *J Parkinsons Dis*, *11*(1), 45-60. https://doi.org/10.3233/jpd-201981

Braak, H., Del Tredici, K., Rüb, U., de Vos, R. A., Jansen Steur, E. N., & Braak, E. (2003). Staging of brain pathology related to sporadic Parkinson's disease. *Neurobiol Aging*, *24*(2), 197-211. https://doi.org/10.1016/s0197-4580(02)00065-9

Braidy, N., Guillemin, G. J., Mansour, H., Chan-Ling, T., Poljak, A., & Grant, R. (2011). Age related changes in NAD+ metabolism oxidative stress and Sirt1 activity in wistar rats. *PLoS One*, *6*(4), e19194. https://doi.org/10.1371/journal.pone.0019194

Braidy, N., Poljak, A., Grant, R., Jayasena, T., Mansour, H., Chan-Ling, T., Guillemin, G. J., Smythe, G., & Sachdev, P. (2014). Mapping NAD(+) metabolism in the brain of ageing Wistar rats: potential targets for influencing brain senescence. *Biogerontology*, *15*(2), 177-198. https://doi.org/10.1007/s10522-013-9489-5

Burré, J., Sharma, M., Tsetsenis, T., Buchman, V., Etherton, M. R., & Südhof, T. C. (2010). Alpha-synuclein promotes SNARE-complex assembly in vivo and in vitro. *Science*, *329*(5999), 1663-1667. https://doi.org/10.1126/science.1195227

Caines, J. K., Barnes, D. A., & Berry, M. D. (2022). The Use of Seahorse XF Assays to Interrogate Real-Time Energy Metabolism in Cancer Cell Lines. *Methods Mol Biol*, *2508*, 225-234. https://doi.org/10.1007/978-1-0716-2376-3_17

Camacho-Pereira, J., Tarragó, M. G., Chini, C. C. S., Nin, V., Escande, C., Warner, G. M., Puranik, A. S., Schoon, R. A., Reid, J. M., Galina, A., & Chini, E. N. (2016). CD38 Dictates Age-Related NAD Decline and Mitochondrial Dysfunction through an SIRT3-Dependent Mechanism. *Cell Metab*, *23*(6), 1127-1139. https://doi.org/10.1016/j.cmet.2016.05.006

Chen, M. L., Lin, C. H., Lee, M. J., & Wu, R. M. (2014). BST1 rs11724635 interacts with environmental factors to increase the risk of Parkinson's disease in a Taiwanese population. *Parkinsonism Relat Disord*, *20*(3), 280-283. https://doi.org/10.1016/j.parkreldis.2013.11.009

Chini, E. N., Chini, C. C. S., Espindola Netto, J. M., de Oliveira, G. C., & van Schooten, W. (2018). The Pharmacology of CD38/NADase: An Emerging Target in Cancer and Diseases of Aging. *Trends Pharmacol Sci*, *39*(4), 424-436. https://doi.org/10.1016/j.tips.2018.02.001

Cockayne, D. A., Muchamuel, T., Grimaldi, J. C., Muller-Steffner, H., Randall, T. D., Lund, F. E., Murray, R., Schuber, F., & Howard, M. C. (1998). Mice deficient for the ecto-nicotinamide adenine dinucleotide glycohydrolase CD38 exhibit altered humoral immune responses. *Blood*, *92*(4), 1324-1333.

Connolly, N. M. C., Theurey, P., Adam-Vizi, V., Bazan, N. G., Bernardi, P., Bolaños, J. P., Culmsee, C., Dawson, V. L., Deshmukh, M., Duchen, M. R., Düssmann, H., Fiskum, G., Galindo, M. F., Hardingham, G. E., Hardwick, J. M., Jekabsons, M. B., Jonas, E. A., Jordán, J., Lipton, S. A., . . . Prehn, J. H. M. (2018). Guidelines on experimental methods to assess mitochondrial dysfunction in cellular models of neurodegenerative diseases. *Cell Death Differ*, *25*(3), 542-572. https://doi.org/10.1038/s41418-017-0020-4

Day, J. O., & Mullin, S. (2021). The Genetics of Parkinson's Disease and Implications for Clinical Practice. *Genes (Basel)*, *12*(7). https://doi.org/10.3390/genes12071006

De Miranda, B. R., Goldman, S. M., Miller, G. W., Greenamyre, J. T., & Dorsey, E. R. (2022). Preventing Parkinson's Disease: An Environmental Agenda. *J Parkinsons Dis*, *12*(1), 45-68. https://doi.org/10.3233/jpd-212922

Deaglio, S., Aydin, S., Vaisitti, T., Bergui, L., & Malavasi, F. (2008). CD38 at the junction between prognostic marker and therapeutic target. *Trends in molecular medicine*, *14*(5), 210-218.

Deaglio, S., Mehta, K., & Malavasi, F. (2001). Human CD38: a (r)evolutionary story of enzymes and receptors. *Leuk Res*, *25*(1), 1-12. https://doi.org/10.1016/s0145-2126(00)00093-x

Deledda, A., Giordano, E., Velluzzi, F., Flore, G., Franceschelli, S., Speranza, L., & Ripari, P. (2022). Mitochondrial Aging and Senolytic Natural Products with Protective Potential. *Int J Mol Sci*, *23*(24). https://doi.org/10.3390/ijms232416219

Derouiche, A., Haseleu, J., & Korf, H. W. (2015). Fine Astrocyte Processes Contain Very Small Mitochondria: Glial Oxidative Capability May Fuel Transmitter Metabolism. *Neurochem Res*, *40*(12), 2402-2413. https://doi.org/10.1007/s11064-015-1563-8

di Domenico, A., Carola, G., Calatayud, C., Pons-Espinal, M., Muñoz, J. P., Richaud-Patin, Y., Fernandez-Carasa, I., Gut, M., Faella, A., Parameswaran, J., Soriano, J., Ferrer, I., Tolosa, E., Zorzano, A., Cuervo, A. M., Raya, A., & Consiglio, A. (2019). Patient-Specific iPSC-Derived Astrocytes Contribute to Non-Cell-Autonomous Neurodegeneration in Parkinson's Disease. *Stem Cell Reports*, *12*(2), 213-229. https://doi.org/10.1016/j.stemcr.2018.12.011

Dong, Y., & Benveniste, E. N. (2001). Immune function of astrocytes. *Glia*, *36*(2), 180-190. https://doi.org/10.1002/glia.1107

Dunn, J., & Grider, M. H. (2020). Physiology, adenosine triphosphate.

Fernández-Calle, R., Konings, S. C., Frontiñán-Rubio, J., García-Revilla, J., Camprubí-Ferrer, L., Svensson, M., Martinson, I., Boza-Serrano, A., Venero, J. L., Nielsen, H. M., Gouras, G. K., & Deierborg, T. (2022). APOE in the bullseye of neurodegenerative diseases: impact of the APOE genotype in Alzheimer's disease pathology and brain diseases. *Mol Neurodegener*, *17*(1), 62. https://doi.org/10.1186/s13024-022-00566-4

Franceschi, C., Garagnani, P., Parini, P., Giuliani, C., & Santoro, A. (2018). Inflammaging: a new immune-metabolic viewpoint for age-related diseases. *Nat Rev Endocrinol*, *14*(10), 576-590. https://doi.org/10.1038/s41574-018-0059-4

Fullard, M. E., Morley, J. F., & Duda, J. E. (2017). Olfactory Dysfunction as an Early Biomarker in Parkinson's Disease. *Neurosci Bull*, *33*(5), 515-525. https://doi.org/10.1007/s12264-017-0170-x

Gan, K. J., & Südhof, T. C. (2020). SPARCL1 Promotes Excitatory But Not Inhibitory Synapse Formation and Function Independent of Neurexins and Neuroligins. *J Neurosci*, *40*(42), 8088-8102. https://doi.org/10.1523/jneurosci.0454-20.2020

Gao, X. Y., Yang, T., Gu, Y., & Sun, X. H. (2022). Mitochondrial Dysfunction in Parkinson's Disease: From Mechanistic Insights to Therapy. *Front Aging Neurosci*, *14*, 885500. https://doi.org/10.3389/fnagi.2022.885500

Ge, Y. J., Ou, Y. N., Deng, Y. T., Wu, B. S., Yang, L., Zhang, Y. R., Chen, S. D., Huang, Y. Y., Dong, Q., Tan, L., & Yu, J. T. (2023). Prioritization of Drug Targets for Neurodegenerative Diseases by Integrating Genetic and Proteomic Data From Brain and Blood. *Biol Psychiatry*, *93*(9), 770-779. https://doi.org/10.1016/j.biopsych.2022.11.002

Grozio, A., Sociali, G., Sturla, L., Caffa, I., Soncini, D., Salis, A., Raffaelli, N., De Flora, A., Nencioni, A., & Bruzzone, S. (2013). CD73 protein as a source of extracellular precursors for sustained NAD+ biosynthesis in FK866-treated tumor cells. *J Biol Chem*, *288*(36), 25938-25949. https://doi.org/10.1074/jbc.M113.470435

GTEx Consortium. (2020). The GTEx Consortium atlas of genetic regulatory effects across human tissues. *Science*, *369*(6509), 1318-1330.

Guerreiro, S., Privat, A. L., Bressac, L., & Toulorge, D. (2020). CD38 in Neurodegeneration and Neuroinflammation. *Cells*, *9*(2). https://doi.org/10.3390/cells9020471

Hattori, T., Cherepanov, S. M., Sakaga, R., Roboon, J., Nguyen, D. T., Ishii, H., Takarada-Iemata, M., Nishiuchi, T., Kannon, T., Hosomichi, K., Tajima, A., Yamamoto, Y., Okamoto, H., Sugawara, A., Higashida, H., & Hori, O. (2023). Postnatal expression of CD38 in astrocytes regulates synapse formation and adult social memory. *Embo j*, *42*(15), e111247. https://doi.org/10.15252/embj.2022111247

Hattori, T., Kaji, M., Ishii, H., Jureepon, R., Takarada-Iemata, M., Minh Ta, H., Manh Le, T., Konno, A., Hirai, H., Shiraishi, Y., Ozaki, N., Yamamoto, Y., Okamoto, H., Yokoyama, S., Higashida, H., Kitao, Y., & Hori, O. (2017). CD38 positively regulates postnatal development of astrocytes cell-autonomously and oligodendrocytes non-cell-autonomously. *Glia*, *65*(6), 974-989. https://doi.org/10.1002/glia.23139

Hayakawa, K., Esposito, E., Wang, X., Terasaki, Y., Liu, Y., Xing, C., Ji, X., & Lo, E. H. (2016). Transfer of mitochondria from astrocytes to neurons after stroke. *Nature*, *535*(7613), 551-555. https://doi.org/10.1038/nature18928

Hayete, B., Wuest, D., Laramie, J., McDonagh, P., Church, B., Eberly, S., Lang, A., Marek, K., Runge, K., Shoulson, I., Singleton, A., Tanner, C., Khalil, I., Verma, A., & Ravina, B. (2017). A Bayesian mathematical model of motor and cognitive outcomes in Parkinson's disease. *PLoS One*, *12*(6), e0178982. https://doi.org/10.1371/journal.pone.0178982

Henry, A. G., Aghamohammadzadeh, S., Samaroo, H., Chen, Y., Mou, K., Needle, E., & Hirst, W. D. (2015). Pathogenic LRRK2 mutations, through increased kinase activity, produce enlarged lysosomes with reduced degradative capacity and increase ATP13A2 expression. *Hum Mol Genet*, *24*(21), 6013-6028. https://doi.org/10.1093/hmg/ddv314

Higashida, H., Salmina, A. B., Olovyannikova, R. Y., Hashii, M., Yokoyama, S., Koizumi, K., Jin, D., Liu, H. X., Lopatina, O., Amina, S., Islam, M. S., Huang, J. J., & Noda, M. (2007). Cyclic ADP-ribose as a universal calcium signal molecule in the nervous system. *Neurochem Int*, *51*(2-4), 192-199. https://doi.org/10.1016/j.neuint.2007.06.023

Higashida, H., Yokoyama, S., Kikuchi, M., & Munesue, T. (2012). CD38 and its role in oxytocin secretion and social behavior. *Horm Behav*, *61*(3), 351-358. https://doi.org/10.1016/j.yhbeh.2011.12.011

Holt, L. M., Hernandez, R. D., Pacheco, N. L., Torres Ceja, B., Hossain, M., & Olsen, M. L. (2019). Astrocyte morphogenesis is dependent on BDNF signaling via astrocytic TrkB.T1. *Elife*, *8*. https://doi.org/10.7554/eLife.44667

Holt, L. M., & Olsen, M. L. (2016). Novel Applications of Magnetic Cell Sorting to Analyze Cell-Type Specific Gene and Protein Expression in the Central Nervous System. *PLoS One*, *11*(2), e0150290. https://doi.org/10.1371/journal.pone.0150290

Holt, L. M., Stoyanof, S. T., & Olsen, M. L. (2019). Magnetic Cell Sorting for In Vivo and In Vitro Astrocyte, Neuron, and Microglia Analysis. *Curr Protoc Neurosci*, *88*(1), e71. https://doi.org/10.1002/cpns.71

Horan, M. P., Pichaud, N., & Ballard, J. W. (2012). Review: quantifying mitochondrial dysfunction in complex diseases of aging. *J Gerontol A Biol Sci Med Sci*, *67*(10), 1022-1035. https://doi.org/10.1093/gerona/glr263

Houfani, A. A., & Foster, L. J. (2022). Review of the Real and Sometimes Hidden Costs in Proteomics Experimental Workflows. *Methods Mol Biol*, *2456*, 1-14. https://doi.org/10.1007/978-1-0716-2124-0_1

Howard, M., Grimaldi, J. C., Bazan, J. F., Lund, F. E., Santos-Argumedo, L., Parkhouse, R. M., Walseth, T. F., & Lee, H. C. (1993). Formation and hydrolysis of cyclic ADP-ribose catalyzed by lymphocyte antigen CD38. *Science*, *262*(5136), 1056-1059. https://doi.org/10.1126/science.8235624

Ilyechova, E. Y., Miliukhina, I. V., Orlov, I. A., Muruzheva, Z. M., Puchkova, L. V., & Karpenko, M. N. (2018). A low blood copper concentration is a co-morbidity burden factor in Parkinson's disease development. *Neurosci Res*, *135*, 54-62. https://doi.org/10.1016/j.neures.2017.11.011

Jha, M. K., Kim, J. H., Song, G. J., Lee, W. H., Lee, I. K., Lee, H. W., An, S. S. A., Kim, S., & Suk, K. (2018). Functional dissection of astrocyte-secreted proteins: Implications in brain health and diseases. *Prog Neurobiol*, *162*, 37-69. https://doi.org/10.1016/j.pneurobio.2017.12.003

Jin, D., Liu, H. X., Hirai, H., Torashima, T., Nagai, T., Lopatina, O., Shnayder, N. A., Yamada, K., Noda, M., Seike, T., Fujita, K., Takasawa, S., Yokoyama, S., Koizumi, K., Shiraishi, Y., Tanaka, S., Hashii, M., Yoshihara, T., Higashida, K., . . . Higashida, H. (2007). CD38

is critical for social behaviour by regulating oxytocin secretion. *Nature*, *446*(7131), 41-45. https://doi.org/10.1038/nature05526
Kalia, L. V., & Lang, A. E. (2015). Parkinson's disease. *Lancet*, *386*(9996), 896-912. https://doi.org/10.1016/s0140-6736(14)61393-3
Kam, T. I., Hinkle, J. T., Dawson, T. M., & Dawson, V. L. (2020). Microglia and astrocyte dysfunction in parkinson's disease. *Neurobiol Dis*, *144*, 105028. https://doi.org/10.1016/j.nbd.2020.105028
Kandel, E. R., Schwartz, J. H., & Thomas, M. J. (2014). The Basal Ganglia. In *Principles of Neural Science, Fifth Edition*. McGraw-Hill Education. neurology.mhmedical.com/content.aspx?aid=1101682080
Karlsson, M., Zhang, C., Méar, L., Zhong, W., Digre, A., Katona, B., Sjöstedt, E., Butler, L., Odeberg, J., Dusart, P., Edfors, F., Oksvold, P., von Feilitzen, K., Zwahlen, M., Arif, M., Altay, O., Li, X., Ozcan, M., Mardinoglu, A., . . . Lindskog, C. (2021). A single-cell type transcriptomics map of human tissues. *Sci Adv*, *7*(31). https://doi.org/10.1126/sciadv.abh2169
Kelley, K. W., Nakao-Inoue, H., Molofsky, A. V., & Oldham, M. C. (2018). Variation among intact tissue samples reveals the core transcriptional features of human CNS cell classes. *Nat Neurosci*, *21*(9), 1171-1184. https://doi.org/10.1038/s41593-018-0216-z
Kent, W. J., Sugnet, C. W., Furey, T. S., Roskin, K. M., Pringle, T. H., Zahler, A. M., & Haussler, D. (2002). The human genome browser at UCSC. *Genome research*, *12*(6), 996-1006.
Khaidizar, F. D., Bessho, Y., & Nakahata, Y. (2021). Nicotinamide Phosphoribosyltransferase as a Key Molecule of the Aging/Senescence Process. *Int J Mol Sci*, *22*(7). https://doi.org/10.3390/ijms22073709
Kia, D. A., Zhang, D., Guelfi, S., Manzoni, C., Hubbard, L., Reynolds, R. H., Botía, J., Ryten, M., Ferrari, R., Lewis, P. A., Williams, N., Trabzuni, D., Hardy, J., & Wood, N. W. (2021). Identification of Candidate Parkinson Disease Genes by Integrating Genome-Wide Association Study, Expression, and Epigenetic Data Sets. *JAMA Neurol*, *78*(4), 464-472. https://doi.org/10.1001/jamaneurol.2020.5257
Kim, S., Kim, T., Lee, H. R., Jang, E. H., Ryu, H. H., Kang, M., Rah, S. Y., Yoo, J., Lee, B., Kim, J. I., Lim, C. S., Kim, S. J., Kim, U. H., Lee, Y. S., & Kaang, B. K. (2016). Impaired learning and memory in CD38 null mutant mice. *Mol Brain*, *9*, 16. https://doi.org/10.1186/s13041-016-0195-5
Konings, S. C., Torres-Garcia, L., Martinsson, I., & Gouras, G. K. (2021). Astrocytic and Neuronal Apolipoprotein E Isoforms Differentially Affect Neuronal Excitability. *Front Neurosci*, *15*, 734001. https://doi.org/10.3389/fnins.2021.734001
Langley, M. R., Choi, C. I., Peclat, T. R., Guo, Y., Simon, W. L., Yoon, H., Kleppe, L., Lucchinetti, C. F., Chini, C. C. S., Chini, E. N., & Scarisbrick, I. A. (2021). Critical Role of Astrocyte NAD(+) Glycohydrolase in Myelin Injury and Regeneration. *J Neurosci*, *41*(41), 8644-8667. https://doi.org/10.1523/jneurosci.2264-20.2021
Larsen, S., Nielsen, J., Hansen, C. N., Nielsen, L. B., Wibrand, F., Stride, N., Schroder, H. D., Boushel, R., Helge, J. W., Dela, F., & Hey-Mogensen, M. (2012). Biomarkers of mitochondrial content in skeletal muscle of healthy young human subjects. *J Physiol*, *590*(14), 3349-3360. https://doi.org/10.1113/jphysiol.2012.230185

Lautrup, S., Sinclair, D. A., Mattson, M. P., & Fang, E. F. (2019). NAD(+) in Brain Aging and Neurodegenerative Disorders. *Cell Metab*, *30*(4), 630-655. https://doi.org/10.1016/j.cmet.2019.09.001

Lawrence, J. M., Schardien, K., Wigdahl, B., & Nonnemacher, M. R. (2023). Roles of neuropathology-associated reactive astrocytes: a systematic review. *Acta Neuropathol Commun*, *11*(1), 42. https://doi.org/10.1186/s40478-023-01526-9

Levy, A., Bercovich-Kinori, A., Alexandrovich, A. G., Tsenter, J., Trembovler, V., Lund, F. E., Shohami, E., Stein, R., & Mayo, L. (2009). CD38 facilitates recovery from traumatic brain injury. *J Neurotrauma*, *26*(9), 1521-1533. https://doi.org/10.1089/neu.2008.0746

Li, J., Luo, J., Liu, L., Fu, H., & Tang, L. (2019). The association between CD157/BST1 polymorphisms and the susceptibility of Parkinson's disease: a meta-analysis. *Neuropsychiatr Dis Treat*, *15*, 1089-1102. https://doi.org/10.2147/ndt.S190935

Li, K., Li, J., Zheng, J., & Qin, S. (2019). Reactive Astrocytes in Neurodegenerative Diseases. *Aging Dis*, *10*(3), 664-675. https://doi.org/10.14336/ad.2018.0720

Lowe, R., Shirley, N., Bleackley, M., Dolan, S., & Shafee, T. (2017). Transcriptomics technologies. *PLoS Comput Biol*, *13*(5), e1005457. https://doi.org/10.1371/journal.pcbi.1005457

Mahlknecht, P., Marini, K., Werkmann, M., Poewe, W., & Seppi, K. (2022). Prodromal Parkinson's disease: hype or hope for disease-modification trials? *Transl Neurodegener*, *11*(1), 11. https://doi.org/10.1186/s40035-022-00286-1

Malavasi, F., Deaglio, S., Funaro, A., Ferrero, E., Horenstein, A. L., Ortolan, E., Vaisitti, T., & Aydin, S. (2008). Evolution and function of the ADP ribosyl cyclase/CD38 gene family in physiology and pathology. *Physiol Rev*, *88*(3), 841-886. https://doi.org/10.1152/physrev.00035.2007

Massudi, H., Grant, R., Braidy, N., Guest, J., Farnsworth, B., & Guillemin, G. J. (2012). Age-associated changes in oxidative stress and NAD+ metabolism in human tissue. *PLoS One*, *7*(7), e42357. https://doi.org/10.1371/journal.pone.0042357

Meade, R. M., Fairlie, D. P., & Mason, J. M. (2019). Alpha-synuclein structure and Parkinson's disease - lessons and emerging principles. *Mol Neurodegener*, *14*(1), 29. https://doi.org/10.1186/s13024-019-0329-1

Meyer, T., Shimon, D., Youssef, S., Yankovitz, G., Tessler, A., Chernobylsky, T., Gaoni-Yogev, A., Perelroizen, R., Budick-Harmelin, N., Steinman, L., & Mayo, L. (2022). NAD(+) metabolism drives astrocyte proinflammatory reprogramming in central nervous system autoimmunity. *Proc Natl Acad Sci U S A*, *119*(35), e2211310119. https://doi.org/10.1073/pnas.2211310119

Michalovicz, L. T., Kelly, K. A., Vashishtha, S., Ben-Hamo, R., Efroni, S., Miller, J. V., Locker, A. R., Sullivan, K., Broderick, G., Miller, D. B., & O'Callaghan, J. P. (2019). Astrocyte-specific transcriptome analysis using the ALDH1L1 bacTRAP mouse reveals novel biomarkers of astrogliosis in response to neurotoxicity. *J Neurochem*, *150*(4), 420-440. https://doi.org/10.1111/jnc.14800

Miyake, Y., Tanaka, K., Fukushima, W., Kiyohara, C., Sasaki, S., Tsuboi, Y., Yamada, T., Oeda, T., Shimada, H., Kawamura, N., Sakae, N., Fukuyama, H., Hirota, Y., & Nagai, M. (2012). Lack of association between BST1 polymorphisms and sporadic Parkinson's disease in a Japanese population. *J Neurol Sci*, *323*(1-2), 162-166. https://doi.org/10.1016/j.jns.2012.09.008

Miyazaki, I., & Asanuma, M. (2020). Neuron-Astrocyte Interactions in Parkinson's Disease. *Cells*, *9*(12). https://doi.org/10.3390/cells9122623

Mizuguchi, M., Otsuka, N., Sato, M., Ishii, Y., Kon, S., Yamada, M., Nishina, H., Katada, T., & Ikeda, K. (1995). Neuronal localization of CD38 antigen in the human brain. *Brain Res*, *697*(1-2), 235-240. https://doi.org/10.1016/0006-8993(95)00885-t

Morandi, F., Airoldi, I., Marimpietri, D., Bracci, C., Faini, A. C., & Gramignoli, R. (2019). CD38, a Receptor with Multifunctional Activities: From Modulatory Functions on Regulatory Cell Subsets and Extracellular Vesicles, to a Target for Therapeutic Strategies. *Cells*, *8*(12). https://doi.org/10.3390/cells8121527

Nalls, M. A., Blauwendraat, C., Vallerga, C. L., Heilbron, K., Bandres-Ciga, S., Chang, D., Tan, M., Kia, D. A., Noyce, A. J., Xue, A., Bras, J., Young, E., von Coelln, R., Simón-Sánchez, J., Schulte, C., Sharma, M., Krohn, L., Pihlstrøm, L., Siitonen, A., . . . Singleton, A. B. (2019). Identification of novel risk loci, causal insights, and heritable risk for Parkinson's disease: a meta-analysis of genome-wide association studies. *Lancet Neurol*, *18*(12), 1091-1102. https://doi.org/10.1016/s1474-4422(19)30320-5

Nedergaard, M., Ransom, B., & Goldman, S. A. (2003). New roles for astrocytes: redefining the functional architecture of the brain. *Trends Neurosci*, *26*(10), 523-530. https://doi.org/10.1016/j.tins.2003.08.008

Nelissen, T. P., Bamford, R. A., Tochitani, S., Akkus, K., Kudzinskas, A., Yokoi, K., Okamoto, H., Yamamoto, Y., Burbach, J. P. H., Matsuzaki, H., & Oguro-Ando, A. (2018). CD38 is Required for Dendritic Organization in Visual Cortex and Hippocampus. *Neuroscience*, *372*, 114-125. https://doi.org/10.1016/j.neuroscience.2017.12.050

Ni, A., & Ernst, C. (2022). Evidence That Substantia Nigra Pars Compacta Dopaminergic Neurons Are Selectively Vulnerable to Oxidative Stress Because They Are Highly Metabolically Active. *Front Cell Neurosci*, *16*, 826193. https://doi.org/10.3389/fncel.2022.826193

Nissanka, N., & Moraes, C. T. (2018). Mitochondrial DNA damage and reactive oxygen species in neurodegenerative disease. *FEBS Lett*, *592*(5), 728-742. https://doi.org/10.1002/1873-3468.12956

Nonnekes, J., Post, B., Tetrud, J. W., Langston, J. W., & Bloem, B. R. (2018). MPTP-induced parkinsonism: an historical case series. *Lancet Neurol*, *17*(4), 300-301. https://doi.org/10.1016/s1474-4422(18)30072-3

Noyce, A. J., Bestwick, J. P., Silveira-Moriyama, L., Hawkes, C. H., Giovannoni, G., Lees, A. J., & Schrag, A. (2012). Meta-analysis of early nonmotor features and risk factors for Parkinson disease. *Annals of neurology*, *72*(6), 893-901.

Osellame, L. D., Blacker, T. S., & Duchen, M. R. (2012). Cellular and molecular mechanisms of mitochondrial function. *Best practice & research Clinical endocrinology & metabolism*, *26*(6), 711-723.

Parkinson, J. (2002). An essay on the shaking palsy. 1817. *J Neuropsychiatry Clin Neurosci*, *14*(2), 223-236; discussion 222. https://doi.org/10.1176/jnp.14.2.223

Patani, R., Hardingham, G. E., & Liddelow, S. A. (2023). Functional roles of reactive astrocytes in neuroinflammation and neurodegeneration. *Nat Rev Neurol*, *19*(7), 395-409. https://doi.org/10.1038/s41582-023-00822-1

Patel, M. G. B., & Chudasama, D. (2021). *Nuclear Magnetic Resonance Spectroscopy NMR*. https://doi.org/10.37591/JoNET

Phatnani, H., & Maniatis, T. (2015). Astrocytes in neurodegenerative disease. *Cold Spring Harb Perspect Biol*, *7*(6). https://doi.org/10.1101/cshperspect.a020628
Pickrell, A. M., & Youle, R. J. (2015). The roles of PINK1, parkin, and mitochondrial fidelity in Parkinson's disease. *Neuron*, *85*(2), 257-273. https://doi.org/10.1016/j.neuron.2014.12.007
Piedra-Quintero, Z. L., Wilson, Z., Nava, P., & Guerau-de-Arellano, M. (2020). CD38: An Immunomodulatory Molecule in Inflammation and Autoimmunity. *Front Immunol*, *11*, 597959. https://doi.org/10.3389/fimmu.2020.597959
Poewe, W., Seppi, K., Tanner, C. M., Halliday, G. M., Brundin, P., Volkmann, J., Schrag, A. E., & Lang, A. E. (2017). Parkinson disease. *Nat Rev Dis Primers*, *3*, 17013. https://doi.org/10.1038/nrdp.2017.13
Rajan, S., & Kaas, B. (2022). Parkinson's Disease: Risk Factor Modification and Prevention. *Semin Neurol*, *42*(5), 626-638. https://doi.org/10.1055/s-0042-1758780
Rannikko, E. H., Weber, S. S., & Kahle, P. J. (2015). Exogenous α-synuclein induces toll-like receptor 4 dependent inflammatory responses in astrocytes. *BMC Neurosci*, *16*, 57. https://doi.org/10.1186/s12868-015-0192-0
Ransom, B. R., Kunis, D. M., Irwin, I., & Langston, J. W. (1987). Astrocytes convert the parkinsonism inducing neurotoxin, MPTP, to its active metabolite, MPP+. *Neurosci Lett*, *75*(3), 323-328. https://doi.org/10.1016/0304-3940(87)90543-x
Rath, S., Sharma, R., Gupta, R., Ast, T., Chan, C., Durham, T. J., Goodman, R. P., Grabarek, Z., Haas, M. E., Hung, W. H. W., Joshi, P. R., Jourdain, A. A., Kim, S. H., Kotrys, A. V., Lam, S. S., McCoy, J. G., Meisel, J. D., Miranda, M., Panda, A., . . . Mootha, V. K. (2021). MitoCarta3.0: an updated mitochondrial proteome now with sub-organelle localization and pathway annotations. *Nucleic Acids Res*, *49*(D1), D1541-d1547. https://doi.org/10.1093/nar/gkaa1011
Roboon, J., Hattori, T., Ishii, H., Takarada-Iemata, M., Le, T. M., Shiraishi, Y., Ozaki, N., Yamamoto, Y., Sugawara, A., Okamoto, H., Higashida, H., Kitao, Y., & Hori, O. (2019). Deletion of CD38 Suppresses Glial Activation and Neuroinflammation in a Mouse Model of Demyelination. *Front Cell Neurosci*, *13*, 258. https://doi.org/10.3389/fncel.2019.00258
Roos, D. S., Klein, M., Deeg, D. J. H., Doty, R. L., & Berendse, H. W. (2022). Prevalence of Prodromal Symptoms of Parkinson's Disease in the Late Middle-Aged Population. *J Parkinsons Dis*, *12*(3), 967-974. https://doi.org/10.3233/jpd-213007
Rose, J., Brian, C., Pappa, A., Panayiotidis, M. I., & Franco, R. (2020). Mitochondrial Metabolism in Astrocytes Regulates Brain Bioenergetics, Neurotransmission and Redox Balance. *Front Neurosci*, *14*, 536682. https://doi.org/10.3389/fnins.2020.536682
Rouillard, A. D., Gundersen, G. W., Fernandez, N. F., Wang, Z., Monteiro, C. D., McDermott, M. G., & Ma'ayan, A. (2016). The harmonizome: a collection of processed datasets gathered to serve and mine knowledge about genes and proteins. *Database (Oxford)*, *2016*. https://doi.org/10.1093/database/baw100
Sakers, K., Lake, A. M., Khazanchi, R., Ouwenga, R., Vasek, M. J., Dani, A., & Dougherty, J. D. (2017). Astrocytes locally translate transcripts in their peripheral processes. *Proc Natl Acad Sci U S A*, *114*(19), E3830-e3838. https://doi.org/10.1073/pnas.1617782114
Saunders, A., Macosko, E. Z., Wysoker, A., Goldman, M., Krienen, F. M., de Rivera, H., Bien, E., Baum, M., Bortolin, L., Wang, S., Goeva, A., Nemesh, J., Kamitaki, N., Brumbaugh, S., Kulp, D., & McCarroll, S. A. (2018). Molecular Diversity and Specializations among

the Cells of the Adult Mouse Brain. *Cell*, *174*(4), 1015-1030.e1016. https://doi.org/10.1016/j.cell.2018.07.028
Savtchouk, I., & Volterra, A. (2018). Gliotransmission: Beyond Black-and-White. *J Neurosci*, *38*(1), 14-25. https://doi.org/10.1523/jneurosci.0017-17.2017
Schildge, S., Bohrer, C., Beck, K., & Schachtrup, C. (2013). Isolation and culture of mouse cortical astrocytes. *J Vis Exp*(71). https://doi.org/10.3791/50079
Schiweck, J., Eickholt, B. J., & Murk, K. (2018). Important Shapeshifter: Mechanisms Allowing Astrocytes to Respond to the Changing Nervous System During Development, Injury and Disease. *Front Cell Neurosci*, *12*, 261. https://doi.org/10.3389/fncel.2018.00261
Sellbach, A. N., Boyle, R. S., Silburn, P. A., & Mellick, G. D. (2006). Parkinson's disease and family history. *Parkinsonism & related disorders*, *12*(7), 399-409.
Sharma, M., Ioannidis, J. P., Aasly, J. O., Annesi, G., Brice, A., Van Broeckhoven, C., Bertram, L., Bozi, M., Crosiers, D., Clarke, C., Facheris, M., Farrer, M., Garraux, G., Gispert, S., Auburger, G., Vilariño-Güell, C., Hadjigeorgiou, G. M., Hicks, A. A., Hattori, N., . . . Krüger, R. (2012). Large-scale replication and heterogeneity in Parkinson disease genetic loci. *Neurology*, *79*(7), 659-667. https://doi.org/10.1212/WNL.0b013e318264e353
Sheng, Z. H. (2014). Mitochondrial trafficking and anchoring in neurons: New insight and implications. *J Cell Biol*, *204*(7), 1087-1098. https://doi.org/10.1083/jcb.201312123
Sidoli, S., Kulej, K., & Garcia, B. A. (2017). Why proteomics is not the new genomics and the future of mass spectrometry in cell biology. *The Journal of cell biology*, *216*(1), 21.
Singh, A., Zhi, L., & Zhang, H. (2019). LRRK2 and mitochondria: Recent advances and current views. *Brain Res*, *1702*, 96-104. https://doi.org/10.1016/j.brainres.2018.06.010
Singh, K., Han, K., Tilve, S., Wu, K., Geller, H. M., & Sack, M. N. (2018). Parkin targets NOD2 to regulate astrocyte endoplasmic reticulum stress and inflammation. *Glia*, *66*(11), 2427-2437. https://doi.org/10.1002/glia.23482
Sjöstedt, E., Zhong, W., Fagerberg, L., Karlsson, M., Mitsios, N., Adori, C., Oksvold, P., Edfors, F., Limiszewska, A., Hikmet, F., Huang, J., Du, Y., Lin, L., Dong, Z., Yang, L., Liu, X., Jiang, H., Xu, X., Wang, J., . . . Mulder, J. (2020). An atlas of the protein-coding genes in the human, pig, and mouse brain. *Science*, *367*(6482). https://doi.org/10.1126/science.aay5947
Skrahina, V., Gaber, H., Vollstedt, E. J., Förster, T. M., Usnich, T., Curado, F., Brüggemann, N., Paul, J., Bogdanovic, X., Zülbahar, S., Olmedillas, M., Skobalj, S., Ameziane, N., Bauer, P., Csoti, I., Koleva-Alazeh, N., Grittner, U., Westenberger, A., Kasten, M., . . . Rolfs, A. (2021). The Rostock International Parkinson's Disease (ROPAD) Study: Protocol and Initial Findings. *Mov Disord*, *36*(4), 1005-1010. https://doi.org/10.1002/mds.28416
Sofroniew, M. V., & Vinters, H. V. (2010). Astrocytes: biology and pathology. *Acta Neuropathol*, *119*(1), 7-35. https://doi.org/10.1007/s00401-009-0619-8
Sonntag, K. C., Ryu, W. I., Amirault, K. M., Healy, R. A., Siegel, A. J., McPhie, D. L., Forester, B., & Cohen, B. M. (2017). Late-onset Alzheimer's disease is associated with inherent changes in bioenergetics profiles. *Sci Rep*, *7*(1), 14038. https://doi.org/10.1038/s41598-017-14420-x
Sontheimer, H. (2021). *Diseases of the nervous system*. Elsevier.
Sun, C., Liu, X., Wang, B., Wang, Z., Liu, Y., Di, C., Si, J., Li, H., Wu, Q., Xu, D., Li, J., Li, G., Wang, Y., Wang, F., & Zhang, H. (2019). Endocytosis-mediated mitochondrial transplantation: Transferring normal human astrocytic mitochondria into glioma cells

rescues aerobic respiration and enhances radiosensitivity. *Theranostics*, *9*(12), 3595-3607. https://doi.org/10.7150/thno.33100
Technologies, S. (2023). *Magnetic Cell Separation and Cell Isolation*. Stemcell Technologies. Retrieved 11/21/2023 from https://www.stemcell.com/cell-separation/magnetic-cell-isolation
Thomas, B., & Beal, M. F. (2010). Mitochondrial therapies for Parkinson's disease. *Mov Disord*, *25 Suppl 1*(Suppl 1), S155-160. https://doi.org/10.1002/mds.22781
Tolosa, E., Garrido, A., Scholz, S. W., & Poewe, W. (2021). Challenges in the diagnosis of Parkinson's disease. *Lancet Neurol*, *20*(5), 385-397. https://doi.org/10.1016/s1474-4422(21)00030-2
Tysnes, O. B., & Storstein, A. (2017). Epidemiology of Parkinson's disease. *J Neural Transm (Vienna)*, *124*(8), 901-905. https://doi.org/10.1007/s00702-017-1686-y
Usmani, A., Shavarebi, F., & Hiniker, A. (2021). The Cell Biology of LRRK2 in Parkinson's Disease. *Mol Cell Biol*, *41*(5). https://doi.org/10.1128/mcb.00660-20
Viegas, M. S., Silva, T., Monteiro, M. M., do Carmo, A., & Martins, T. C. (2011). Knocking out of CD38 accelerates development of a lupus-like disease in lpr mice. *Rheumatology (Oxford)*, *50*(9), 1569-1577. https://doi.org/10.1093/rheumatology/ker178
Vollstedt, E. J., Schaake, S., Lohmann, K., Padmanabhan, S., Brice, A., Lesage, S., Tesson, C., Vidailhet, M., Wurster, I., Hentati, F., Mirelman, A., Giladi, N., Marder, K., Waters, C., Fahn, S., Kasten, M., Brüggemann, N., Borsche, M., Foroud, T., . . . Klein, C. (2023). Embracing Monogenic Parkinson's Disease: The MJFF Global Genetic PD Cohort. *Mov Disord*, *38*(2), 286-303. https://doi.org/10.1002/mds.29288
Wakade, C., Chong, R., Bradley, E., Thomas, B., & Morgan, J. (2014). Upregulation of GPR109A in Parkinson's disease. *PLoS One*, *9*(10), e109818. https://doi.org/10.1371/journal.pone.0109818
Walter, W., Sanchez-Cabo, F., & Ricote, M. (2015). GOplot: an R package for visually combining expression data with functional analysis. *Bioinformatics*, *31*(17), 2912-2914. https://doi.org/10.1093/bioinformatics/btv300
Wang, Y., Ni, J., Gao, T., Gao, C., Guo, L., & Yin, X. (2020). Activation of astrocytic sigma-1 receptor exerts antidepressant-like effect via facilitating CD38-driven mitochondria transfer. *Glia*, *68*(11), 2415-2426. https://doi.org/10.1002/glia.23850
Wang, Y. M., Liu, Z. Y., Ai, Y. H., Zhang, L. N., Zou, Y., & Peng, Q. Y. (2017). Blocking the CD38/cADPR pathway plays a double-edged role in LPS stimulated microglia. *Neuroscience*, *361*, 34-42. https://doi.org/10.1016/j.neuroscience.2017.08.010
Wei, W., Graeff, R., & Yue, J. (2014). Roles and mechanisms of the CD38/cyclic adenosine diphosphate ribose/Ca(2+) signaling pathway. *World J Biol Chem*, *5*(1), 58-67. https://doi.org/10.4331/wjbc.v5.i1.58
Wilson, D. M., 3rd, Cookson, M. R., Van Den Bosch, L., Zetterberg, H., Holtzman, D. M., & Dewachter, I. (2023). Hallmarks of neurodegenerative diseases. *Cell*, *186*(4), 693-714. https://doi.org/10.1016/j.cell.2022.12.032
World Health Organization. (2023, 8/09/2023). *Parkinson disease*. World Health Organization. Retrieved 11/19/2023 from https://www.who.int/news-room/fact-sheets/detail/parkinson-disease
Wu, M., Neilson, A., Swift, A. L., Moran, R., Tamagnine, J., Parslow, D., Armistead, S., Lemire, K., Orrell, J., Teich, J., Chomicz, S., & Ferrick, D. A. (2007). Multiparameter metabolic analysis reveals a close link between attenuated mitochondrial bioenergetic function and

enhanced glycolysis dependency in human tumor cells. *Am J Physiol Cell Physiol*, *292*(1), C125-136. https://doi.org/10.1152/ajpcell.00247.2006

Yamada, M., Mizuguchi, M., Otsuka, N., Ikeda, K., & Takahashi, H. (1997). Ultrastructural localization of CD38 immunoreactivity in rat brain. *Brain Res*, *756*(1-2), 52-60. https://doi.org/10.1016/s0006-8993(97)00117-0

Yang, W., Hamilton, J. L., Kopil, C., Beck, J. C., Tanner, C. M., Albin, R. L., Ray Dorsey, E., Dahodwala, N., Cintina, I., Hogan, P., & Thompson, T. (2020). Current and projected future economic burden of Parkinson's disease in the U.S. *NPJ Parkinsons Dis*, *6*, 15. https://doi.org/10.1038/s41531-020-0117-1

Yang, Y. J., Zhang, S., Ding, J. H., Zhou, F., & Hu, G. (2009). Iptakalim protects against MPP+-induced degeneration of dopaminergic neurons in association with astrocyte activation. *Int J Neuropsychopharmacol*, *12*(3), 317-327. https://doi.org/10.1017/s1461145708009243

Yao, S., Zhang, X., Zou, S. C., Zhu, Y., Li, B., Kuang, W. P., Guo, Y., Li, X. S., Li, L., & Wang, X. Y. (2021). A transcriptome-wide association study identifies susceptibility genes for Parkinson's disease. *NPJ Parkinsons Dis*, *7*(1), 79. https://doi.org/10.1038/s41531-021-00221-7

Ye, H., Robak, L. A., Yu, M., Cykowski, M., & Shulman, J. M. (2023). Genetics and Pathogenesis of Parkinson's Syndrome. *Annu Rev Pathol*, *18*, 95-121. https://doi.org/10.1146/annurev-pathmechdis-031521-034145

Yu, G., Wang, L. G., Han, Y., & He, Q. Y. (2012). clusterProfiler: an R package for comparing biological themes among gene clusters. *OMICS*, *16*(5), 284-287. https://doi.org/10.1089/omi.2011.0118

Zhang, W., Xiao, D., Mao, Q., & Xia, H. (2023). Role of neuroinflammation in neurodegeneration development. *Signal Transduct Target Ther*, *8*(1), 267. https://doi.org/10.1038/s41392-023-01486-5

Zhou, S., Tian, Y., Song, X., Xiong, J., & Cheng, G. (2023). Brain Proteome-Wide and Transcriptome-Wide Asso-ciation Studies, Bayesian Colocalization, and Mendelian Randomization Analyses Reveal Causal Genes of Parkinson's Disease. *J Gerontol A Biol Sci Med Sci*, *78*(4), 563-568. https://doi.org/10.1093/gerona/glac245

Zhu, X. C., Cao, L., Tan, M. S., Jiang, T., Wang, H. F., Lu, H., Tan, C. C., Zhang, W., Tan, L., & Yu, J. T. (2017). Association of Parkinson's Disease GWAS-Linked Loci with Alzheimer's Disease in Han Chinese. *Mol Neurobiol*, *54*(1), 308-318. https://doi.org/10.1007/s12035-015-9649-5